PHYSIOLOGICAL AND HORMONAL REGULATION OF INSULIN ACTION IN THE PREGNANT AND GROWING EWE

A Dissertation

Presented to the Faculty of the Graduate School

Of Cornell University

In Partial Fulfillment of the Requirements for the Degree of

Doctor of Philosophy

By

Cassandra Lynn Orndorff Lamb

August 2021

PHYSIOLOGICAL AND HORMONAL REGULATION OF INSULIN ACTION IN THE PREGNANT AND GROWING EWE

Cassandra Lynn Orndorff Lamb, Ph.D.
Cornell University 2021

Visceral adipose tissue depots have been implicated as major contributors to the insulin resistance of obesity in humans and rodents, but whether they are similarly as important in ruminants is unknown. Understanding the metabolic influence of fat depots is important to balance animal performance with maternal health in pregnancy and lactation. To explore this issue, lean and obese ewes were obtained by feeding to energy requirements or allowing unlimited energy consumption for a 50-day premating period and during pregnancy; both groups were energy-restricted during lactation. Ewes were evaluated in mid- and late pregnancy and in early lactation for adiposity by computed tomography (CT) and for insulin resistance by glucose (GTT) and insulin tolerance tests (ITT). By CT scan analysis, obese ewes were 2-fold fatter by mid-pregnancy; similar differences remained in late pregnancy and in lactation. Adiposity was further evaluated by using the CT scans to quantify internal (sum of omental, mesenteric, perirenal, and retroperitoneal) and external fat (remaining fat not included in internal fat). Unexpectedly, external fat accounted for greater than 2/3 of lipid accretion during pregnancy and mobilization during lactation. Obese ewes were more insulin resistant than lean ewes during pregnancy, but this effect disappeared during lactation. Surprisingly, correlation analysis suggested external fat as a more significant contributor to insulin resistance than internal fat. Overall, the dynamics of external fat appear to be a more important determinant of insulin action in pregnant and lactating ewes. Further work is needed to determine if a specific depot (i.e., intermuscular fat) is driving the influence of external fat.

In the second part of this dissertation, we asked whether exogenous administration of the hormone fibroblast growth factor-21 (FGF21) can improve insulin action in growing sheep. FGF21 is a known insulin-sensitizer in well-fed, obese rodents and primates. However, it was recently shown to have no such effect in energy-deficient early lactating dairy cows. Whether this reflects absence of insulin-sensitizing FGF21 action in ruminants or simply loss of action during energy insufficiency was unknown. Therefore, we studied FGF21 in well-fed growing sheep. First, we showed that the FGF21 system is similarly organized in sheep compared with other species. Briefly, liver is the main tissue expressing FGF21 and adipose is an important target tissue. Next, we administered recombinant human FGF21 (FGF21) or excipient solution (control) to the sheep via subcutaneous injection and found FGF21 acutely reduced both plasma glucose and insulin concentrations. Finally, chronic FGF21 administration improved insulin response as evaluated by GTT, as well as increased circulating adiponectin. Furthermore, FGF21 increased epinephrine-stimulated lipolysis. These results are similar to those reported in rodents and primates, but contrast with work previously obtained in energy-deficient dairy cattle. Energy balance may therefore be an important determinant of FGF21 action, but further work is needed in the same ruminant species to confirm these findings.

BIOGRAPHICAL SKETCH

Cassandra Lynn Orndorff Lamb was born in Morgantown, West Virginia on September 1, 1993. Her parents, Corbly and Christy Orndorff raised her on their fourth-generation Belgian draft horse farm in Waynesburg, Pennsylvania. Growing up, she was involved in the local 4-H and FFA programs, gaining an extensive background in livestock production by raising and showing lambs, pigs, and steers. In FFA, she served as the 2011 Chapter President, and then received her American FFA degree in 2012, which is the highest achievable degree. After graduating from Waynesburg Central High School at the top of her class in 2011, she chose to enroll at West Virginia University. In 2013, she began in the lab of Dr. Alexey Ivanov in the Mary Babb Randolph Cancer Center as an intern where she assisted Dr. Joseph Addison with his experiments to understand the mechanisms that regulate gene expression in tumor formation. Then in 2014, she joined the lab of Dr. Joseph McFadden where she assisted with an experiment designed to understand the physiological and biochemical changes in lean and overweight dairy cows transitioning from gestation to lactation. In May 2015, she graduated as a WVU Outstanding Senior with a Bachelor of Science degree in Biochemistry from the Davis College of Agriculture, Natural Resources and Design at WVU. In August 2015, she began her doctoral studies at Cornell University under the mentorship of Dr. Yves Boisclair to study physiological and hormonal mechanisms regulating insulin action in ewes.

ACKNOWLEDGEMENTS

First and foremost, I would like to thank my mentor, Dr. Yves Boisclair. I have the utmost respect for you as a scientist and am grateful to have had the opportunity to learn from the best. You have taught me to never settle and always strive to be my greatest. I am a better scientist and teacher because of your persistence.

Next, I would like to thank Dr. Sarah Giesy. From helping me "man-handle" sheep to teaching me how to critically review data, you are truly a person of many talents. When I met with you during my interview, you said that if I ever needed help with anything, you would be the person to ask. At the time, I didn't realize just how true that statement was; I'm not sure I would have made it through all of my studies without your moral support and scientific expertise.

In addition, I would like to thank present and past members of the Boisclair lab. First, Dr. Chris Krumm for showing me the ropes of what it means to be a graduate student, and always answering my questions – no matter how silly they may have been. I feel fortunate to have gotten to work with you during the last part of your PhD. Antonio Ramos and Molly McGuckin, thank you both for assisting with my experiments, helping me with some analysis, and providing support during the last couple years of my PhD. You are both very talented scientists and I wish you luck in your future endeavors!

I would also like to extend gratitude to my PhD special committee members, Dr. Vimal Selvaraj, Dr. Joseph McFadden, and Dr. Anna Thalacker-Mercer. Thank you for always answering any questions I had and pushing me to be the best scientist I could be. To Dr. McFadden

specifically, thank you for all of the experiences I gained in your lab as an undergraduate student at WVU. Working in your lab sparked my interest in transition period biology and metabolism, and you are a big reason I decided to pursue my doctoral degree.

Next, I would like to extend many thanks to supporting staff directly involved in my sheep studies. First, to Bruce Berggren-Thomas. I am positive no animal study would be possible at Cornell without your assistance! Next to Jessica Waltemeyer, Jeff Jebbett, and the rest of the LARTU staff. You may not hear this enough, but all of us graduate students really appreciate the work you do setting up pens and accommodating our sometimes-crazy requests!

I also gratefully acknowledge the support I had from all assisting undergraduate students – Remington Chan, Megan Hollister, Max Marwin, Adam Frosolone, Avni Bhalla, Chloe Mikles, Nneka Williams, and Shane Langbauer. I feel very fortunate to have gotten to work with such an excellent group.

A special thank you to all of our collaborators for all of their expertise in conducting my final sheep experiment. Dr. Richard Ehrhardt, Dr. Ramona Ehrhardt, and Barbara Makela for conducting the Michigan portion of our study and also fielding several sheep questions. Dr. Peter Scrivani and the entire radiology team at Cornell Vet for guiding us through the CT scanning process and then assisting us in analyzing our scans. And finally, Dr. Anthony Reeves and Raisa Rasul for developing and then fine-tuning the computer algorithm used to analyze our scans. I cannot thank you all enough for all the support you have given me!

Additional faculty and staff who supported me along the way include Dr. Jeremy Allen, Dr. Mike Thonney, Dr. Ron Butler, and Susanne Pelton. Additional graduate students who assisted me along the way include Dr. Robert Wijma, Dr. Niko Kochendoerfer, Dr. Amanda Davis, Dr. Billy Myers, Ananda Fontoura, Dr. Martin Perez, Dr. Kasey Schalich, and Dr. Viju Pillai. Thank you all for the guidance and assistance you provided!

I can't forget to thank my life-long support system: my parents, Corbly and Christy Orndorff and my sister, Caitlin Morton. I've lost track of how many late-night and supportive phone calls we've shared over the last 6 years. I am also very appreciative of all the hands-on skills Caitlin and I learned on the farm which provided me with the knowledge base I needed for my sheep research. Thank you all for always being on my side and in my corner, supporting everything I set out to do. Love you guys!

Finally, I would like to thank my husband and my better half, Kyle Lamb, for all of his support during the final and most crucial part of my degree. I knew when you were willing to come with me to virtually all of the 3AM lambing checks and stay with me while we waited for the ewe to expel her placenta that you would always be by my side. You know what they say – you will become like those who you are around most, and I guess I have finally spent enough time around lambs to become one! The last few months we've spent as husband and wife have been my favorite, and I am excited to see what else life has in store for us!

TABLE OF CONTENTS

LIST OF FIGURES

LIST OF TABLES

LIST OF ABBREVIATIONS

AARE	Amino Acid Response Element
ACC	Acetyl-CoA Carboxylase
AKT	Protein Kinase B or AKT
ALS	Acid Labile Subunit
AMPK	Adenosine Monophosphate-Activated Protein Kinase
ATGL	Adipose Triglyceride Lipase
BAT	Brown Adipose Tissue
BHBA	β-hydroxybutyric Acid
CNS	Central Nervous System
CSF	Cerebrospinal Fluid
DAG	Diacylglycerol
DGAT2	Diacylglycerol Acyltransferase
DIO	Diet-Induced Obesity
Dio2	Iodothyronine Deiodinase 2
EC	Epinephrine Challenge
EL	Early Lactation
ERK	Extracellular Signal-Regulated Kinase
FAS	Fatty Acid Synthase
FGF	Fibroblast Growth Factor
FGF21	Fibroblast Growth Factor-21
FGFR	Fibroblast Growth Factor Receptor
GH	Growth Hormone
GLUT	Glucose Transporter
GTT	Glucose Tolerance Test
HBD	Heparin-binding Domain
HDL	High Density Lipoprotein
HSL	Hormone Sensitive Lipase
IGF1	Insulin-like Growth Factor 1
IL-6	Interleukin 6
IR	Insulin Resistance

IRS1/2	Insulin Receptor Substrate 1 or 2
ITT	Insulin Tolerance Test
KD	Ketogenic Diet
KO	Knockout
LDL	Low Density Lipoprotein
LP	Late Pregnancy
MBW	Metabolic Body Weight ($BW^{0.75}$)
mTORC2	Mechanistic Target of Rapamycin Complex 2
NEB	Negative Energy Balance
NEFA	Non-esterified Fatty Acids
PDK1	Phosphoinositide-dependent Kinase 1
PGC-1α	Proliferator-Activated Receptor γ Coactivator-1^{α}
PGH	Placental Growth Hormone
PI3K	Phosphatidylinositol-3 Kinase
PIP2	Phosphatidylinositol-4,5-bisphosphate
PIP3	Phosphatidylinositol-3,4,5-trisphosphate
PKC	Protein Kinase C
PL	Placental Lactogen
PP2A	Protein Phosphatase 2A
PTP1B	Protein Tyrosine Phosphatase 1B
SAA	Serum Amyloid A
SCD	Stearoyl-CoA Desaturase
SCN	Suprachiasmatic Nucleus
SREBP-1c	Sterol Regulatory Element Binding Protein 1c
STAT5	Signal Transducer and Activator of Transcription 5
T2D	Type 2 Diabetes
TNFα	Tumor Necrosis Factor α
UCP1	Uncoupling Protein 1
WAT	White Adipose Tissue
WT	Wild Type

CHAPTER 1

INTRODUCTION

Insulin resistance is a key adaptation in ruminants to accommodate the glucose needs of the placenta and mammary gland (Bell and Bauman, 1997). Glucose uptake in these tissues occurs independently of plasma insulin and therefore insulin resistance improves their access to the pool of available glucose (Bell and Bauman, 1997). Although a reduction in insulin action is a normal homeorhetic response in pregnant and lactating ruminants, excessive insulin resistance increases the risk for infectious diseases (Leblanc, 2010). Adiposity is detrimental to insulin action and overall metabolic health (McCann et al., 1986; Bergman et al., 1989; Bonadonna et al., 1990; Kahn and Flier, 2000; Chen et al., 2012). Furthermore, the dynamics of internal (sum of omental, mesenteric, perirenal, and retroperitoneal) and external (fat not included in internal depot) fat depots differ. Previous work in sheep and cows revealed preferential fat accretion in dissectible internal versus external depots (Chay-Canul et al., 2011; Drackley et al., 2014). This was also suggested by Ruda et al. who used ultrasonography to infer greater fat mobilization from internal than external adipose depots in early lactating cows (Ruda et al., 2019). Moreover, internal fat exhibits additional differences such as increased lipolysis relative to subcutaneous fat (Ibrahim, 2010).

Various studies in ewes show that obesity reduces insulin action (Bergman et al., 1989; Wallace et al., 2005; Ford et al., 2009; Tuersunjiang et al., 2013). In a recent study, total body fatness quantified by DEXA scanning was negatively correlated with insulin action in pregnant ewes (Tuersunjiang et al., 2013). However, no studies have attempted to assess the relative contribution of internal and external depots to insulin resistance in ruminants. Computed tomography (CT) scanning has been widely used in humans (Nemoto et al., 2014; Sato et al., 2017), dogs (Nagao et al., 2019), and mice (Herrera et al., 2018; Ma et al., 2019) to not only quantify total fatness, but also accurately assess relative importance of different depots. More

recently, this method was applied to sheep and proved to be repeatable and accurate in quantifying internal fat volume (Rosenblatt et al., 2017). The first experimental chapter of this thesis reports work evaluating the relationship between internal and external fat depots and insulin action in pregnant and lactating ewes using computed tomography (Chapter 3).

A number of pharmacological approaches have been developed to improve insulin action. One of the most recent insulin-sensitizing agents studied in insulin-resistant states is the novel hormone, fibroblast growth factor 21 (FGF21). Functionally, exogenous FGF21 administration lowers plasma insulin and glucose and improves glucose clearance in well-fed, obese primates and rodents (Kharitonenkov et al., 2005; Véniant et al., 2012; Adams et al., 2013). These effects are commonly coupled with an increase in plasma adiponectin, an insulin-sensitizing adipokine (Holland et al., 2013). Recent work in early lactating dairy cattle, however, showed that FGF21 had no effect on basal plasma insulin or glucose, nor did it improve glucose clearance during glucose tolerance tests (Krumm et al., 2019). However, early lactating dairy cattle are in a state of negative energy balance, whereas previous work in rodents and monkeys was performed in conditions of positive energy balance (Kharitonenkov et al., 2005; Kharitonenkov et al., 2007; Véniant et al., 2012). It is therefore unclear whether FGF21 can act as an insulin-sensitizer in well-fed ruminants. This question will be addressed in the second experimental chapter (Chapter 4).

REFERENCES

Adams, A. C., C. A. Halstead, B. C. Hansen, A. R. Irizarry, J. A. Martin, S. R. Myers, V. L. Reynolds, H. W. Smith, V. J. Wroblewski, and A. Kharitonenkov. 2013. LY2405319, an Engineered FGF21 Variant, Improves the Metabolic Status of Diabetic Monkeys. PloS One 8(6):e65763. doi: 10.1371/journal.pone.0065763 PMID - 23823755

Bell, A. W., and D. E. Bauman. 1997. Adaptations of glucose metabolism during pregnancy and lactation. Journal of Mammary Gland Biology and Neoplasia 2(3):265-278.

Bergman, E. N., S. S. Reulein, and R. E. Corlett. 1989. Effects of obesity on insulin sensitivity and responsiveness in sheep. American Journal of Physiology Endocrinology and Metabolism 257(5):E772-E781. doi: 10.1152/ajpendo.1989.257.5.e772 PMID - 2688439

Bonadonna, R. C., G. Leif, N. Kraemer, E. Ferrannini, S. D. Prato, and R. A. DeFronzo. 1990. Obesity and insulin resistance in humans: A dose-response study. Metabolism 39(5):452-459. doi: https://doi.org/10.1016/0026-0495(90)90002-T

Chay-Canul, A. J., A. J. Ayala-Burgos, J. C. Ku-Vera, J. G. Magaña-Monforte, and L. O. Tedeschi. 2011. The effects of metabolizable energy intake on body fat depots of adult Pelibuey ewes fed roughage diets under tropical conditions. Tropical Animal Health and Production 43(5):929-936. doi: 10.1007/s11250-011-9785-5 PMID - 21240653

Chen, W., J. L. Wilson, M. Khaksari, M. A. Cowley, and P. J. Enriori. 2012. Abdominal fat analyzed by DEXA scan reflects visceral body fat and improves the phenotype description and the assessment of metabolic risk in mice. American Journal of Physiology Endocrinology and Metabolism 303(5):E635-643. doi: 10.1152/ajpendo.00078.2012 PMID - 22761161

Drackley, J. K., R. L. Wallace, D. Graugnard, J. Vasquez, B. F. Richards, and J. J. Loor. 2014. Visceral adipose tissue mass in nonlactating dairy cows fed diets differing in energy density. Journal of Dairy Science 97(6):3420-3430. doi: 10.3168/jds.2014-8014 PMID - 24704224

Ford, S. P., L. Zhang, M. Zhu, M. M. Miller, D. T. Smith, B. W. Hess, G. E. Moss, P. W. Nathanielsz, and M. J. Nijland. 2009. Maternal obesity accelerates fetal pancreatic β-cell but not α-cell development in sheep: prenatal consequences. American Journal of Physiology Regulatory, Integrative and Comparative Physiology 297(3):R835-R843. doi: 10.1152/ajpregu.00072.2009 PMID - 19605766

Herrera, S., K. Vincent, A. Poole, G. Olson, I. Patrikeev, J. Saada, P. Gamble, M. Motamedi, G. Saade, A. Stuebe, and E. B. Prewit. 2018. Long-Term Effect of Lactation on Maternal Cardiovascular Function and Adiposity in a Murine Model. American Journal of Perinatology 36(05):490-497. doi: 10.1055/s-0038-1669443 PMID - 30193385

Holland, W. L., A. C. Adams, J. T. Brozinick, H. H. Bui, Y. Miyauchi, C. M. Kusminski, S. M. Bauer, M. Wade, E. Singhal, C. C. Cheng, K. Volk, M.-S. S. Kuo, R. Gordillo, A. Kharitonenkov, and P. E. Scherer. 2013. An FGF21-adiponectin-ceramide axis controls

energy expenditure and insulin action in mice. Cell Metabolism 17(5):790-797. doi: 10.1016/j.cmet.2013.03.019 PMID - 23663742

Ibrahim, M. M. 2010. Subcutaneous and visceral adipose tissue: structural and functional differences. Obesity Reviews 11(1):11-18. doi: 10.1111/j.1467-789x.2009.00623.x PMID - 19656312

Kahn, B. B., and J. S. Flier. 2000. Obesity and insulin resistance. Journal of Clinical Investigation 106(4):473-481. doi: 10.1172/jci10842

Kharitonenkov, A., T. L. Shiyanova, A. Koester, A. M. Ford, R. Micanovic, E. J. Galbreath, G. E. Sandusky, L. J. Hammond, J. S. Moyers, R. A. Owens, J. Gromada, J. T. Brozinick, E. D. Hawkins, V. J. Wroblewski, D.-S. S. Li, F. Mehrbod, S. R. Jaskunas, and A. B. Shanafelt. 2005. FGF-21 as a novel metabolic regulator. Journal of Clinical Investigation 115(6):1627-1635. doi: 10.1172/JCI23606 PMID - 15902306

Kharitonenkov, A., V. J. Wroblewski, A. Koester, Y.-F. F. Chen, C. K. Clutinger, X. T. Tigno, B. C. Hansen, A. B. Shanafelt, and G. J. Etgen. 2007. The metabolic state of diabetic monkeys is regulated by fibroblast growth factor-21. Endocrinology 148(2):774-781. doi: 10.1210/en.2006-1168 PMID - 17068132

Krumm, C. S., S. L. Giesy, L. S. Caixeta, J. W. Perfield, H. Sauerwein, B. L. Moore, and Y. R. Boisclair. 2019. Fibroblast growth factor-21 (FGF21) administration to early-lactating dairy cows. I. Effects on signaling and indices of insulin action. Journal of Dairy Science doi: 10.3168/jds.2019-16695 PMID - 31548053

Leblanc, S. 2010. Monitoring Metabolic Health of Dairy Cattle in the Transition Period. Journal of Reproduction and Development 56(S):S29-S35. doi: 10.1262/jrd.1056S29 PMID - 20629214

Ma, M.-m., C.-c. Jin, X.-l. Huang, L. Sun, H. Zhou, X.-j. Wen, X.-q. Huang, J.-y. Du, H.-s. Sun, Z.-x. Ren, J. Liu, Y.-y. Guan, X.-m. Zhao, and G.-l. Wang. 2019. Clcn3 deficiency ameliorates high-fat diet-induced obesity and adipose tissue macrophage inflammation in mice. Acta Pharmacologica Sinica 40(12):1532-1543. doi: 10.1038/s41401-019-0229-5 PMID - 31165783

McCann, J. P., M. B. Ullmann, M. R. Temple, T. J. Reimers, and E. N. Bergman. 1986. Insulin and glucose responses to glucose injection in fed and fasted obese and lean sheep. Journal of Nutrition 116(7):1287-1297. doi: 10.1093/jn/116.7.1287 PMID - 3528428

Nagao, I., K. Ohno, T. Nagahara, N. Yokoyama, T. Nakagawa, R. Fujiwara, K. Yamamoto, Y. Goto-Koshino, H. Tomiyasu, and H. Tsujimoto. 2019. Evaluation of visceral fat mass in dogs by computed tomography. Journal of Veterinary Medical Science 81(11):1552-1557. doi: 10.1292/jvms.19-0254 PMID - 31554745

Nemoto, M., T. Yeernuer, Y. Masutani, Y. Nomura, S. Hanaoka, S. Miki, T. Yoshikawa, N. Hayashi, and K. Ohtomo. 2014. Development of automatic visceral fat volume

calculation software for CT volume data. Journal of Obesity 2014:495084. doi: 10.1155/2014/495084

Rosenblatt, A. J., P. V. Scrivani, Y. R. Boisclair, A. P. Reeves, J. M. Ramos-Nieves, Y. Xie, and H. N. Erb. 2017. Evaluation of a semi-automated computer algorithm for measuring total fat and visceral fat content in lambs undergoing in vivo whole body computed tomography. Veterinary Journal 228:46-52. doi: 10.1016/j.tvjl.2017.10.012 PMID - 29153108

Ruda, L., C. Raschka, K. Huber, R. Tienken, U. Meyer, S. Dänicke, and J. Rehage. 2019. Gain and loss of subcutaneous and abdominal fat depot mass from late pregnancy to 100 days in milk in German Holsteins. Journal of Dairy Research 86(3):296-302. doi: 10.1017/s0022029919000542 PMID - 31409432

Sato, F., N. Maeda, T. Yamada, H. Namazui, S. Fukuda, T. Natsukawa, H. Nagao, J. Murai, S. Masuda, Y. Tanaka, Y. Obata, Y. Fujishima, H. Nishizawa, T. Funahashi, and I. Shimomura. 2017. Association of Epicardial, Visceral, and Subcutaneous Fat With Cardiometabolic Diseases. Circulation Journal 82(2):CJ-17-0820. doi: 10.1253/circj.cj-17-0820 PMID - 28954947

Tuersunjiang, N., J. F. Odhiambo, N. M. Long, D. R. Shasa, P. W. Nathanielsz, and S. P. Ford. 2013. Diet reduction to requirements in obese/overfed ewes from early gestation prevents glucose/insulin dysregulation and returns fetal adiposity and organ development to control levels. American Journal of Physiology Endocrinology and Metabolism 305(7):E868-878. doi: 10.1152/ajpendo.00117.2013 PMID - 23921140

Véniant, M. M., R. Komorowski, P. Chen, S. Stanislaus, K. Winters, T. Hager, L. Zhou, R. Wada, R. Hecht, and J. Xu. 2012. Long-Acting FGF21 Has Enhanced Efficacy in Diet-Induced Obese Mice and in Obese Rhesus Monkeys. Endocrinology 153(9):4192-4203. doi: 10.1210/en.2012-1211 PMID - 22798348

Wallace, J. M., J. S. Milne, and R. P. Aitken. 2005. The effect of overnourishing singleton-bearing adult ewes on nutrient partitioning to the gravid uterus. British Journal of Nutrition 94(4):533-539.

CHAPTER 2

LITERATURE REVIEW

Introduction:

The main focus of this thesis is relating to sheep metabolism. However, in some areas, more extensive work was completed in other species (i.e. humans, rodents, and cows). Therefore, additional details from these other species will be utilized as necessary to help address some of the areas that are lacking or to provide further support.

Part I: Maternal metabolism during pregnancy and lactation in ewes:

In the sheep, gestation length is 146 days and lactation typically lasts for about 5 months (Forbes, 1967; Lérias et al., 2014). Classically, we refer to the period of time surrounding parturition as the transition period (Drackley, 1999). Glucose provides a good example of the metabolic challenge faced by sheep during pregnancy and lactation. Total glucose demands increase by more than 2-fold in ewes carrying twins in late pregnancy compared with nonpregnant ewes (Bell and Bauman, 1997), and during lactation, the demands of the mammary gland increases the total glucose turnover rate to about twice that of twin pregnancy (Bergman and Hogue, 1967). At the same time, sheep have insufficient appetite around parturition to cover their nutritional requirements, leading to a state of negative energy balance (NEB) (Forbes, 1970). As a consequence, plasma fatty acids rise during the transition period leading to an increase in plasma β-hydroxybutyric acid (BHBA), the main ketone in ruminants (Hammon et al., 2009; Zamuner et al., 2020). There is still some debate about the drivers of inadequate feed intake during this period, but they could include a limitation of physical space imposed by the uterus and increased estrogen, but there are likely additional contributing factors (Hadjipieris and Holmes, 1966; Forbes, 1977; Grummer et al., 2004). In the following section, I will focus on glucose and insulin action as they represent the most obvious illustration of the reorganization

needed to cover the nutrient needs of the placenta, mammary gland, and other maternal tissues (Block et al., 2001).

Glucose Metabolism in the Placenta

The placenta is a transient organ that experiences rapid growth starting around day 40 of pregnancy and ending around day 80 in the sheep (Ehrhardt and Bell, 1995). A major function of the placenta is to transport nutrients from the maternal blood supply to the fetus to support growth. Glucose and fatty acids are transported by facilitated diffusion, whereas amino acid uptake involves active transport (Hay Jr., 1994). The major glucose transporters in the sheep placenta are glucose transporter (GLUT)-1 and GLUT3. Their protein abundance in the placenta increases 2-3 fold from mid- to late pregnancy (Ehrhardt and Bell, 1997). These transporters function in an insulin-independent manner as opposed to GLUT4; GLUT4 is virtually absent in the placenta (Ehrhardt and Bell, 1997; Wooding et al., 2004). This ability of the placenta to uptake glucose independently of insulin is an important mechanism to secure a large fraction of maternal glucose for the fetus. Glucose uptake by the uterus is 26 mg/min in mid-pregnancy and increases to 47 mg/min in late pregnancy in ewes pregnant with singletons (Oddy et al., 1985). Finally, evaluation of placental glucose transport capacity by use of a glucose clamp in the maternal femoral vein reveals a five-fold increase in this capacity from mid- to late gestation (Molina et al., 1991).

Two hormones produced in the placenta that are thought to aid in the repartitioning of maternal nutrients include placental growth hormone (PGH) and placental lactogen (PL). PGH is expressed in the trophectoderm and syncytial cells of the placenta between days 27 and 75 in pregnant ewes. The function of PGH is not known, although its expression pattern corresponds to the period of greatest placental growth in sheep (Gootwine, 2004). PL is produced in

binucleate cells in the trophectoderm starting around day 16 of pregnancy and peaks between 120 and 140 days of pregnancy (Gootwine, 2004). It is suggested to regulate fetal growth and is correlated with both fetal number and placental mass in late pregnancy; PL may also stimulate maternal intake (Min et al., 1996; Gootwine, 2004). Finally, there is evidence PL increases insulin-like growth factor 1 (IGF-1) in fetal sheep, further indicating its role in fetal growth (Anthony et al., 1995). The exact role and mechanism of both PGH and PL remain poorly understood, however.

Glucose Metabolism in the Mammary Gland

The mammary gland is a unique organ which goes through periods of proliferation, secretion, and involution. The majority of mammary gland growth occurs during pregnancy in sheep and corresponds to the formation of lobulo-alveolar structures (Anderson, 1975; Smith et al., 1989). The primary hormones driving this proliferation are prolactin, PL, estrogen, and progesterone (Schams et al., 1984; Lérias et al., 2014). The secretory activities of the mammary gland are initiated by the drop in plasma progesterone near parturition (Forsyth, 1986). Ewes typically reach peak lactation by about 3-4 weeks, followed by a gradual production decline (Lérias et al., 2014). Once the lambs are weaned, intra-alveolar pressure increases and triggers involution of the secretory structures via apoptosis (Tatarczuch et al., 1997).

During lactation, the mammary gland requires a large supply of nutrients for milk synthesis. For example, mammary glucose uptake in lactating goats accounts for 60-85% of the available maternal supply; 79-95% of this uptake is used for the synthesis of lactose, the major determinant of milk volume, and for the synthesis of glycerol (Annison and Linzell, 1964). Similar to the placenta, the mammary gland relies predominantly on the insulin-independent glucose transporter GLUT1 for glucose transport (Zhao and Keating, 2007). In addition to

GLUT1, GLUT8 is also not dependent on insulin, highly expressed, and regulated in relation to physiological stage. In late pregnancy, GLUT8 mRNA is upregulated by more than 10-fold and in early lactation it increases again by almost 4-fold relative to late pregnancy. Overall, there is comparable expression between GLUT1 and GLUT8, but GLUT1 is the predominant functional glucose transporter (Zhao et al., 2004; Zhao, 2014). Some other glucose transporters expressed in the bovine mammary gland are GLUT12, SGLT1, and SGLT2 (Miller et al., 2005).

A peculiarity of ruminant species is that they do not utilize glucose for *de novo* fatty acid synthesis, and instead rely on acetate as the carbon source for this process (Bauman et al., 1973; Moore and Christie, 1979). While glucose cannot serve as the carbon source for *de novo* synthesis, it is used for the generation of ~40% of the NADPH used in fatty acid synthesis and for the generation of glycerol for triglyceride synthesis. Although *in vitro* studies with sheep mammary slices demonstrate that acetate alone can be utilized for fatty acid synthesis when glucose is absent or lacking in sheep, the presence of glucose increases the efficiency of this process (Balmain et al., 1952). This is one potential mechanism to aid in sparing glucose during a period with such high glucose demands (Balmain et al., 1952; Bauman et al., 1973; Chaiyabutr et al., 1980).

Glucose Metabolism in Other Peripheral Tissues

The main peripheral tissues aside from the placenta and mammary gland, relevant to glucose metabolism are liver, adipose tissue, and skeletal muscle. Ruminants differ from nonruminants in that they do not obtain much glucose from their diet. In fact, gluconeogenesis provides up to 90-95% of the total glucose supply (Young, 1977; Aschenbach et al., 2010). Studies in sheep estimate that the liver and kidney respectively account for 85% and 10-15% of gluconeogenesis (Bergman et al., 1974; Aschenbach et al., 2010). The top three glucose

precursors in ruminants are propionate, lactate, and alanine, in that order (Aschenbach et al., 2010). In sheep, the glucose turnover rate increases from 4.6 g/hr to 7.5 g/hr between the nonpregnant and late pregnant state and finally to 13.3 g/hr in early lactation; these changes reflect increased hepatic gluconeogenesis (Bergman et al., 1974). An *in vitro* experiment demonstrated that the increase in gluconeogenic activity in the ovine liver during lactation was due to an increased ability of primary hepatocytes to utilize pyruvate derived from lactate as a precursor. In fact, gluconeogenesis from lactate is increased by 2-fold in hepatocytes from lactating animals (Faulkner and Pollock, 1991). Furthermore, pyruvate carboxylase, the gluconeogenic enzyme catalyzing the carboxylation of pyruvate to form oxaloacetate, is increased more than 6-fold between the nonpregnant and late pregnant state and remains elevated through lactation (Smith and Walsh, 1982).

While liver is the main tissue for glucose production, adipose and muscle are the main glucose-utilizing tissues besides the placenta and the mammary gland. Looking at glucose utilization, there are two main things to consider – glucose transport and insulin action. Glucose can be transported into these tissues by either GLUT1 under basal conditions or GLUT4 under insulin stimulation (Duhlmeier et al., 2005). Changes in GLUT1 and GLUT4 abundance in adipose tissue and muscle can help explain the changes we see in glucose metabolism during pregnancy and lactation. GLUT1 expression in bovine adipose tissue is decreased in early lactation (EL) relative to nonlactating or late lactating animals (Komatsu et al., 2005; Zhao and Keating, 2007). GLUT4 protein in adipose tissue was decreased during EL compared with late pregnancy (LP) in Holstein dairy cows (Ji et al., 2012; Jaakson et al., 2018). At the mRNA level, there were no changes in GLUT4 mRNA abundance in neither adipose tissue nor muscle between nonlactating and early lactating cattle. This suggests that GLUT4 may be under post-

transcriptional regulation in adipose tissue across the transition period (Komatsu et al., 2005). GLUT expression has not been studied extensively in ruminant muscle during pregnancy and lactation. One study showed that lactating goats also have reduced GLUT4 protein expression in skeletal muscle compared with nonlactating goats (Balage et al., 1997).

In addition to changes in glucose transporters, insulin action also fluctuates across the transition period. Ewes become more sensitive to insulin during early pregnancy compared to their nonpregnant state. This change favors lipogenesis and storage of macronutrients. This is followed in LP and EL by a substantial reduction in adipose tissue response to insulin (Guesnet et al., 1991). In late pregnancy, decreased insulin responsiveness is associated with a decrease in the number of insulin receptors in adipocytes (Vernon et al., 1981). In addition, insulin-stimulated glucose utilization in the hind limb (skeletal muscle) is reduced in sheep during lactation. However, the number of insulin receptors across the transition period in sheep remains unchanged in muscle (Vernon et al., 1990). The insulin receptor itself is not defective, suggesting that the defect in insulin signaling during lactation is downstream of the receptor (Wilson et al., 1996). This characteristic fluctuation in insulin action across pregnancy and lactation will be explored in greater depth later in this review.

Hormonal Changes in Plasma

A series of homeorhetic signals favor use of maternal glucose by the placenta or mammary gland at the expense of other tissues. The signals are thought to be hormones such as insulin, adiponectin, and glucagon. Across the periparturient period, plasma adiponectin reaches a nadir at parturition in dairy cattle (Giesy et al., 2012). The driver behind this decrease is still unknown, although it must be post-transcriptional because adiponectin mRNA remains unchanged in adipose tissue across this time (Krumm et al., 2017; Krumm et al., 2018). In

ruminants, many efforts have been put into characterizing insulin and glucagon profiles and action during the periparturient period: plasma insulin decreases across the transition period, whereas plasma glucagon increases.

The somatotropic axis also influences homeorhetic adaptations across this time. There is an uncoupling of the growth hormone (GH) axis across the transition period, which is characterized by an increase in circulating GH, while circulating IGF-1 is decreased (Kim, 2014). This uncoupling is due to a decrease in GH receptor expression in the liver (Kim et al., 2004). It is not clear what is driving the decreased expression, although it is not due to the state of NEB during EL (Rhoads et al., 2007).

Insulin action and resistance during pregnancy and lactation

Insulin resistance (IR) is the inability of a tissue (or whole animal) to respond to insulin. Given the importance of insulin in regulating glucose utilization, IR results in reduced glucose disposal during dynamic tests such as GTT or ITT (Kahn, 1978). IR is the result of some defect in signal transmission, whether that is at the level of the receptor or at some point downstream (Petersen and Shulman, 2018).

In terms of structure, the insulin receptor is composed of 2 α and 2 β subunits linked via a disulfide bond to form a heterotetramer (Hubbard, 2013). Insulin binding elicits a conformational change, causing autophosphorylation of the receptor followed by the recruitment of various scaffold proteins. These scaffold proteins then allow engagement of different signaling cascades (Lee and Pilch, 1994; Menting et al., 2013). In the case of glucose metabolism, the main scaffold proteins of interest are insulin receptor substrate 1 or 2 (IRS1/2). Both IRS1 and IRS2 are important in the insulin signaling pathway, but IRS1 is the most important isoform in muscle and adipose, the main insulin-stimulated glucose consuming tissues

(Petersen and Shulman, 2018). Following recruitment, IRS1 then recruits phosphatidylinositol-3 kinase (PI3K), which then catalyzes the formation of phosphatidylinositol-3,4,5-trisphosphate (PIP3) from phosphatidylinositol-4,5-bisphosphate (PIP2). PIP3 then binds protein kinase B (AKT), allowing AKT activation via sequential phosphorylation events by phosphoinositide-dependent kinase 1 (PDK1) and mechanistic target of rapamycin complex 2 (mTORC2). It is unclear exactly how this pathway leads to translocation of GLUT4 to the plasma membrane, but AKT as well as additional PI3K targets are involved (Petersen and Shulman, 2018). Of note, insulin-stimulated glucose uptake in ruminants is lower compared with that in nonruminants due in part to a lower number of insulin receptors and reduced translocation of GLUT4 by insulin (De Koster and Opsomer, 2013).

IR during pregnancy and lactation could relate to reduced insulin receptor abundance or activity or reduced signaling. Regarding receptor abundance, the number of insulin receptors and the percentage of insulin binding increases in the liver across pregnancy in sheep (Gill and Hart, 1982). Conversely, insulin receptor expression is decreased in both retroperitoneal and subcutaneous adipose tissue depots of Holstein dairy cattle (Kenéz et al., 2019). Factors occurring during the transition period in ruminants and capable of causing IR include inflammation, increased diacylglycerol (DAG), and increased ceramide. Across the periparturient period, acute phase proteins such as serum amyloid A (SAA) and haptoglobin are elevated in both sheep and cattle, indicating a state of heightened inflammation (Ceciliani et al., 2012; Bradford et al., 2015; Greguła-Kania et al., 2020). Tumor necrosis factor α (TNF-α) is a pro-inflammatory cytokine that is upregulated across the transition period in adipose tissue in cattle (Sadri et al., 2010). TNFα impairs insulin signaling through different mechanisms, including inhibiting tyrosine phosphorylation of IRS1 as well as activating proteins involved in

signal termination, such as protein tyrosine phosphatase 1B (PTP1B) (Borst, 2004; Ito et al., 2012). On the other hand, another pro-inflammatory marker, interleukin 6 (IL-6), induces insulin resistance through impaired phosphorylation of both the insulin receptor and IRS1 (Rehman et al., 2017).

The excessive lipid mobilization of early lactation also causes the generation of two known negative regulators of insulin action, namely DAG and ceramide. Their generation and action are particularly well-described in the liver. Mechanistically, DAG and ceramides affect insulin signaling similarly, but there are some differences. DAG activates protein kinase Cε (PKCε), which then triggers serine phosphorylation of IRS1, thereby disrupting tyrosine phosphorylation and blunting the rest of the insulin response (Petersen and Shulman, 2018; Vázquez-Jiménez et al., 2019). Ceramides target a second PKC isoform known as PKCζ, which targets AKT phosphorylation. In addition, ceramides activate protein phosphatase 2 (PP2A) which dephosphorylates the threonine residue on AKT which is necessary for activation (Vázquez-Jiménez et al., 2019). While some of these mechanisms have yet to be fully elucidated in ruminants, there is evidence that periparturient dairy cattle exhibit an increase in ceramides, and that ceramide treatment of primary bovine adipocytes causes a decrease in AKT phosphorylation (Rico et al., 2017; Rico et al., 2018).

Effect of over- or underfeeding during transition period

Ruminants are susceptible to a number of diseases during the transition from LP to EL, including ketosis, fatty liver, clinical hypocalcemia, retained placenta, metritis, and displaced abomasum (Mulligan and Doherty, 2008). In the case of sheep, the most common metabolic disease in late pregnancy is known as pregnancy toxemia. Pregnancy toxemia is clinically characterized by circulating BHBA levels greater than 3.0 mmol/L. This condition has a very

fast progression; if left untreated, the animal will become recumbent followed by death within 3-6 days (Andrews, 1997). Major risk factors for this disease include overnutrition, undernutrition, obesity, and carrying multiple fetuses (Fthenakis et al., 2012).

The metabolic adaptations of pregnancy favoring partitioning of glucose to the fetus are likely involved. For example, ewes that were moderately undernourished for 2 weeks in late pregnancy exhibited a 50% increase in glucose transport capacity across the placenta. This allowed the fetus to receive the same amount of glucose, at the expense of glucose availability to the ewe (Bell and Ehrhardt, 2002). This could be due in part to a further reduction in insulin action in peripheral tissues; ewes that were fed to meet 60% of requirements in late pregnancy exhibited a ~50% reduction of GLUT4 protein in perirenal adipose and a ~25% reduction of GLUT4 protein in muscle (Bell and Bauman, 1997). However, placental glucose transport will also drop when maternal feed intake covers only 30-40% of maternal requirements (Leury et al., 1990).

On the other hand, overfeeding during pregnancy and lactation can have just as severe metabolic consequences. We know from human (Amatruda et al., 1985) and rodent (Nagy and Einwallner, 2018) data that overfeeding and obesity lead to insulin resistance. Recent data suggest that this also occurs in ruminants. For example, overconditioned Holstein cows [body condition score (BCS) $\geq$ 3.75] had reduced GLUT4 protein expression in adipose tissue compared with their lean counterparts at day -21 relative to parturition (Jaakson et al., 2018). Further, overconditioned cows displayed an overall reduction in insulin sensitivity relative to the lean animals at day -21 as determined by the insulin response during a GTT (Jaakson et al., 2018). This was further supported in another study in dairy cows which found a negative association between insulin action and body fat accumulation (De Koster et al., 2015). In

addition, serum adiponectin is negatively correlated with BCS and positively correlated with insulin responsiveness in cattle (De Koster et al., 2017). In terms of the effects of overfeeding on insulin action, there have been a handful of studies evaluating this in sheep. Ford and colleagues published a series of papers in which they fed ewes at either 100% or 150% of their predicted requirements starting 2 months prior to breeding, and maintained throughout gestation. In ewes carrying either singletons (Ford et al., 2009) or twins (Tuersunjiang et al., 2013), the insulin response curve during a GTT was exaggerated in obese ewes compared with their lean counterparts, suggesting a reduction in insulin sensitivity. Furthermore, ewes carrying twins were evaluated again in late pregnancy, and again obese sheep displayed decreased insulin sensitivity as well as reduced glucose clearance. In addition to these responses, the basal glucose and insulin concentrations were also elevated in obese animals at both mid- and late pregnancy (Tuersunjiang et al., 2013).

Overall, IR development during the transition period is an important and necessary homeorhetic adaptation to support fetal growth and milk production (De Koster and Opsomer, 2013). However, excessive IR increases the risk of various diseases and loss of productivity (Leblanc, 2010). In addition, increased adiposity is one of the most common causes for excess IR during this transition (Rukkwamsuk et al., 1999; Pascottini et al., 2020).

Dynamics of visceral adipose tissue and insulin action

While overall fatness is positively associated with the development of IR, there is evidence of varying contribution by different fat depots. One of the first studies identifying these differences reported that the subcutaneous fat depot was less responsive to insulin than the retroperitoneal or epididymal depots in rats (Fried et al., 1982). Since then, visceral depots have been consistently identified as more dynamic and responsive than subcutaneous depots. There is

limited work in ruminants in this area, but they also suggest that the visceral fat depots are more responsive to changes in nutrition or energy balance. A first study reported differences between subcutaneous and visceral depots in nonpregnant, nonlactating Holstein cows receiving either a high or low energy diet. At slaughter, cows had similar BCS, suggesting a similar amount of subcutaneous fat. In contrast, the weight of visceral fat was 2-fold higher in cows receiving the high energy diet than cows receiving the low energy diet (Drackley et al., 2014). Ultrasonography in German Holstein dairy cattle also revealed that there was increased mobilization of the abdominal adipose depot compared with the subcutaneous depot during the very early part of lactation (Ruda et al., 2019). Furthermore, periparturient dairy cattle have a plasma fatty acid profile that is more similar to the fatty acid composition of omental fat than that of subcutaneous fat (Hostens et al., 2012).

Not only are internal fat depots more dynamic, but they are also more likely to contribute to the development of insulin resistance due to their anatomical location (Lafontan and Girard, 2008; Ibrahim, 2010). This was demonstrated in rats where pregnancy was accompanied by an increase in visceral fat accumulation and a decrease in hepatic insulin sensitivity; hepatic insulin sensitivity was completely restored by surgical removal of visceral fat (Einstein et al., 2008). The effects of fat depot distribution was evaluated in mice suffering from diet-induced obesity. Negative correlations were found between indices of insulin responsiveness and visceral fat mass, but no such relation was seen with subcutaneous fat (Chen et al., 2012).

Summary

In the overfeeding studies of Ford et al., insulin resistance was correlated with fatness by the end of pregnancy as determined by DEXA scanning (>40% vs <20% at 135 days of gestation), but there were no observations pertaining to the location of the fat depots

(Tuersunjiang et al., 2013). To date, there have not been any studies examining the longitudinal effects of pregnancy on the dynamics of the internal adipose depots in ruminants utilizing a method with the level of precision that can be obtained via CT scanning. Furthermore, the dynamics of adipose depots during times of accretion and mobilization remain poorly understood in ruminants. We therefore sought to investigate the effects of pregnancy as well as overfeeding on adipose depots and how this might relate to insulin action in sheep. We hypothesized that internal fat (sum of omental, mesenteric, perirenal, and retroperitoneal) would be the most dynamic. In addition, we hypothesized internal fat would be more detrimental for insulin action relative to external (remaining fat not included in internal fat) fat.

Part II: Fibroblast Growth Factor-21 (FGF21):

Discovery and Structure

Fibroblast growth factor-21 is a member of the fibroblast growth factor (FGF) superfamily (Ornitz and Itoh, 2001; Itoh and Ornitz, 2004). There are 22 members within the FGF superfamily, grouped into 7 subfamilies on the basis of sequence similarity and biochemical and developmental properties (Ornitz and Itoh, 2001; Itoh and Ornitz, 2004). FGF21 falls within the FGF19 subfamily, along with FGF19 and FGF23 (Itoh and Ornitz, 2004). FGF19 is involved in bile acid metabolism, and FGF23 is important in maintaining phosphate and vitamin D homeostasis (Fukumoto, 2008).

FGF21 was discovered by homology-based PCR in mouse embryos in 2000 by Nishimura et al. and was found to be 210 amino acids long (Nishimura et al., 2000). Investigation into adult mouse tissues revealed that FGF21 was preferentially expressed in the liver. Other tissues investigated include brain, heart, kidney, spleen, lung, stomach, small

intestine, and thymus; only the thymus showed some FGF21 expression, although it was very minimal. Because FGFs are predominantly factors that act locally, FGF21 was originally predicted to exert some function within the liver (Nishimura et al., 2000). However, FGF21 belongs to the FGF19 subfamily, which is the only branch within the superfamily to contain endocrine-acting FGFs (Itoh and Ornitz, 2010). The endocrine-acting FGFs lack a heparin-binding domain (HBD), which enables them to leave the tissue of production. All other FGFs remain localized at the site of production as a consequence of HBD interacting with heparin sulfate proteoglycans in the extra-cellular matrix (Ornitz, 2000).

Receptors and Signaling

The HBD domain facilitates FGF binding to FGF receptors (FGFRs) (Ornitz, 2000; Mohammadi et al., 2005). In absence of the HBD domain in FGF21, this facilitating role is fulfilled by the co-receptor β-klotho (Kharitonenkov et al., 2008; Suzuki et al., 2008). Structurally, β-klotho consists of an extracellular domain (ECD), a single-pass transmembrane region and a short cytoplasmic tail (Shi et al., 2018). The c-terminus of FGF21 interacts with two tandem repeats in β-klotho, called KL1 and KL2, whereas the N-terminus of FGF21 binds and interacts with the FGFR (Micanovic et al., 2009; Yie et al., 2009). Due to a relatively short intracellular domain, β-klotho is unlikely to directly activate intracellular signaling, but is instead involved in stabilizing the interaction of FGF21 with the FGFR moiety; there is also thought of some FGF21 domain interacting with the hydrophobic groove in the immunoglobulin-like domain III of FGFR (Goetz et al., 2012).

FGF receptors are encoded by four different genes: FGFR1, FGFR2, FGFR3, and FGFR4. For FGFR1 to 3, alternative splicing produces either the c or b isoform. β-klotho only binds to the c isoforms of FGFR1-3 and FGFR4 (Goetz et al., 2012; Kilkenny and Rocheleau,

2016). Among these β-klotho interacting FGFRs, FGF21 prefers FGFR1c but can also bind to and activate FGFR2c and 3c (Kharitonenkov et al., 2005; Suzuki et al., 2008). To demonstrate the necessity of β-klotho for FGF21 action, a global β-klotho knockout (KO) mouse model was generated. The global KO mice are completely refractory to typical downstream gene responses by FGF21 treatment and do not exhibit the same improvement in insulin sensitivity as the wild type (WT) mice (Ding et al., 2012).

Components of the FGF receptor system have been characterized extensively in mice. FGFR expression is ubiquitous in the mouse. In contrast, meaningful β-klotho expression is seen only in liver, adipose tissue, pancreas, and brain, with the consequence that FGF21 signaling is limited to these tissues (Kurosu et al., 2007; Tacer et al., 2010; Schoenberg et al., 2011; Cui et al., 2014; Douris et al., 2015). The main target tissue for FGF21 in the mouse is adipose tissue based on combined expression of β-klotho and FGFR1c. Other target tissues include liver, placenta, and pancreas (Cui et al., 2014). The FGF21 system has been characterized to some extent in humans and monkeys as well, showing that it is very similar to the mouse. Using β-klotho expression as an indicator, FGF21 target tissues were identified in primates as liver, adipose tissue, pancreas, and brain (Nygaard et al., 2014; Lee et al., 2018; Hultman et al., 2019).

FGF21 binding is followed by activation of the FGFR receptor tyrosine kinase and phosphorylation of FGF receptor substrate 2 (FRS2) (Fisher et al., 2011). FRS2 then activates the Ras-Raf-ERK pathway; ERK activation is commonly used to demonstrate FGF21 signaling (Dailey et al., 2005; Fisher and Maratos-Flier, 2015; Ornitz and Itoh, 2015). In addition, FRS2 can activate the PI3K kinase, which through a phosphorylation cascade, activates AKT (Mendoza et al., 2011; Ornitz and Itoh, 2015). Aside from FRS2, the FGF receptor is also reported to activate Liver Kinase B1 (LKB1), which activates adenosine monophosphate-

activated protein kinase (AMPK); AMPK improves insulin sensitivity and increases glucose uptake (Steinberg and Kemp, 2009; Chau et al., 2010; Salminen et al., 2017). An alternative mechanism by which FGF21 indirectly activates AMPK is via the adipokine adiponectin (Yamauchi et al., 2002; Salminen et al., 2017). Various studies show FGF21 stimulates adiponectin secretion from adipose in mice and monkeys, and that adiponectin is an insulin sensitizer (Kharitonenkov et al., 2007; Lin et al., 2013).

Metabolic FGF21 Regulation in Rodents and Primates

In both rodents and primates, the sites of significant FGF21 production are liver, pancreas, muscle, and adipose tissue, with liver contributing most to circulating FGF21 (Izumiya et al., 2008; Muise et al., 2008; Dushay et al., 2010; Cui et al., 2014; Nygaard et al., 2014). Accordingly, the information given in this section relates predominantly to liver FGF21 production.

FGF21 is upregulated in response to a few different conditions. These conditions include fasting (Inagaki et al., 2007; Fazeli et al., 2015), exercise (Kim et al., 2013), ketogenic diet (KD) (Badman et al., 2007), protein restriction (Laeger et al., 2014), obesity (Zhang et al., 2008; Fisher et al., 2010), and alcohol consumption (Zhao et al., 2015; Søberg et al., 2018; Lanng et al., 2019). While each of these conditions leads to upregulation in mice and primates, there are some key differences. In WT mice, acute fasting for 6 hrs is enough to significantly increase plasma FGF21, followed by further elevation after 24 hrs of fasting. Conversely, fasting increased plasma FGF21 in humans only after 7-10 days (Fazeli et al., 2015). This has been confirmed in several other studies reporting that fasting up to 72 hrs is not sufficient to increase FGF21 in humans (Christodoulides et al., 2009a; Dushay et al., 2010; Andersen et al., 2011). However, there are some effects observed in humans that stimulates FGF21. Following 1 hr of endurance

exercise, FGF21 reaches a peak in plasma concentration by 1 hr of recovery (Morville et al., 2018). Similarly, mice exercised for 60 min experience an increase in both hepatic and serum FGF21 (Kim et al., 2013).

Ketogenic diets have also been shown to induce FGF21 in mice. Mice fed a KD for 4 weeks exhibited markedly increased hepatic and serum FGF21 compared to chow-fed mice; the increase in hepatic FGF21 was observed after just 3 days of KD intervention (Badman et al., 2007). However, a human study that put participants on a KD for 3 months saw the opposite effect – plasma FGF21 was actually decreased by 42% (Christodoulides et al., 2009b). This decrease in FGF21 after initiation of a KD was again observed by another group, further demonstrating the differences between mice and humans (Rosenbaum et al., 2019). Protein is another factor impacting FGF21 production. FGF21 was increased after just 4 days of low protein diet in mice and 28 days in humans (Laeger et al., 2014).

Finally, obesity also increases both hepatic and plasma FGF21 in monkeys (Nygaard et al., 2014). Similarly, overweight mice have 20-fold higher FGF21 mRNA expression in liver and more than 3-fold higher serum FGF21 compared to their lean counterparts (Fisher et al., 2010). Finally, mice fed a liquid-based diet containing 5% alcohol for 12 days showed a 4-fold increase in plasma FGF21 relative to pairfed mice. Hepatic FGF21 mRNA was also increased both *in vivo* in the same mice and *in vitro* in primary mouse hepatocytes following incubation with alcohol (Zhao et al., 2015). Similar to mice, when people consumed an alcoholic drink, plasma FGF21 increased within 2 hrs by almost 3-fold compared to those who consumed a non-alcoholic drink (Song et al., 2018).

Mechanistically, plasma NEFA, glucagon, and the transcription factor, peroxisome proliferator-activated receptor α (PPARα), play a major role in increasing transcription of the

FGF21 gene in liver (Badman et al., 2007; Inagaki et al., 2007; Mai et al., 2010; Habegger et al., 2013; Cyphert et al., 2014). Increased NEFA not only increases PPARα, but also increases cAMP-responsive element-binding protein H (CREBH) (Gentile et al., 2010). CREBH and PPARα form a complex that binds directly to the FGF21 promoter and increases FGF21 in the liver in mice (Inagaki et al., 2007; Kim et al., 2014; Xue et al., 2019). While glucagon also increases PPARα activity (von Meyenn et al., 2013; Cyphert et al., 2014), there is also a translational or post-translational mechanism involving protein kinase A (PKA) and exchange protein activated by cAMP (EPAC) (Cyphert et al., 2014). In the case of protein restriction, a reduction in amino acids activates general control nonderepressible 2 (GCN2), which induces phosphorylation of eukaryotic translation initiation factor 2α (eIF2α). This ultimately results in an upregulation of activating transcription factor 4 (ATF4), which binds to amino acid response element (AARE) sites in the promoter region of the FGF21 gene (Sousa-Coelho et al., 2012; Laeger et al., 2014; Wilson et al., 2015; Maruyama et al., 2016).

FGF21 Actions in Mice

Fibroblast growth factor 21 is involved in several different physiological processes including insulin action (Kharitonenkov et al., 2005; Li et al., 2018), lipid metabolism (Schlein et al., 2016), and white adipose tissue browning (Fisher et al., 2012; Douris et al., 2015). Its positive effects on insulin action have been demonstrated, primarily in diabetic or diet-induced obese (DIO) models. The initial study suggesting FGF21 acting on glucose metabolism was aimed at finding secreted molecules that could affect glucose uptake in mouse 3T3-L1 adipocytes. FGF21 increased GLUT1 receptors in these adipocytes, demonstrating that this can also partly account for the increase in glucose uptake (Kharitonenkov et al., 2005). Upon identifying FGF21 as a potent stimulator of glucose uptake, Kharitonenkov et al. then moved on

to an *in vivo* model – the *ob/ob* mouse (Kharitonenkov et al., 2005). The leptin-deficient *ob/ob* mouse model displays insulin resistance and is widely used to study diabetes (Dubuc, 1976; Belfiore et al., 1984; Zhang et al., 1994). Like the observations in the 3T3-L1 cells, these mice had increased GLUT1 expression in adipose tissue in response to FGF21 administration. FGF21 therapy of *ob/ob* mice resulted in basal plasma glucose and insulin concentrations that were essentially back to a normal, non-diabetic level after 7 days of treatment. Oral glucose tolerance tests (GTT) were also performed in these mice at the end of the 7-day treatment, and both glucose and insulin area under the curve (AUC) were decreased, indicating an improvement in insulin action (Kharitonenkov et al., 2005). In addition, FGF21 administration to DIO mice for 4 weeks led to a greater decline in plasma glucose during an insulin tolerance test (ITT) (Lin et al., 2013). The insulin-sensitizing nature of FGF21 was also shown using a hyperinsulinemic-euglycemic clamp, the "gold standard" method to assess insulin response: FGF21 administration at the dosage of either 0.1 or 10 mg/kg/day increased the glucose infusion rate in DIO mice by approximately 7- and 17-fold over the control animals respectively (Xu et al., 2009a). Another group investigated the acute effects of FGF21 in *ob/ob* mice and found that a single FGF21 dose reduced basal glucose by 40% within 1 hr of injection and that this effect was sustained for 6 hrs (Xu et al., 2009b).

In addition to its effects on insulin action and glucose uptake, FGF21 modulates lipid metabolism. Obese mice treated with FGF21 for 2 weeks lost ~3 g of body weight, mostly through loss of fat. Interestingly, this was not accompanied by any reduction in food intake (Coskun et al., 2008). Furthermore, when obese mice were treated with FGF21, plasma triglycerides and cholesterol were significantly reduced (Kharitonenkov et al., 2005; Xu et al., 2009a). Liver triglycerides are also reduced in these animals (Xu et al., 2009a). Beyond

triglyceride content, FGF21 treatment decreases lipid intermediates as well. Specifically, liver and muscle diacylglycerol (DAG) and circulating and liver ceramides are reduced in FGF21-treated mice; these effects may contribute to the improvement of insulin sensitivity by FGF21 (Holland et al., 2013).

FGF21 improves dyslipidemia through a few different mechanisms, such as increasing total body energy expenditure and hepatic β-oxidation, as well as decreasing hepatic lipogenesis (Xu et al., 2009a; Fisher et al., 2014; Schlein et al., 2016). In transgenic mice overexpressing FGF21, hormone sensitive lipase (HSL) and adipose triglyceride lipase (ATGL) mRNA and protein were significantly increased in white adipose tissue (WAT), suggesting increased lipolysis. The increase in energy expenditure can be explained in part by increased brown adipose tissue (BAT) activity, demonstrated by increased expression of uncoupling protein 1 (UCP1) and iodothyronine deiodinase 2 (Dio2) mRNA in mouse white adipose following FGF21 treatment (Schlein et al., 2016).

There has been a debate over the role of the brain in mediating FGF21 action, but recent work has shown its importance (Owen et al., 2014; Douris et al., 2015). FGF21 can cross the blood brain barrier (Hsuchou et al., 2007), and FGF receptors and β-klotho are expressed in the brain (Tacer et al., 2010; Bookout et al., 2013; Owen et al., 2013). Specifically, while FGF receptors are expressed across the central nervous system (CNS), β-klotho is restricted to the suprachiasmatic nucleus (SCN) (Hultman et al., 2019). Acting through the brain, FGF21 improves hepatic insulin sensitivity (Sarruf et al., 2010), increases energy expenditure, promotes weight loss, and browns white adipose tissue (Owen et al., 2014).

Additional actions of FGF21 in mice include impairing GH action and increasing adiponectin. In transgenic mice overexpressing FGF21, plasma GH is elevated, while IGF-1 is

decreased; moreover, these mice suffer a growth deficit by adulthood. Taken together, this indicates an impairment in GH action (Inagaki et al., 2008). Finally, FGF21 is reported to increase adiponectin under both acute and chronic FGF21 treatment (Lin et al., 2013), but the importance of this effect for the insulin-sensitizing effects of FGF21 is still a debate. In a first study, FGF21 treatment increased plasma adiponectin and reduced insulin stimulated glucose disposal in WT mice, but the latter effect was not seen in adiponectin KO (ADNKO) mice (Lin et al., 2013). However, in the study by BonDurant et al., ADNKO mice treated with FGF21 experienced the same decrease in plasma glucose when challenged with insulin as the WT mice treated with FGF21 (BonDurant et al., 2017).

FGF21 Actions in Primates

Similar to its actions in mice, FGF21 improves insulin action and glucose uptake in primates. Primary human adipocytes treated with FGF21 exhibit a 65% increase in glucose uptake relative to baseline (Lee et al., 2014). FGF21 lowered basal glucose and insulin in diabetic monkeys when administered for 6 wks (Kharitonenkov et al., 2007). Further, in a separate study, obese rhesus monkeys treated for 6 wks with FGF21 have improved glucose clearance during an oral GTT as well as a lower insulin response, indicating an improvement in insulin action (Véniant et al., 2012). Administration of 3, 10, or 20 mg of FGF21 daily to obese humans with type II diabetes (T2D) led to dose-dependent numerical reduction in fasting glucose and insulin after 28 days of treatment. These effects were associated with dose-dependent increases in the insulin sensitizing adipokine, adiponectin (Gaich et al., 2013).

In addition to modulating insulin action and glucose uptake, FGF21 reduces body weight in both humans and monkeys. While this is also observed in rodents, monkeys differ in that they also experience a decrease in intake with FGF21 treatment (Adams et al., 2013). Furthermore,

when obese humans with T2D and overweight monkeys were treated with FGF21, plasma triglycerides and cholesterol were significantly reduced (Kharitonenkov et al., 2007; Gaich et al., 2013). Another study administered 5, 25, 100, or 140 mg of long-acting FGF21 twice weekly for 4 weeks to obese humans with T2D. Although the effects on glucose and insulin were small, there was a significant reduction in total plasma triglycerides by 33-51% from baseline in those receiving at least the 25 mg dose as well as a reduction in total plasma cholesterol by ~10-15% from baseline in those receiving at least the 100 mg dose. In addition, not only was total cholesterol reduced, but there was also a shift from low density lipoprotein (LDL) to high density lipoprotein (HDL) with the 2 highest doses. This group also administered FGF21 to monkeys and observed a similar effect in the plasma lipid profile (Talukdar et al., 2016). These effects were further confirmed by Adams et al (Adams et al., 2013). At the cellular level, FGF21 decreases mRNA expression of lipogenic genes acetyl-CoA carboxylase (ACC), fatty acid synthase (FAS), stearoyl-CoA desaturase (SCD), and diacylglycerol acyltransferase (DGAT2) in the human liver-derived HepG2 cells *in vitro*. These genes were found to be downregulated as a consequence of FGF21 repression of sterol regulatory element binding protein 1c (SREBP-1c) (Zhang et al., 2011).

The presence of FGF21 was detected in human cerebrospinal fluid (CSF) (Tan et al., 2011). There have been studies speculating that part of its function may be to protect the brain during neurological disorders such as Parkinson's Disease. Specifically in the case of Parkinson's Disease, FGF21 enhances mitochondrial capacity and increases the peroxisome proliferator-activated receptor γ coactivator-1α (PGC-1α) pathway in dopaminergic neurons cultured *in vitro* (Mäkelä et al., 2014). Although FGF21 action in primate brains may be

expected based on rodent studies, there is yet to be any study supporting these actions in primate models.

FGF21 also appears to modulate the GH actions in primates. In both nondiabetic patients and patients with anorexia nervosa, plasma FGF21 is not only increased, but there is also a negative relationship between plasma FGF21 and IGF-1 and a positive association between plasma FGF21 and GH (Fazeli et al., 2010; Kralisch et al., 2013). Furthermore, human HepG2 cells treated with FGF21 exhibit a reduction in IGF-1 secretion (Kralisch et al., 2013). In addition, infant length in premature infants was negatively correlated with plasma FGF21, suggesting increased FGF21 may be responsible for decreased linear growth (Guasti et al., 2014). Upon further investigation, FGF21 was found to inhibit GH action in chondrocytes. Specifically, FGF21 treatment of primary human chondrocytes cultured *in vitro* upregulated both basal and GH-stimulated suppressor of cytokine signaling (SOCS2), a suppressor of the GH signaling pathway. In addition, FGF21 blocked the GH-induced phosphorylation of signal transducer and activator of transcription 5 (STAT5) in these same cells (Guasti et al., 2014). These data suggest FGF21 inhibits the positive effects of GH on long bone growth.

FGF21 Biology in Ruminants

Schoenberg et al. investigated FGF21 across the periparturient period and observed that plasma FGF21 increased from 75 pg/mL in late pregnancy to 1600 pg/mL on the day of parturition, followed by chronically elevated levels for the next 4 weeks. FGF21 was expressed predominantly in liver, with low expression in adipose tissue and mammary gland and no expression in muscle (Schoenberg et al., 2011). In terms of target tissues, β-klotho was highly expressed in WAT and to a lesser extent in the liver. Other tissues were also analyzed (lung, pituitary, hypothalamus, muscle, intestine, adrenal gland, kidney, heart, spleen, uterus, and

ovaries), but expression across these tissues was minimal to non-existent. If we take into account FGFR1c expression as well, like the mouse, the primary FGF21 target tissue in cattle is adipose and the secondary target tissue is the liver (Schoenberg et al., 2011). Other studies measuring hepatic FGF21 mRNA confirmed its induction in early lactating cows (Carriquiry et al., 2009; Schlegel et al., 2013).

Previous work by Caixeta et al shows that elevated NEFA increases both hepatic FGF21 mRNA and plasma FGF21, while glucagon increases only hepatic FGF21 mRNA in nonpregnant dairy cows (Caixeta et al., 2017). Further supporting NEFA increasing FGF21 production, incubation of primary calf hepatocytes with NEFA increased not only FGF21 mRNA abundance but also FGF21 in the media. Importantly, this was demonstrated with NEFA concentrations ranging from 0.6 – 2.4 mmol/L, consistent with plasma concentrations prevailing in early lactating dairy cows (Wang et al., 2018). More recently, early lactating dairy cattle were infused with FGF21 over the course of 9 days. There were no effects on any indices of production (milk energy, milk yield, dry matter intake) (Caixeta et al., 2019). Activation of extracellular signal-regulated kinase (ERK) signaling was observed in adipose tissue, but not liver, further supporting adipose tissue as a major target tissue. This is likely due to the insufficient expression of the FGFR1c isoform in the liver. Metabolically, there was no effect by FGF21 on basal or stimulated indices of insulin action. There was also no effect on circulating levels of the adipokine adiponectin (Krumm et al., 2019). On the other hand, liver triglycerides were reduced by almost 50% with FGF21 treatment. In addition, IGF-1 was decreased while there was a tendency toward increased GH, suggesting that FGF21 attenuates GH action (Caixeta et al., 2019).

Summary

Research on FGF21 biology in rodents and primates has been performed nearly exclusively in the context of obesity and energy excess. Under these conditions, FGF21 treatment results in a number of beneficial effects, including correction of insulin resistance and loss of adiposity. In ruminants, however, FGF21 treatment has been limited to energy-deficient dairy cows and few effects were seen. We therefore asked the question if this difference in FGF21 action could relate to energy balance. Because of these reasons, we chose to administer FGF21 to a ruminant that would be in positive energy balance: 8-month-old growing female sheep fed ad libitum. We hypothesized FGF21 would lower basal plasma insulin and glucose, as well as improve insulin sensitivity under these conditions.

References

Adams, A. C., C. A. Halstead, B. C. Hansen, A. R. Irizarry, J. A. Martin, S. R. Myers, V. L. Reynolds, H. W. Smith, V. J. Wroblewski, and A. Kharitonenkov. 2013. LY2405319, an Engineered FGF21 Variant, Improves the Metabolic Status of Diabetic Monkeys. PloS One 8(6):e65763. doi: 10.1371/journal.pone.0065763 PMID - 23823755

Amatruda, J. M., J. N. Livingston, and D. H. Lockwood. 1985. Cellular mechanisms in selected states of insulin resistance: Human obesity, glucocorticoid excess, and chronic renal failure. Diabetes/Metabolism Reviews 1(3):293-317. doi: 10.1002/dmr.5610010304 PMID - 3915256

Andersen, B., H. Beck-Nielsen, and K. Højlund. 2011. Plasma FGF21 displays a circadian rhythm during a 72-h fast in healthy female volunteers. Clinical Endocrinology 75(4):514-519. doi: 10.1111/j.1365-2265.2011.04084.x PMID - 21521350

Anderson, R. R. 1975. Mammary Gland Growth in Sheep. Journal of Animal Science 41(1):118-123. doi: 10.2527/jas1975.411118x PMID - 1158789

Andrews, A. 1997. Pregnancy toxaemia in the ewe. In Practice 19(6):306. doi: 10.1136/inpract.19.6.306

Annison, E. F., and J. L. Linzell. 1964. The oxidation and utilization of glucose and acetate by the mammary gland of the goat in relation to their over-all metabolism and to milk formation. Journal of Physiology 175(3):372-385. doi: 10.1113/jphysiol.1964.sp007522 PMID - 14241838

Anthony, R. V., R. Liang, E. P. Kayl, and S. L. Pratt. 1995. The growth hormone/prolactin gene family in ruminant placentae. Journal of Reproduction and Fertility Supplement doi: 10.1530/biosciprocs.3.007

Aschenbach, J. R., N. B. Kristensen, S. S. Donkin, H. M. Hammon, and G. B. Penner. 2010. Gluconeogenesis in dairy cows: The secret of making sweet milk from sour dough. IUBMB Life 62(12):869-877. doi: 10.1002/iub.400 PMID - 21171012

Badman, M. K., P. Pissios, A. R. Kennedy, G. Koukos, J. S. Flier, and E. Maratos-Flier. 2007. Hepatic Fibroblast Growth Factor 21 Is Regulated by PPARα and Is a Key Mediator of Hepatic Lipid Metabolism in Ketotic States. Cell Metabolism 5(6):426-437. doi: 10.1016/j.cmet.2007.05.002 PMID - 17550778

Balage, M., J. F. Hocquette, B. Graulet, P. Ferre, and J. Grizard. 1997. Skeletal muscle glucose transporter (GLUT-4) protein is decreased in lactating goats. Journal of Animal Science 65(2):257-265. doi: 10.1017/s1357729800016568

Balmain, J. H., S. J. Folley, and R. F. Glascock. 1952. Effects of insulin and of glycerol in vitro on the incorporation of [carboxy-14C]acetate into the fatty acids of lactating mammary gland slices with special reference to species differences. Biochemical Journal 52(2):301-306. doi: 10.1042/bj0520301 PMID - 13018225

Bauman, D. E., R. W. Mellenberger, and R. G. Derrig. 1973. Fatty Acid Synthesis in Sheep Mammary Tissue1. Journal of Dairy Science 56(10):1312-1318. doi: 10.3168/jds.s0022-0302(73)85352-4 PMID - 4742113

Belfiore, F., A. M. Rabuazzo, S. Iannello, D. Vasta, and R. Campione. 1984. Insulin resistance in the obese hyperglycemic (ob/ob) mouse. Failure of hyperinsulinemia to activate hepatic pyruvate kinase (PK). Metabolism: Clinical and Experimental 33(2):104-106. doi: 10.1016/0026-0495(84)90119-7 PMID - 6694552

Bell, A. W., and D. E. Bauman. 1997. Adaptations of glucose metabolism during pregnancy and lactation. Journal of Mammary Gland Biology and Neoplasia 2(3):265-278.

Bell, A. W., and R. A. Ehrhardt. 2002. Regulation of placental nutrient transport and implications for fetal growth. Nutrition Research Reviews 15(2):211-230. doi: 10.1079/nrr200239 PMID - 19087405

Bergman, E. N., R. P. Brockman, and C. F. Kaufman. 1974. Glucose metabolism in ruminants: comparison of whole-body turnover with production by gut, liver, and kidneys. Federation Proceedings 33(7):1849-1854.

Bergman, E. N., and D. E. Hogue. 1967. Glucose turnover and oxidation rates in lactating sheep. American Journal of Physiology Legacy Content 213(6):1378-1384. doi: 10.1152/ajplegacy.1967.213.6.1378 PMID - 5624433

Block, S. S., W. R. Butler, R. A. Ehrhardt, A. W. Bell, M. E. V. Amburgh, and Y. R. Boisclair. 2001. Decreased concentration of plasma leptin in periparturient dairy cows is caused by negative energy balance. Journal of Endocrinology 171(2):339-348.

BonDurant, L. D., M. Ameka, M. C. Naber, K. R. Markan, S. O. Idiga, M. R. Acevedo, S. A. Walsh, D. M. Ornitz, and M. J. Potthoff. 2017. FGF21 Regulates Metabolism Through Adipose-Dependent and -Independent Mechanisms. Cell Metabolism 25(4):935-944.e934. doi: 10.1016/j.cmet.2017.03.005 PMID - 28380381

Bookout, A. L., M. H. M. d. Groot, B. M. Owen, S. Lee, L. Gautron, H. L. Lawrence, X. Ding, J. K. Elmquist, J. S. Takahashi, D. J. Mangelsdorf, and S. A. Kliewer. 2013. FGF21 regulates metabolism and circadian behavior by acting on the nervous system. Nature Medicine 19(9):1147-1152. doi: 10.1038/nm.3249 PMID - 23933984

Borst, S. E. 2004. The role of TNF-α in insulin resistance. Endocrine 23(2-3):177-182. doi: 10.1385/endo:23:2-3:177 PMID - 15146098

Bradford, B. J., K. Yuan, J. K. Farney, L. K. Mamedova, and A. J. Carpenter. 2015. Invited review: Inflammation during the transition to lactation: New adventures with an old flame. Journal of Dairy Science 98(10):6631-6650. doi: 10.3168/jds.2015-9683 PMID - 26210279

Caixeta, L. S., S. L. Giesy, C. S. Krumm, J. W. Perfield, A. Butterfield, and Y. R. Boisclair. 2019. Fibroblast growth factor-21 (FGF21) administration to early-lactating dairy cows.

II. Pharmacokinetics, whole-animal performance, and lipid metabolism. Journal of Dairy Science doi: 10.3168/jds.2019-16696 PMID - 31548064

Caixeta, L. S., S. L. Giesy, C. S. Krumm, J. W. Perfield, A. Butterfield, K. M. Schoenberg, D. C. Beitz, and Y. R. Boisclair. 2017. Effect of circulating glucagon and free fatty acids on hepatic FGF21 production in dairy cows. American Journal of Physiology: Regulatory, Integrative and Comparative Physiology:ajpregu.00197.02017. doi: 10.1152/ajpregu.00197.2017 PMID - 28794103

Carriquiry, M., W. J. Weber, S. C. Fahrenkrug, and B. A. Crooker. 2009. Hepatic gene expression in multiparous Holstein cows treated with bovine somatotropin and fed n-3 fatty acids in early lactation 1. Journal of Dairy Science 92(10):4889-4900. doi: 10.3168/jds.2008-1676 PMID - 19762804

Ceciliani, F., J. J. Ceron, P. D. Eckersall, and H. Sauerwein. 2012. Acute phase proteins in ruminants. Journal of Proteomics 75(14):4207-4231. doi: 10.1016/j.jprot.2012.04.004 PMID - 22521269

Chaiyabutr, N., A. Faulkner, and M. Peaker. 1980. The utilization of glucose for the synthesis of milk components in the fed and starved lactating goat in vivo. Biochemical Journal 186(1):301-308. doi: 10.1042/bj1860301 PMID - 7370016

Chau, M. D. L., J. Gao, Q. Yang, Z. Wu, and J. Gromada. 2010. Fibroblast growth factor 21 regulates energy metabolism by activating the AMPK–SIRT1–PGC-1α pathway. Proceedings of the National Academy of Sciences 107(28):12553-12558. doi: 10.1073/pnas.1006962107 PMID - 20616029

Chen, W., J. L. Wilson, M. Khaksari, M. A. Cowley, and P. J. Enriori. 2012. Abdominal fat analyzed by DEXA scan reflects visceral body fat and improves the phenotype description and the assessment of metabolic risk in mice. American Journal of Physiology Endocrinology and Metabolism 303(5):E635-643. doi: 10.1152/ajpendo.00078.2012 PMID - 22761161

Christodoulides, C., P. Dyson, and S.-D. of …. 2009a. Circulating fibroblast growth factor 21 is induced by peroxisome proliferator-activated receptor agonists but not ketosis in man. The Journal of Clinical Endocrinology & Metabolism

Christodoulides, C., P. Dyson, D. Sprecher, K. Tsintzas, and F. Karpe. 2009b. Circulating Fibroblast Growth Factor 21 Is Induced by Peroxisome Proliferator-Activated Receptor Agonists But Not Ketosis in Man. Journal of Clinical Endocrinology and Metabolism 94(9):3594-3601. doi: 10.1210/jc.2009-0111 PMID - 19531592

Coskun, T., H. A. Bina, M. A. Schneider, J. D. Dunbar, C. C. Hu, Y. Chen, D. E. Moller, and A. Kharitonenkov. 2008. Fibroblast growth factor 21 corrects obesity in mice. Endocrinology 149(12):6018-6027. doi: 10.1210/en.2008-0816 PMID - 18687777

Cui, Y., S. L. Giesy, M. Hassan, K. Davis, S. Zhao, and Y. R. Boisclair. 2014. Hepatic FGF21 production is increased in late pregnancy in the mouse. American Journal of Physiology:

Regulatory, Integrative and Comparative Physiology 307(3):R290-298. doi: 10.1152/ajpregu.00554.2013 PMID - 24898837

Cyphert, H. A., K. M. Alonge, S. M. Ippagunta, and F. B. Hillgartner. 2014. Glucagon stimulates hepatic FGF21 secretion through a PKA- and EPAC-dependent posttranscriptional mechanism. PloS One 9(4):e94996. doi: 10.1371/journal.pone.0094996 PMID - 24733293

Dailey, L., D. Ambrosetti, A. Mansukhani, and C. Basilico. 2005. Mechanisms underlying differential responses to FGF signaling. Cytokine & Growth Factor Reviews 16(2):233-247. doi: 10.1016/j.cytogfr.2005.01.007 PMID - 15863038

De Koster, J., M. Hostens, M. Van Eetvelde, K. Hermans, S. Moerman, H. Bogaert, E. Depreester, W. Van den Broeck, and G. Opsomer. 2015. Insulin response of the glucose and fatty acid metabolism in dry dairy cows across a range of body condition scores. Journal of Dairy Science 98(7):4580-4592. doi: 10.3168/jds.2015-9341

De Koster, J., C. Urh, M. Hostens, W. Van den Broeck, H. Sauerwein, and G. Opsomer. 2017. Relationship between serum adiponectin concentration, body condition score, and peripheral tissue insulin response of dairy cows during the dry period. Domestic Animal Endocrinology 59:100-104. doi: 10.1016/j.domaniend.2016.12.004

De Koster, J. D., and G. Opsomer. 2013. Insulin resistance in dairy cows. Veterinary Clinics of North America: Food Animal Practice 29(2):299-322. doi: 10.1016/j.cvfa.2013.04.002

Ding, X., J. Boney-Montoya, B. M. Owen, A. L. Bookout, K. C. Coate, D. J. Mangelsdorf, and S. A. Kliewer. 2012. βKlotho is required for fibroblast growth factor 21 effects on growth and metabolism. Cell Metabolism 16(3):387-393. doi: 10.1016/j.cmet.2012.08.002 PMID - 22958921

Douris, N., D. M. Stevanovic, M. f. Fisher, T. I. Cisu, M. J. Chee, N. L. Nguyen, E. Zarebidaki, A. C. Adams, A. Kharitonenkov, J. S. Flier, T. J. Bartness, and E. Maratos-Flier. 2015. Central Fibroblast Growth Factor 21 Browns White Fat via Sympathetic Action in Male Mice. Endocrinology 156(7):2470-2481. doi: 10.1210/en.2014-2001 PMID - 25924103

Drackley, J. K. 1999. ADSA Foundation Scholar Award. Biology of dairy cows during the transition period: the final frontier? Journal of Dairy Science 82(11):2259-2273.

Drackley, J. K., R. L. Wallace, D. Graugnard, J. Vasquez, B. F. Richards, and J. J. Loor. 2014. Visceral adipose tissue mass in nonlactating dairy cows fed diets differing in energy density. Journal of Dairy Science 97(6):3420-3430. doi: 10.3168/jds.2014-8014 PMID - 24704224

Dubuc, P. U. 1976. The development of obesity, hyperinsulinemia, and hyperglycemia in ob/ob mice. Metabolism 25(12):1567-1574. doi: 10.1016/0026-0495(76)90109-8 PMID - 994838

Duhlmeier, R., A. Hacker, A. Widdel, W. von Engelhardt, and H. P. Sallmann. 2005. Mechanisms of insulin-dependent glucose transport into porcine and bovine skeletal muscle. American Journal of Physiology Regulatory Integrative and Comparative Physiology 289(1):R187-197. doi: 10.1152/ajpregu.00502.2004

Dushay, J., P. C. Chui, G. S. Gopalakrishnan, M. Varela–Rey, M. Crawley, F. M. Fisher, M. K. Badman, M. L. Martinez–Chantar, and E. Maratos–Flier. 2010. Increased Fibroblast Growth Factor 21 in Obesity and Nonalcoholic Fatty Liver Disease. Gastroenterology 139(2):456-463. doi: 10.1053/j.gastro.2010.04.054 PMID - 20451522

Ehrhardt, R. A., and A. W. Bell. 1995. Growth and metabolism of the ovine placenta during mid-gestation. Placenta 16(8):727-741. doi: 10.1016/0143-4004(95)90016-0 PMID - 8710803

Ehrhardt, R. A., and A. W. Bell. 1997. Developmental increases in glucose transporter concentration in the sheep placenta. American Journal of Physiology 273(3 Pt 2):R1132-1141. doi: 10.1152/ajpregu.1997.273.3.r1132 PMID - 9321896

Einstein, F. H., S. Fishman, R. H. Muzumdar, X. M. Yang, G. Atzmon, and N. Barzilai. 2008. Accretion of visceral fat and hepatic insulin resistance in pregnant rats. American Journal of Physiology Endocrinology and Metabolism 294(2):E451-E455. doi: 10.1152/ajpendo.00570.2007 PMID - 18073320

Faulkner, A., and H. T. Pollock. 1991. Effect of lactation on gluconeogenesis and ketogenesis in ovine hepatocytes. Comparative Biochemistry and Physiology 98(2-3):283-286. doi: 10.1016/0305-0491(91)90180-l PMID - 1873985

Fazeli, P. K., M. Lun, S. M. Kim, M. A. Bredella, S. Wright, Y. Zhang, H. Lee, C. Catana, A. Klibanski, P. Patwari, and M. L. Steinhauser. 2015. FGF21 and the late adaptive response to starvation in humans. Journal of Clinical Investigation 125(12):4601-4611. doi: 10.1172/JCI83349 PMID - 26529252

Fazeli, P. K., M. Misra, M. Goldstein, K. K. Miller, and A. Klibanski. 2010. Fibroblast Growth Factor-21 May Mediate Growth Hormone Resistance in Anorexia Nervosa. Journal of Clinical Endocrinology and Metabolism 95(1):369-374. doi: 10.1210/jc.2009-1730 PMID - 19926712

Fisher, f. M., P. C. Chui, P. J. Antonellis, H. A. Bina, A. Kharitonenkov, J. S. Flier, and E. Maratos-Flier. 2010. Obesity Is a Fibroblast Growth Factor 21 (FGF21)-Resistant State. Diabetes 59(11):2781-2789. doi: 10.2337/db10-0193 PMID - 20682689

Fisher, F. M., P. C. Chui, I. A. Nasser, Y. Popov, J. C. Cunniff, T. Lundasen, A. Kharitonenkov, D. Schuppan, J. S. Flier, and E. Maratos-Flier. 2014. Fibroblast Growth Factor 21 Limits Lipotoxicity by Promoting Hepatic Fatty Acid Activation in Mice on Methionine and Choline-Deficient Diets. Gastroenterology 147(5):1073-1083.e1076. doi: 10.1053/j.gastro.2014.07.044 PMID - 25083607

Fisher, F. M., J. L. Estall, A. C. Adams, P. J. Antonellis, H. A. Bina, J. S. Flier, A. Kharitonenkov, B. M. Spiegelman, and E. Maratos-Flier. 2011. Integrated Regulation of

Hepatic Metabolism by Fibroblast Growth Factor 21 (FGF21) in Vivo. Endocrinology 152(8):2996-3004. doi: 10.1210/en.2011-0281 PMID - 21712364

Fisher, F. M., S. Kleiner, N. Douris, E. C. Fox, R. J. Mepani, F. Verdeguer, J. Wu, A. Kharitonenkov, J. S. Flier, E. Maratos-Flier, and B. M. Spiegelman. 2012. FGF21 regulates PGC-1α and browning of white adipose tissues in adaptive thermogenesis. Genes and Development 26(3):271-281. doi: 10.1101/gad.177857.111 PMID - 22302939

Fisher, F. M., and E. Maratos-Flier. 2015. Understanding the Physiology of FGF21. Annual Review of Physiology 78(1):1-19. doi: 10.1146/annurev-physiol-021115-105339 PMID - 26654352

Forbes, J. M. 1967. Factors affecting the gestation length in sheep. The Journal of Agricultural Science 68(2):191-194. doi: 10.1017/s0021859600016221

Forbes, J. M. 1970. Voluntary Food Intake of Pregnant Ewes. Journal of Animal Science 31(6):1222-1227. doi: 10.2527/jas1970.3161222x

Forbes, J. M. 1977. Interrelationships between physical and metabolic control of voluntary food intake in fattening, pregnant and lactating mature sheep: a model. Journal of Animal Science 24(1):91-101. doi: 10.1017/s0003356100039258

Ford, S. P., L. Zhang, M. Zhu, M. M. Miller, D. T. Smith, B. W. Hess, G. E. Moss, P. W. Nathanielsz, and M. J. Nijland. 2009. Maternal obesity accelerates fetal pancreatic β-cell but not α-cell development in sheep: prenatal consequences. American Journal of Physiology: Regulatory, Integrative and Comparative Physiology 297(3):R835-R843. doi: 10.1152/ajpregu.00072.2009 PMID - 19605766

Forsyth, I. A. 1986. Variation Among Species in the Endocrine Control of Mammary Growth and Function: The Roles of Prolactin, Growth Hormone, and Placental Lactogen. Journal of Dairy Science 69(3):886-903. doi: 10.3168/jds.s0022-0302(86)80479-9 PMID - 3519707

Fried, S. K., M. Lavau, and F. X. Pi-Sunyer. 1982. Variations in glucose metabolism by fat cells from three adipose depots of the rat. Metabolism 31(9):876-883. doi: 10.1016/0026-0495(82)90176-7 PMID - 7121259

Fthenakis, G. C., G. Arsenos, C. Brozos, I. A. Fragkou, N. D. Giadinis, I. Giannenas, V. S. Mavrogianni, E. Papadopoulos, and I. Valasi. 2012. Health management of ewes during pregnancy. Animal Reproduction Science 130(3-4):198-212. doi: 10.1016/j.anireprosci.2012.01.016 PMID - 22356932

Fukumoto, S. 2008. Actions and Mode of Actions of FGF19 Subfamily Members. Endocrine Journal 55(1):23-31. doi: 10.1507/endocrj.kr07e-002 PMID - 17878606

Gaich, G., J. Y. Chien, H. Fu, L. C. Glass, M. A. Deeg, W. L. Holland, A. Kharitonenkov, T. Bumol, H. K. Schilske, and D. E. Moller. 2013. The effects of LY2405319, an FGF21

analog, in obese human subjects with type 2 diabetes. Cell Metabolism 18(3):333-340. doi: 10.1016/j.cmet.2013.08.005 PMID - 24011069

Gentile, C. L., D. Wang, K. T. Pfaffenbach, R. Cox, Y. Wei, and M. J. Pagliassotti. 2010. Fatty acids regulate CREBh via transcriptional mechanisms that are dependent on proteasome activity and insulin. Molecular and Cellular Biochemistry 344(1-2):99-107. doi: 10.1007/s11010-010-0533-3 PMID - 20607591

Giesy, S. L., B. Yoon, W. B. Currie, J. W. Kim, and Y. R. Boisclair. 2012. Adiponectin deficit during the precarious glucose economy of early lactation in dairy cows. Endocrinology 153(12):5834-5844. doi: 10.1210/en.2012-1765 PMID - 23077076

Gill, R. D., and I. C. Hart. 1982. Hepatic receptors for insulin and glucagon in relation to plasma hormones and metabolites in pregnant and unmated ewes. Journal of Endocrinology 93(2):231-238. doi: 10.1677/joe.0.0930231 PMID - 6283005

Goetz, R., M. Ohnishi, X. Ding, H. Kurosu, L. Wang, J. Akiyoshi, J. Ma, W. Gai, Y. Sidis, N. Pitteloud, M. Kuro-o, M. S. Razzaque, and M. Mohammadi. 2012. Klotho Coreceptors Inhibit Signaling by Paracrine Fibroblast Growth Factor 8 Subfamily Ligands. Molecular and Cellular Biology 32(10):1944-1954. doi: 10.1128/mcb.06603-11 PMID - 22451487

Gootwine, E. 2004. Placental hormones and fetal–placental development. Animal Reproduction Science

Greguła-Kania, M., U. Kosior-Korzecka, K. Patkowski, E. Juszczuk-Kubiak, M. Plewik, and T. M. Gruszecki. 2020. Acute-phase proteins, cortisol and haematological parameters in ewes during the periparturient period. Reproduction in Domestic Animals 55(3):393-400. doi: 10.1111/rda.13628 PMID - 31916297

Grummer, R. R., D. G. Mashek, and A. Hayirli. 2004. Dry matter intake and energy balance in the transition period. Veterinary Clinics of North America: Food Animal Practice 20(3):447-470. doi: 10.1016/j.cvfa.2004.06.013 PMID - 15471620

Guasti, L., S. Silvennoinen, N. W. Bulstrode, P. Ferretti, U. Sankilampi, and L. Dunkel. 2014. Elevated FGF21 Leads to Attenuated Postnatal Linear Growth in Preterm Infants Through GH Resistance in Chondrocytes. Journal of Clinical Endocrinology and Metabolism 99(11):E2198-E2206. doi: 10.1210/jc.2014-1566 PMID - 25137423

Guesnet, P. M., M. J. Massoud, and Y. Demarne. 1991. Regulation of adipose tissue metabolism during pregnancy and lactation in the ewe: the role of insulin1. Journal of Animal Science 69(5):2057-2065. doi: 10.2527/1991.6952057x PMID - 2066315

Habegger, K. M., K. Stemmer, C. Cheng, T. D. Müller, K. M. Heppner, N. Ottaway, J. Holland, J. L. Hembree, D. Smiley, V. Gelfanov, R. Krishna, A. M. Arafat, A. Konkar, S. Belli, M. Kapps, S. C. Woods, S. M. Hofmann, D. D'Alessio, P. T. Pfluger, D. Perez-Tilve, R. J. Seeley, M. Konishi, N. Itoh, A. Kharitonenkov, J. Spranger, R. D. DiMarchi, and M. H. Tschöp. 2013. Fibroblast Growth Factor 21 Mediates Specific Glucagon Actions. Diabetes 62(5):1453-1463. doi: 10.2337/db12-1116 PMID - 23305646

Hadjipieris, G., and W. Holmes. 1966. Studies on feed intake and feed utilization by sheep I. Voluntary feed intake of dry, pregnant and lactating ewes. The Journal of Agricultural Science 66(02):217. doi: 10.1017/s0021859600062626

Hammon, H. M., G. Stürmer, F. Schneider, A. Tuchscherer, H. Blum, T. Engelhard, A. Genzel, R. Staufenbiel, and W. Kanitz. 2009. Performance and metabolic and endocrine changes with emphasis on glucose metabolism in high-yielding dairy cows with high and low fat content in liver after calving 1. Journal of Dairy Science 92(4):1554-1566. doi: 10.3168/jds.2008-1634 PMID - 19307636

Hay Jr., W. W. 1994. Placental Transport of Nutrients to the Fetus. Hormone Research 42(4-5):215-222. doi: 10.1159/000184196 PMID - 7868076

Holland, W. L., A. C. Adams, J. T. Brozinick, H. H. Bui, Y. Miyauchi, C. M. Kusminski, S. M. Bauer, M. Wade, E. Singhal, C. C. Cheng, K. Volk, M.-S. S. Kuo, R. Gordillo, A. Kharitonenkov, and P. E. Scherer. 2013. An FGF21-adiponectin-ceramide axis controls energy expenditure and insulin action in mice. Cell Metabolism 17(5):790-797. doi: 10.1016/j.cmet.2013.03.019 PMID - 23663742

Hostens, M., V. Fievez, J. L. M. R. Leroy, J. V. Ranst, B. Vlaeminck, and G. Opsomer. 2012. The fatty acid profile of subcutaneous and abdominal fat in dairy cows with left displacement of the abomasum. Journal of Dairy Science 95(7):3756-3765. doi: 10.3168/jds.2011-5092 PMID - 22720932

Hsuchou, H., W. Pan, and A. J. Kastin. 2007. The fasting polypeptide FGF21 can enter brain from blood. Peptides 28(12):2382-2386. doi: 10.1016/j.peptides.2007.10.007 PMID - 17996984

Hubbard, S. R. 2013. The Insulin Receptor: Both a Prototypical and Atypical Receptor Tyrosine Kinase. Cold Spring Harbor Perspectives in Biology 5(3):a008946. doi: 10.1101/cshperspect.a008946 PMID - 23457259

Hultman, K., J. M. Scarlett, A. F. Baquero, A. Cornea, Y. Zhang, C. B. G. Salinas, J. Brown, G. J. Morton, E. J. Whalen, K. L. Grove, F. H. Koegler, M. W. Schwartz, and A. J. Mercer. 2019. The central fibroblast growth factor receptor/beta klotho system: Comprehensive mapping in Mus musculus and comparisons to nonhuman primate and human samples using an automated in situ hybridization platform. Journal of Comparative Neurology 527(12):2069-2085. doi: 10.1002/cne.24668 PMID - 30809795

Ibrahim, M. M. 2010. Subcutaneous and visceral adipose tissue: structural and functional differences. Obesity Reviews 11(1):11-18. doi: 10.1111/j.1467-789x.2009.00623.x PMID - 19656312

Inagaki, T., P. Dutchak, G. Zhao, X. Ding, L. Gautron, V. Parameswara, Y. Li, R. Goetz, M. Mohammadi, V. Esser, J. K. Elmquist, R. D. Gerard, S. C. Burgess, R. E. Hammer, D. J. Mangelsdorf, and S. A. Kliewer. 2007. Endocrine regulation of the fasting response by PPARalpha-mediated induction of fibroblast growth factor 21. Cell Metabolism 5(6):415-425. doi: 10.1016/j.cmet.2007.05.003 PMID - 17550777

Inagaki, T., V. Y. Lin, R. Goetz, M. Mohammadi, D. J. Mangelsdorf, and S. A. Kliewer. 2008. Inhibition of growth hormone signaling by the fasting-induced hormone FGF21. Cell Metabolism 8(1):77-83. doi: 10.1016/j.cmet.2008.05.006 PMID - 18585098

Ito, Y., R. Banno, S. Hagimoto, Y. Ozawa, H. Arima, and Y. Oiso. 2012. TNFα increases hypothalamic PTP1B activity via the NFκB pathway in rat hypothalamic organotypic cultures. Regulatory Peptides 174(1-3):58-64. doi: 10.1016/j.regpep.2011.11.010

Itoh, N., and D. M. Ornitz. 2004. Evolution of the Fgf and Fgfr gene families. Trends in Genetics 20(11):563-569. doi: 10.1016/j.tig.2004.08.007 PMID - 15475116

Itoh, N., and D. M. Ornitz. 2010. Fibroblast growth factors: from molecular evolution to roles in development, metabolism and disease. Journal of Biochemistry 149(2):121-130. doi: 10.1093/jb/mvq121 PMID - 20940169

Izumiya, Y., H. A. Bina, N. Ouchi, Y. Akasaki, A. Kharitonenkov, and K. Walsh. 2008. FGF21 is an Akt-regulated myokine. FEBS Letters 582(27):3805-3810. doi: 10.1016/j.febslet.2008.10.021 PMID - 18948104

Jaakson, H., P. Karis, K. Ling, A. Ilves-Luht, J. Samarütel, M. Henno, I. Jõudu, A. Waldmann, E. Reimann, P. Pärn, R. M. Bruckmaier, J. J. Gross, T. Kaart, M. Kass, and M. Ots. 2018. Adipose tissue insulin receptor and glucose transporter 4 expression, and blood glucose and insulin responses during glucose tolerance tests in transition Holstein cows with different body condition. Journal of Dairy Science 101(1):752-766. doi: 10.3168/jds.2017-12877 PMID - 29102144

Ji, P., J. S. Osorio, J. K. Drackley, and J. J. Loor. 2012. Overfeeding a moderate energy diet prepartum does not impair bovine subcutaneous adipose tissue insulin signal transduction and induces marked changes in peripartal gene network expression 1. Journal of Dairy Science 95(8):4333-4351. doi: 10.3168/jds.2011-5079 PMID - 22818447

Kahn, C. R. 1978. Insulin resistance, insulin insensitivity, and insulin unresponsiveness: A necessary distinction. Metabolism 27(12):1893-1902. doi: 10.1016/s0026-0495(78)80007-9 PMID - 723640

Kenéz, Á., L. Ruda, S. Dänicke, and K. Huber. 2019. Insulin signaling and insulin response in subcutaneous and retroperitoneal adipose tissue in Holstein cows during the periparturient period. Journal of Dairy Science 102(12):11718-11729. doi: 10.3168/jds.2019-16873 PMID - 31563314

Kharitonenkov, A., J. D. Dunbar, H. A. Bina, S. Bright, J. S. Moyers, C. Zhang, L. Ding, R. Micanovic, S. F. Mehrbod, M. D. Knierman, J. E. Hale, T. Coskun, and A. B. Shanafelt. 2008. FGF-21/FGF-21 receptor interaction and activation is determined by βKlotho. Journal of Cellular Physiology 215(1):1-7. doi: 10.1002/jcp.21357 PMID - 18064602

Kharitonenkov, A., T. L. Shiyanova, A. Koester, A. M. Ford, R. Micanovic, E. J. Galbreath, G. E. Sandusky, L. J. Hammond, J. S. Moyers, R. A. Owens, J. Gromada, J. T. Brozinick, E. D. Hawkins, V. J. Wroblewski, D.-S. S. Li, F. Mehrbod, S. R. Jaskunas, and A. B.

Shanafelt. 2005. FGF-21 as a novel metabolic regulator. Journal of Clinical Investigation 115(6):1627-1635. doi: 10.1172/JCI23606 PMID - 15902306

Kharitonenkov, A., V. J. Wroblewski, A. Koester, Y.-F. F. Chen, C. K. Clutinger, X. T. Tigno, B. C. Hansen, A. B. Shanafelt, and G. J. Etgen. 2007. The metabolic state of diabetic monkeys is regulated by fibroblast growth factor-21. Endocrinology 148(2):774-781. doi: 10.1210/en.2006-1168 PMID - 17068132

Kilkenny, D. M., and J. V. Rocheleau. 2016. The FGF21 Receptor Signaling Complex: Klothoβ, FGFR1c, and Other Regulatory Interactions. Vitamins and Hormones 101:17-58. doi: 10.1016/bs.vh.2016.02.008 PMID - 27125737

Kim, H., R. Mendez, Z. Zheng, L. Chang, J. Cai, R. Zhang, and K. Zhang. 2014. Liver-Enriched Transcription Factor CREBH Interacts With Peroxisome Proliferator-Activated Receptor α to Regulate Metabolic Hormone FGF21. Endocrinology 155(3):769-782. doi: 10.1210/en.2013-1490 PMID - 24424044

Kim, J. W. 2014. Modulation of the Somatotropic Axis in Periparturient Dairy Cows. Asian-Australasian Journal of Animal Sciences 27(1):147-154. doi: 10.5713/ajas.2013.13139 PMID - 25049937

Kim, J. W., R. P. Rhoads, S. S. Block, T. R. Overton, S. J. Frank, and Y. R. Boisclair. 2004. Dairy cows experience selective reduction of the hepatic growth hormone receptor during the periparturient period. Journal of Endocrinology 181(2):281-290. doi: 10.1677/joe.0.1810281 PMID - 15128276

Kim, K., S. Kim, Y.-K. Min, H.-M. Yang, J.-B. Lee, and M.-S. Lee. 2013. Acute Exercise Induces FGF21 Expression in Mice and in Healthy Humans. PloS One 8(5):e63517. doi: 10.1371/journal.pone.0063517 PMID - 23667629

Komatsu, T., F. Itoh, S. Kushibiki, and K. Hodate. 2005. Changes in gene expression of glucose transporters in lactating and nonlactating cows. Journal of Animal Science 83(3):557-564. doi: 10.2527/2005.833557x PMID - 15705752

Kralisch, S., A. Tönjes, K. Krause, J. Richter, U. Lossner, P. Kovacs, T. Ebert, M. Blüher, M. Stumvoll, and M. Fasshauer. 2013. Fibroblast growth factor-21 serum concentrations are associated with metabolic and hepatic markers in humans. Journal of Endocrinology 216(2):135-143. doi: 10.1530/joe-12-0367 PMID - 23129782

Krumm, C. S., S. L. Giesy, L. S. Caixeta, W. R. Butler, H. Sauerwein, J. W. Kim, and Y. R. Boisclair. 2017. Effect of hormonal and energy-related factors on plasma adiponectin in transition dairy cows. Journal of Dairy Science doi: 10.3168/jds.2017-13274 PMID - 28843695

Krumm, C. S., S. L. Giesy, L. S. Caixeta, J. W. Perfield, H. Sauerwein, B. L. Moore, and Y. R. Boisclair. 2019. Fibroblast growth factor-21 (FGF21) administration to early-lactating dairy cows. I. Effects on signaling and indices of insulin action. Journal of Dairy Science doi: 10.3168/jds.2019-16695 PMID - 31548053

Krumm, C. S., S. L. Giesy, C. L. Orndorff, and Y. R. Boisclair. 2018. Variation in x-box binding protein 1 (XBP1) expression and its dependent endoplasmic reticulum chaperones does not regulate adiponectin secretion in dairy cows. Journal of Dairy Science doi: 10.3168/jds.2017-14048 PMID - 29550138

Kurosu, H., M. Choi, Y. Ogawa, A. S. Dickson, R. Goetz, A. V. Eliseenkova, M. Mohammadi, K. P. Rosenblatt, S. A. Kliewer, and M. Kuro-o. 2007. Tissue-specific Expression of βKlotho and Fibroblast Growth Factor (FGF) Receptor Isoforms Determines Metabolic Activity of FGF19 and FGF21. Journal of Biological Chemistry 282(37):26687-26695. doi: 10.1074/jbc.m704165200 PMID - 17623664

Laeger, T., T. M. Henagan, D. C. Albarado, L. M. Redman, G. A. Bray, R. C. Noland, H. Münzberg, S. M. Hutson, T. W. Gettys, M. W. Schwartz, and C. D. Morrison. 2014. FGF21 is an endocrine signal of protein restriction. Journal of Clinical Investigation 124(9):3913-3922. doi: 10.1172/JCI74915 PMID - 25133427

Lafontan, M., and J. Girard. 2008. Impact of visceral adipose tissue on liver metabolism Part I: Heterogeneity of adipose tissue and functional properties of visceral adipose tissue. Diabetes and Metabolism 34(4):317-327. doi: 10.1016/j.diabet.2008.04.001 PMID - 18550411

Lanng, A. R. R., L. S. Gasbjerg, N. C. Bergmann, S. Bermann, M. M. Helsted, M. P. Gillum, B. Hartmann, J. J. Holst, T. Vilsbøll, and F. K. Knop. 2019. Gluco-metabolic effects of oral and intravenous alcohol administration in men. Endocrine Connections -1(aop)doi: 10.1530/ec-19-0317

Leblanc, S. 2010. Monitoring Metabolic Health of Dairy Cattle in the Transition Period. Journal of Reproduction and Development 56(S):S29-S35. doi: 10.1262/jrd.1056S29 PMID - 20629214

Lee, D. V., D. Li, Q. Yan, Y. Zhu, B. Goodwin, R. Calle, M. B. Brenner, and S. Talukdar. 2014. Fibroblast Growth Factor 21 Improves Insulin Sensitivity and Synergizes with Insulin in Human Adipose Stem Cell-Derived (hASC) Adipocytes. PloS One 9(11):e111767. doi: 10.1371/journal.pone.0111767 PMID - 25365322

Lee, J., and P. F. Pilch. 1994. The insulin receptor: structure, function, and signaling. American Journal of Physiology Cell Physiology 266(2):C319-C334. doi: 10.1152/ajpcell.1994.266.2.c319 PMID - 8141246

Lee, K. J., Y. O. Jang, S.-K. Cha, M. Y. Kim, K.-S. Park, Y. W. Eom, and S. K. Baik. 2018. Expression of Fibroblast Growth Factor 21 and β-Klotho Regulates Hepatic Fibrosis through the Nuclear Factor-κB and c-Jun N-Terminal Kinase Pathways. Gut and Liver 12(4):449-456. doi: 10.5009/gnl17443 PMID - 29699061

Lérias, J. R., L. E. Hernández-Castellano, A. Suárez-Trujillo, N. Castro, A. Pourlis, and A. M. Almeida. 2014. The mammary gland in small ruminants: major morphological and functional events underlying milk production – a review. Journal of Dairy Research 81(3):304-318. doi: 10.1017/s0022029914000235 PMID - 24901899

Leury, B. J., A. R. Bird, K. D. Chandler, and A. W. Bell. 1990. Glucose partitioning in the pregnant ewe: Effects of undernutrition and exercise. British Journal of Nutrition 64(2):449-462. doi: 10.1079/bjn19900045 PMID - 2223746

Li, H., G. Wu, Q. Fang, M. Zhang, X. Hui, B. Sheng, L. Wu, Y. Bao, P. Li, A. Xu, and W. Jia. 2018. Fibroblast growth factor 21 increases insulin sensitivity through specific expansion of subcutaneous fat. Nature Communications 9(1):272. doi: 10.1038/s41467-017-02677-9 PMID - 29348470

Lin, Z., H. Tian, Karen S. L. Lam, S. Lin, Ruby C. L. Hoo, M. Konishi, N. Itoh, Y. Wang, Stefan R. Bornstein, A. Xu, and X. Li. 2013. Adiponectin Mediates the Metabolic Effects of FGF21 on Glucose Homeostasis and Insulin Sensitivity in Mice. Cell Metabolism 17(5):779-789. doi: 10.1016/j.cmet.2013.04.005 PMID - 23663741

Mai, K., T. Bobbert, C. Groth, A. Assmann, S. Meinus, J. Kraatz, J. Andres, A. M. Arafat, A. F. H. Pfeiffer, M. Möhlig, and J. Spranger. 2010. Physiological modulation of circulating FGF21: relevance of free fatty acids and insulin. American Journal of Physiology Endocrinology and Metabolism 299(1):E126-E130. doi: 10.1152/ajpendo.00020.2010 PMID - 20424140

Mäkelä, J., T. V. Tselykh, F. Maiorana, O. Eriksson, H. Do, G. Mudò, L. T. Korhonen, N. Belluardo, and D. Lindholm. 2014. Fibroblast growth factor-21 enhances mitochondrial functions and increases the activity of PGC-1α in human dopaminergic neurons via Sirtuin-1. SpringerPlus 3(1):2. doi: 10.1186/2193-1801-3-2 PMID - 25932355

Maruyama, R., M. Shimizu, J. Li, J. Inoue, and R. Sato. 2016. Fibroblast growth factor 21 induction by activating transcription factor 4 is regulated through three amino acid response elements in its promoter region. Bioscience, Biotechnology, and Biochemistry 80(5):929-934. doi: 10.1080/09168451.2015.1135045 PMID - 27010621

Mendoza, M. C., E. E. Er, and J. Blenis. 2011. The Ras-ERK and PI3K-mTOR pathways: cross-talk and compensation. Trends in Biochemical Sciences 36(6):320-328. doi: 10.1016/j.tibs.2011.03.006 PMID - 21531565

Menting, J. G., J. Whittaker, M. B. Margetts, L. J. Whittaker, G. K. W. Kong, B. J. Smith, C. J. Watson, L. Žáková, E. Kletvíková, J. Jiráček, S. J. Chan, D. F. Steiner, G. G. Dodson, A. M. Brzozowski, M. A. Weiss, C. W. Ward, and M. C. Lawrence. 2013. How insulin engages its primary binding site on the insulin receptor. Nature 493(7431):241-245. doi: 10.1038/nature11781 PMID - 23302862

Micanovic, R., D. W. Raches, J. D. Dunbar, D. A. Driver, H. A. Bina, C. D. Dickinson, and A. Kharitonenkov. 2009. Different roles of N- and C- termini in the functional activity of FGF21. Journal of Cellular Physiology 219(2):227-234. doi: 10.1002/jcp.21675 PMID - 19117008

Miller, P. J., K. A. Finucane, M. Hughes, and F.-Q. Zhao. 2005. Cloning and Expression of Bovine Glucose Transporter GLUT12. Mammalian Genome 16(11):873-883. doi: 10.1007/s00335-005-0080-5 PMID - 16284803

Min, S. H., D. D. Mackenzie, B. H. Breier, S. N. McCutcheon, and P. D. Gluckman. 1996. Growth-promoting effects of ovine placental lactogen (oPL) in young lambs: comparison with bovine growth hormone provides evidence for a distinct effect of oPL on food intake. Growth Regulation 6(3):144-151.

Mohammadi, M., S. K. Olsen, and O. A. Ibrahimi. 2005. Structural basis for fibroblast growth factor receptor activation. Cytokine & Growth Factor Reviews 16(2):107-137. doi: 10.1016/j.cytogfr.2005.01.008 PMID - 15863029

Molina, R. D., G. Meschia, F. C. Battaglia, and W. W. Hay. 1991. Gestational maturation of placental glucose transfer capacity in sheep. American Journal of Physiology Regulatory, Integrative and Comparative Physiology 261(3):R697-R704. doi: 10.1152/ajpregu.1991.261.3.r697 PMID - 1887958

Moore, J. H., and W. W. Christie. 1979. Lipid metabolism in the mammary gland of ruminant animals. Progress in Lipid Research 17(4):347-395. doi: 10.1016/0079-6832(79)90012-0 PMID - 38463

Morville, T., R. E. Sahl, S. A. J. Trammell, J. S. Svenningsen, M. P. Gillum, J. W. Helge, and C. Clemmensen. 2018. Divergent effects of resistance and endurance exercise on plasma bile acids, FGF19, and FGF21 in humans. JCI Insight 3(15):e122737. doi: 10.1172/jci.insight.122737 PMID - 30089729

Muise, E. S., B. Azzolina, D. W. Kuo, M. El-Sherbeini, Y. Tan, X. Yuan, J. Mu, J. R. Thompson, J. P. Berger, and K. K. Wong. 2008. Adipose fibroblast growth factor 21 is up-regulated by peroxisome proliferator-activated receptor gamma and altered metabolic states. Molecular Pharmacology 74(2):403-412. doi: 10.1124/mol.108.044826 PMID - 18467542

Mulligan, F. J., and M. L. Doherty. 2008. Production diseases of the transition cow. Veterinary Journal 176(1):3-9. doi: 10.1016/j.tvjl.2007.12.018 PMID - 18342556

Nagy, C., and E. Einwallner. 2018. Study of In Vivo Glucose Metabolism in High-fat Diet-fed Mice Using Oral Glucose Tolerance Test (OGTT) and Insulin Tolerance Test (ITT). Journal of Visualized Experiments (131)doi: 10.3791/56672 PMID - 29364280

Nishimura, T., Y. Nakatake, M. Konishi, and I. N. e. Acta. 2000. Identification of a novel FGF, FGF-21, preferentially expressed in the liver. Biochimica et Biophysica Acta

Nygaard, E. B., C. L. Møller, P. Kievit, K. L. Grove, and B. Andersen. 2014. Increased fibroblast growth factor 21 expression in high-fat diet-sensitive non-human primates (Macaca mulatta). International Journal of Obesity 38(2):183-191. doi: 10.1038/ijo.2013.79 PMID - 23736354

Oddy, V. H., J. M. Gooden, G. M. Hough, E. Teleni, and E. F. Annison. 1985. Partitioning of nutrients in merino ewes. II. Glucose utilization by skeletal muscle, the pregnant uterus and the lactating mammary gland in relation to whole body glucose utilization. Australian Journal of Biological Sciences 38(1):95-108. doi: 10.1071/bi9850095 PMID - 4062698

Ornitz, D. M. 2000. FGFs, heparan sulfate and FGFRs: complex interactions essential for development. Bioessays 22(2):108-112. doi: 10.1002/(sici)1521-1878(200002)22:2<108::aid-bies2>3.0.co;2-m PMID - 10655030

Ornitz, D. M., and N. Itoh. 2001. Fibroblast growth factors. Genome Biology 2(3):1.

Ornitz, D. M., and N. Itoh. 2015. The Fibroblast Growth Factor signaling pathway. Wiley Interdisciplinary Reviews: Developmental Biology 4(3):215-266. doi: 10.1002/wdev.176 PMID - 25772309

Owen, B. M., A. L. Bookout, X. Ding, V. Y. Lin, and S. D. Atkin. 2013. FGF21 contributes to neuroendocrine control of female reproduction. Nature Medicine

Owen, B. M., X. Ding, D. A. Morgan, K. C. Coate, A. L. Bookout, K. Rahmouni, S. A. Kliewer, and D. J. Mangelsdorf. 2014. FGF21 acts centrally to induce sympathetic nerve activity, energy expenditure, and weight loss. Cell Metabolism 20(4):670-677. doi: 10.1016/j.cmet.2014.07.012 PMID - 25130400

Pascottini, O. B., J. L. M. R. Leroy, and G. Opsomer. 2020. Metabolic Stress in the Transition Period of Dairy Cows: Focusing on the Prepartum Period. Animals : an open access journal from MDPI 10(8):1419. doi: 10.3390/ani10081419

Petersen, M. C., and G. I. Shulman. 2018. Mechanisms of Insulin Action and Insulin Resistance. Physiological Reviews 98(4):2133-2223. doi: 10.1152/physrev.00063.2017 PMID - 30067154

Rehman, K., M. S. H. Akash, A. Liaqat, S. Kamal, M. I. Qadir, and A. Rasul. 2017. Role of Interleukin-6 in Development of Insulin Resistance and Type 2 Diabetes Mellitus. Critical Reviews in Eukaryotic Gene Expression 27(3):229-236. doi: 10.1615/critreveukaryotgeneexpr.2017019712 PMID - 29199608

Rhoads, R. P., J. W. Kim, M. E. V. Amburgh, R. A. Ehrhardt, S. J. Frank, and Y. R. Boisclair. 2007. Effect of nutrition on the GH responsiveness of liver and adipose tissue in dairy cows. Journal of Endocrinology 195(1):49-58. doi: 10.1677/joe-07-0068 PMID - 17911396

Rico, J. E., W. A. Myers, D. J. Laub, A. N. Davis, Q. Zeng, and J. W. McFadden. 2018. Hot topic: Ceramide inhibits insulin sensitivity in primary bovine adipocytes. Journal of Dairy Science doi: 10.3168/jds.2017-13983 PMID - 29395144

Rico, J. E., S. S. Samii, A. T. Mathews, J. Lovett, N. J. Haughey, and J. W. McFadden. 2017. Temporal changes in sphingolipids and systemic insulin sensitivity during the transition from gestation to lactation. PloS One 12(5):e0176787. doi: 10.1371/journal.pone.0176787 PMID - 28486481

Rosenbaum, M., K. D. Hall, J. Guo, E. Ravussin, L. S. Mayer, M. L. Reitman, S. R. Smith, B. T. Walsh, and R. L. Leibel. 2019. Glucose and Lipid Homeostasis and Inflammation in

Humans Following an Isocaloric Ketogenic Diet. Obesity 27(6):971-981. doi: 10.1002/oby.22468 PMID - 31067015

Ruda, L., C. Raschka, K. Huber, R. Tienken, U. Meyer, S. Dänicke, and J. Rehage. 2019. Gain and loss of subcutaneous and abdominal fat depot mass from late pregnancy to 100 days in milk in German Holsteins. Journal of Dairy Research 86(3):296-302. doi: 10.1017/s0022029919000542 PMID - 31409432

Rukkwamsuk, T., T. A. Kruip, and T. Wensing. 1999. Relationship between overfeeding and overconditioning in the dry period and the problems of high producing dairy cows during the postparturient period. Veterinary Quarterly 21(3):71-77. doi: 10.1080/01652176.1999.9694997

Sadri, H., R. M. Bruckmaier, H. R. Rahmani, G. R. Ghorbani, I. Morel, and H. A. V. Dorland. 2010. ORIGINAL ARTICLE: Gene expression of tumour necrosis factor and insulin signalling-related factors in subcutaneous adipose tissue during the dry period and in early lactation in dairy cows. Journal of Animal Physiology and Animal Nutrition 94(5):e194-e202. doi: 10.1111/j.1439-0396.2010.01005.x PMID - 20579185

Salminen, A., A. Kauppinen, and K. Kaarniranta. 2017. FGF21 activates AMPK signaling: impact on metabolic regulation and the aging process. Journal of Molecular Medicine 95(2):123-131. doi: 10.1007/s00109-016-1477-1 PMID - 27678528

Sarruf, D. A., J. P. Thaler, G. J. Morton, J. German, J. D. Fischer, K. Ogimoto, and M. W. Schwartz. 2010. Fibroblast Growth Factor 21 Action in the Brain Increases Energy Expenditure and Insulin Sensitivity in Obese Rats. Diabetes 59(7):1817-1824. doi: 10.2337/db09-1878 PMID - 20357365

Schams, D., I. Rüsse, E. Schallenberger, S. Prokopp, and J. S. D. Chant. 1984. The role of steroid hormones, prolactin and placental lactogen on mammary gland development in ewes and heifers. Journal of Endocrinology 102(1):121-NP. doi: 10.1677/joe.0.1020121 PMID - 6736849

Schlegel, G., R. Ringseis, J. Keller, F. J. Schwarz, W. Windisch, and K. Eder. 2013. Expression of fibroblast growth factor 21 in the liver of dairy cows in the transition period and during lactation. Journal of Animal Physiology and Animal Nutrition 97(5):820-829. doi: 10.1111/j.1439-0396.2012.01323.x PMID - 22805261

Schlein, C., S. Talukdar, M. Heine, Alexander W. Fischer, Lucia M. Krott, Stefan K. Nilsson, Martin B. Brenner, J. Heeren, and L. Scheja. 2016. FGF21 Lowers Plasma Triglycerides by Accelerating Lipoprotein Catabolism in White and Brown Adipose Tissues. Cell Metabolism 23(3):441-453. doi: 10.1016/j.cmet.2016.01.006 PMID - 26853749

Schoenberg, K. M., S. L. Giesy, K. J. Harvatine, M. R. Waldron, C. Cheng, A. Kharitonenkov, and Y. R. Boisclair. 2011. Plasma FGF21 is elevated by the intense lipid mobilization of lactation. Endocrinology 152(12):4652-4661. doi: 10.1210/en.2011-1425 PMID - 21990311

Shi, S., Y.-W. Lu, J. Richardson, X. Min, J. Weiszmann, W. G. Richards, Z. Wang, Z. Zhang, J. Zhang, and Y. Li. 2018. A systematic dissection of sequence elements determining β-Klotho and FGF interaction and signaling. Scientific Reports 8(1):11045. doi: 10.1038/s41598-018-29396-5 PMID - 30038432

Smith, J. J., A. V. Capuco, W. E. Beal, and R. M. Akers. 1989. Association of prolactin and insulin receptors with mammogenesis and lobulo-alveolar formation in pregnant ewes. International Journal of Biochemistry 21(1):73-81. doi: 10.1016/0020-711x(89)90029-3 PMID - 2473930

Smith, R. W., and A. Walsh. 1982. Effects of pregnancy and lactation on the activities in sheep liver of some enzymes of glucose metabolism. The Journal of Agricultural Science 98(3):563-565. doi: 10.1017/s0021859600054332

Søberg, S., E. S. Andersen, N. B. Dalgaard, I. Jarlhelt, N. L. Hansen, N. Hoffmann, T. Vilsbøll, A. Chenchar, M. Jensen, T. J. Grevengoed, S. A. J. Trammell, F. K. Knop, and M. P. Gillum. 2018. FGF21, a liver hormone that inhibits alcohol intake in mice, increases in human circulation after acute alcohol ingestion and sustained binge drinking at Oktoberfest. Molecular Metabolism doi: 10.1016/j.molmet.2018.03.010 PMID - 29627377

Song, P., C. Zechner, G. Hernandez, J. Cánovas, Y. Xie, V. Sondhi, M. Wagner, V. Stadlbauer, A. Horvath, B. Leber, M. C. Hu, O. W. Moe, D. J. Mangelsdorf, and S. A. Kliewer. 2018. The Hormone FGF21 Stimulates Water Drinking in Response to Ketogenic Diet and Alcohol. Cell Metabolism doi: 10.1016/j.cmet.2018.04.001 PMID - 29657029

Sousa-Coelho, A. L. D., P. F. Marrero, and D. Haro. 2012. Activating transcription factor 4-dependent induction of FGF21 during amino acid deprivation. The Biochemical journal 443(1):165-171. doi: 10.1042/BJ20111748 PMID - 22233381

Steinberg, G. R., and B. E. Kemp. 2009. AMPK in Health and Disease. Physiological Reviews 89(3):1025-1078. doi: 10.1152/physrev.00011.2008 PMID - 19584320

Suzuki, M., Y. Uehara, K. Motomura-Matsuzaka, J. Oki, Y. Koyama, M. Kimura, M. Asada, A. Komi-Kuramochi, S. Oka, and T. Imamura. 2008. betaKlotho is required for fibroblast growth factor (FGF) 21 signaling through FGF receptor (FGFR) 1c and FGFR3c. Molecular Endocrinology 22(4):1006-1014. doi: 10.1210/me.2007-0313 PMID - 18187602

Tacer, K. F., A. L. Bookout, X. Ding, H. Kurosu, G. B. John, L. Wang, R. Goetz, M. Mohammadi, M. Kuro-o, D. J. Mangelsdorf, and S. A. Kliewer. 2010. Research resource: Comprehensive expression atlas of the fibroblast growth factor system in adult mouse. Molecular Endocrinology 24(10):2050-2064. doi: 10.1210/me.2010-0142 PMID - 20667984

Talukdar, S., Y. Zhou, D. Li, M. Rossulek, J. Dong, V. Somayaji, Y. Weng, R. Clark, A. Lanba, Bryn M. Owen, Martin B. Brenner, Jeffrey K. Trimmer, Kathryn E. Gropp, Jeffrey R. Chabot, Derek M. Erion, Timothy P. Rolph, B. Goodwin, and Roberto A. Calle. 2016. A

Long-Acting FGF21 Molecule, PF-05231023, Decreases Body Weight and Improves Lipid Profile in Non-human Primates and Type 2 Diabetic Subjects. Cell Metabolism 23(3):427-440. doi: 10.1016/j.cmet.2016.02.001 PMID - 26959184

Tan, B. K., M. Hallschmid, R. Adya, W. Kern, H. Lehnert, and H. S. Randeva. 2011. Fibroblast Growth Factor 21 (FGF21) in Human Cerebrospinal Fluid. Diabetes 60(11):2758-2762. doi: 10.2337/db11-0672 PMID - 21926274

Tatarczuch, L., C. Philip, and C. S. Lee. 1997. Involution of the sheep mammary gland. Journal of Anatomy 190(3):405-416. doi: 10.1046/j.1469-7580.1997.19030405.x PMID - 9147226

Tuersunjiang, N., J. F. Odhiambo, N. M. Long, D. R. Shasa, P. W. Nathanielsz, and S. P. Ford. 2013. Diet reduction to requirements in obese/overfed ewes from early gestation prevents glucose/insulin dysregulation and returns fetal adiposity and organ development to control levels. American Journal of Physiology Endocrinology and Metabolism 305(7):E868-878. doi: 10.1152/ajpendo.00117.2013 PMID - 23921140

Vázquez-Jiménez, J. G., A. Roura-Guiberna, L. R. Jiménez-Mena, and J. A. Olivares-Reyes. 2019. Role of free fatty acids on insulin resistance. Gaceta Medica de México 153(7)doi: 10.24875/gmm.m18000092

Véniant, M. M., R. Komorowski, P. Chen, S. Stanislaus, K. Winters, T. Hager, L. Zhou, R. Wada, R. Hecht, and J. Xu. 2012. Long-Acting FGF21 Has Enhanced Efficacy in Diet-Induced Obese Mice and in Obese Rhesus Monkeys. Endocrinology 153(9):4192-4203. doi: 10.1210/en.2012-1211 PMID - 22798348

Vernon, R. G., R. A. Clegg, and D. J. Flint. 1981. Metabolism of sheep adipose tissue during pregnancy and lactation. Adaptation and regulation. Biochemical Journal 200(2):307-314. doi: 10.1042/bj2000307 PMID - 7041893

Vernon, R. G., A. Faulkner, W. W. Hay, D. T. Calvert, and D. J. Flint. 1990. Insulin resistance of hind-limb tissues in vivo in lactating sheep. Biochemical journal 270(3):783-786. doi: 10.1042/bj2700783 PMID - 2241910

von Meyenn, F., T. Porstmann, E. Gasser, N. Selevsek, A. Schmidt, R. Aebersold, and M. Stoffel. 2013. Glucagon-induced acetylation of Foxa2 regulates hepatic lipid metabolism. Cell Metabolism 17(3):436-447. doi: 10.1016/j.cmet.2013.01.014

Wang, J. G., Y. Z. Guo, Y. Z. Kong, S. Dai, and B. Y. Zhao. 2018. High non-esterified fatty acid concentrations promote expression and secretion of fibroblast growth factor 21 in calf hepatocytes cultured in vitro. Journal of Animal Physiology and Animal Nutrition 102(1)doi: 10.1111/jpn.12699 PMID - 28447390

Wilson, G. J., B. A. Lennox, P. She, E. T. Mirek, R. J. T. Baghdadi, M. E. Fusakio, J. L. Dixon, G. C. Henderson, R. C. Wek, and T. G. Anthony. 2015. GCN2 is required to increase fibroblast growth factor 21 and maintain hepatic triglyceride homeostasis during

asparaginase treatment. American Journal of Physiology Endocrinology and Metabolism 308(4):E283-E293. doi: 10.1152/ajpendo.00361.2014 PMID - 25491724

Wilson, L. A., S. E. Mills, E. Finley, E. Kilgour, P. J. Buttery, and R. G. Vernon. 1996. Effect of lactation on insulin signal transduction in sheep adipose tissue and skeletal muscle. Journal of Endocrinology 151(3):469-480. doi: 10.1677/joe.0.1510469 PMID - 8994392

Wooding, F. B. P., A. L. Fowden, A. W. Bell, R. A. Ehrhardt, S. W. Limesand, and W. W. Hay. 2004. Localisation of glucose transport in the ruminant placenta: implications for sequential use of transporter isoforms. Placenta 26(8-9):626-640. doi: 10.1016/j.placenta.2004.09.013 PMID - 16085042

Xu, J., D. J. Lloyd, C. Hale, S. Stanislaus, M. Chen, G. Sivits, S. Vonderfecht, R. Hecht, Y.-S. S. Li, R. A. Lindberg, J.-L. L. Chen, D. Y. Jung, Z. Zhang, H.-J. J. Ko, J. K. Kim, and M. M. Véniant. 2009a. Fibroblast growth factor 21 reverses hepatic steatosis, increases energy expenditure, and improves insulin sensitivity in diet-induced obese mice. Diabetes 58(1):250-259. doi: 10.2337/db08-0392 PMID - 18840786

Xu, J., S. Stanislaus, N. Chinookoswong, Y. Y. Lau, T. Hager, J. Patel, H. Ge, J. Weiszmann, S.-C. C. Lu, M. Graham, J. Busby, R. Hecht, Y.-S. S. Li, Y. Li, R. Lindberg, and M. M. Véniant. 2009b. Acute glucose-lowering and insulin-sensitizing action of FGF21 in insulin-resistant mouse models--association with liver and adipose tissue effects. American Journal of Physiology Endocrinology and Metabolism 297(5):E1105-1114. doi: 10.1152/ajpendo.00348.2009 PMID - 19706786

Xue, Y., C. Guo, F. Hu, W. Zhu, and S. Mao. 2019. PPARA/RXRA signalling regulates the fate of hepatic non-esterified fatty acids in a sheep model of maternal undernutrition. Biochimica et Biophysica Acta (BBA) - Molecular and Cell Biology of Lipids:158548. doi: 10.1016/j.bbalip.2019.158548 PMID - 31676441

Yamauchi, T., J. Kamon, Y. Minokoshi, Y. Ito, H. Waki, S. Uchida, S. Yamashita, M. Noda, S. Kita, K. Ueki, K. Eto, Y. Akanuma, P. Froguel, F. Foufelle, P. Ferre, D. Carling, S. Kimura, R. Nagai, B. B. Kahn, and T. Kadowaki. 2002. Adiponectin stimulates glucose utilization and fatty-acid oxidation by activating AMP-activated protein kinase. Nature Medicine 8(11):1288-1295. doi: 10.1038/nm788 PMID - 12368907

Yie, J., R. Hecht, J. Patel, J. Stevens, W. Wang, N. Hawkins, S. Steavenson, S. Smith, D. Winters, S. Fisher, L. Cai, E. Belouski, C. Chen, M. L. Michaels, Y.-S. S. Li, R. Lindberg, M. Wang, M. Véniant, and J. Xu. 2009. FGF21 N- and C-termini play different roles in receptor interaction and activation. FEBS Letters 583(1):19-24. doi: 10.1016/j.febslet.2008.11.023 PMID - 19059246

Young, J. W. 1977. Gluconeogenesis in Cattle: Significance and Methodology. Journal of Dairy Science 60(1):1-15. doi: 10.3168/jds.s0022-0302(77)83821-6 PMID - 320235

Zamuner, F., K. DiGiacomo, A. W. N. Cameron, and B. J. Leury. 2020. Endocrine and metabolic status of commercial dairy goats during the transition period. Journal of Dairy Science doi: 10.3168/jds.2019-18040

Zhang, X., D. C. Y. Yeung, M. Karpisek, D. Stejskal, Z.-G. Zhou, F. Liu, R. L. C. Wong, W.-S. Chow, A. W. K. Tso, K. S. L. Lam, and A. Xu. 2008. Serum FGF21 Levels Are Increased in Obesity and Are Independently Associated With the Metabolic Syndrome in Humans. Diabetes 57(5):1246-1253. doi: 10.2337/db07-1476 PMID - 18252893

Zhang, Y., T. Lei, J. F. Huang, S. B. Wang, and Z.-L. L. a. cellular …. 2011. The link between fibroblast growth factor 21 and sterol regulatory element binding protein 1c during lipogenesis in hepatocytes. Molecular and Cellular Endocrinology

Zhang, Y., R. Proenca, M. Maffei, M. Barone, L. Leopold, and J. M. Friedman. 1994. Positional cloning of the mouse obese gene and its human homologue. Nature 372(6505):425-432. doi: 10.1038/372425a0 PMID - 7984236

Zhao, C., Y. Liu, J. Xiao, L. Liu, S. Chen, M. Mohammadi, C. J. McClain, X. Li, and W. Feng. 2015. FGF21 mediates alcohol-induced adipose tissue lipolysis by activation of systemic release of catecholamine in mice. Journal of Lipid Research 56(8):1481-1491. doi: 10.1194/jlr.m058610 PMID - 26092866

Zhao, F.-Q., P. J. Miller, E. H. Wall, Y.-C. Zheng, B. Dong, M. C. Neville, and T. B. McFadden. 2004. Bovine glucose transporter GLUT8: cloning, expression, and developmental regulation in mammary gland. Biochimica et Biophysica Acta (BBA) - Gene Structure and Expression 1680(2):103-113. doi: 10.1016/j.bbaexp.2004.09.001 PMID - 15488990

Zhao, F. Q. 2014. Biology of glucose transport in the mammary gland. Journal of Mammary Gland Biology and Neoplasia 19(1):3-17. doi: 10.1007/s10911-013-9310-8

Zhao, F. Q., and A. F. Keating. 2007. Expression and Regulation of Glucose Transporters in the Bovine Mammary Gland. Journal of Dairy Science 90:E76-E86. doi: 10.3168/jds.2006-470 PMID - 17517754

CHAPTER 3

INSULIN ACTION AND ADIPOSITY DURING PREGNANCY AND LACTATION IN LEAN AND OBESE EWES

INTRODUCTION

Ruminants develop insulin resistance as a mechanism to spare glucose for fetal growth and milk production (Bell and Bauman, 1997). Dairy cows with insufficient or excessive adiposity entering the transition period are at increased risk of developing infectious or metabolic diseases such as ketosis, fatty liver, clinical hypocalcemia, retained placenta, metritis, and displaced abomasum (Mulligan and Doherty, 2008). Similarly, under- or overweight ewes carrying multiple fetuses are susceptible to developing pregnancy toxemia and reduced productivity (Andrews, 1997; Duehlmeier et al., 2013). Furthermore, the dynamics of internal and external adipose depots are known to be different. For example, Drackley et al. reported that excess nutrition over a period of 8 weeks caused a 2-fold increase in visceral fat mass but had no effect on body condition score (i.e. subcutaneous fat) (Drackley et al., 2014). More recently, Ruda et al. used predictive equations based on ultrasonographic measurements to infer higher mobilization from abdominal than subcutaneous depots during early lactation (Ruda et al., 2019). Finally, visceral adipose tissue is more strongly correlated with insulin resistance than subcutaneous depots in dogs and mice (Lottati et al., 2009; Chen et al., 2012). These observations raise the possibility of a disproportionate role for internal fat depots in modulating insulin action during the pregnancy-lactation cycle in ruminants.

Ford and colleagues have demonstrated the correlation between insulin resistance and fatness as determined by DEXA scanning in pregnant ewes (Tuersunjiang et al., 2013). However, they did not differentiate between internal and external depots. Moreover, we are not aware of studies examining the longitudinal effects of pregnancy and obesity on the dynamics of the fat depots utilizing a precise scanning method. Computed tomography (CT) scanning has been widely accepted as a highly accurate method to repeatedly quantify internal adipose depots.

This technique has recently been used in growing sheep and showed to yield accurate determination of internal fat depots (Rosenblatt et al., 2017).

In the present work, we use nutrition to create substantial fatness differences in pregnant and lactating ewes and performed CT scanning to differentiate between the internal and external adipose depots. We hypothesized that the internal depots will be negatively correlated with insulin sensitivity. Another goal of this experiment was to evaluate the differences between depots during periods of accretion and mobilization of adipose reserves. Based on recent data obtained in dairy cows (Drackley et al., 2014; Ruda et al., 2019), we hypothesize the internal depots will also be more responsive than external fat depots to energy balance changes.

MATERIALS AND METHODS

Animals and Design

An animal experiment consisting of 3 phases was performed with the approval of the Michigan State University and the Cornell University Institutional Care and Use Committees.

Multiparous Polypay X Dorset ewes were selected on the basis of uniform age (1.64 ± 0.16 yrs), body condition (2.92 ± 0.04), and weight (72.66 ± 1.43 kg). Phase I was performed at Michigan State University and lasted 105 days. Immediately before treatment initiation, CT data were obtained by performing whole body computed tomography (CT) on a representative reference group of 8 ewes. Ewes were then randomly allocated to two pens and fed amounts of a moderate energy total mixed ration (TMR) (Table 3.1) providing 100% energy requirements (Lean group), or unlimited amounts of a high energy TMR (Obese group). Feeding was 1X/day at 1600 h. Ewes were mated to a single purebred Polypay ram 45-55 days after treatment initiation, followed by ultrasonographic determination of pregnancy status and fetal number 40 days later using either a GE LOGIQ Book XP Vet (Boston, MA, USA) with a 4 MHz convex transducer or a Chison ECO 6 (Wuxi, Jiangsu, China) with a 3.5 MHz convex transducer. Other procedures performed during Phase I were as follows. Body weight was recorded weekly at 1530 h. Blood samples were obtained by jugular venipuncture at 1530 h on days -196, -147, and -96 (all times given relative to parturition on day 0). Blood samples were mixed with heparin (15 U/mL) and centrifuged at 3,000 rpm (2171 × *g*) for 15 min at 4˚C. Resulting plasma was stored at -20˚C until analyzed later for metabolites and hormones. Body condition scoring and ultrasonographic determination of fat were performed on days -196, -147, and -96.

The rest of the experiment was conducted at Cornell University and consisted of the second half of pregnancy (Phase II, day -91 to day 0) and early lactation (Phase III, through day

24 or day 38). A first cohort of twin-bearing lean and obese ewes (n=8) continued on the same dietary treatment by consuming soy hull diets (Table 1; moderate energy soy hull for the lean and high energy soy hull for the obese). A second cohort of ewes bearing 2 (4 lean, 3 obese) or 3 lambs (2 lean, 3 obese) were treated similarly but consumed a single corn diet (Table 3.1) instead of the soy hull diets. Feeding for both cohorts was 1X/day at 0800 h. Other routine procedures during Phase II were as follows. Ewes were weighed weekly at 1500 h. In the case of lean ewes, feed allowances were increased with advancing pregnancy in accordance with NRC recommendations (NRC Nutrient Requirements of Sheep, 1985). Blood samples were collected by jugular venipuncture at 0730 h 3X/week beginning on day -46. Following collection, samples were processed and stored as described before.

In addition, ewes were studied during 5-day long study windows between days -71 to -67 (mid-pregnancy) and days -21 to -17 (late pregnancy). The standard set of procedures during study windows is as follows. On day 1, ewes were fitted with bilateral intrajugular catheters (Tygon S-54-HL, 1.02-mm i.d. × 1.78-mm o.d.; Saint-Gobain Performance Plastics, Akron, OH). Starting at 0800 h the following morning, blood samples were collected every 30 min until feeding at 0900 h. Glucose tolerance tests (GTT) and insulin tolerance tests (ITT) were respectively performed on day 3 and 4. On these days, feed was offered at 0600 h and removed 2 h later. The metabolic tests were then performed at 1600 h using a dose of 0.25 g/kg BW glucose for the GTT (50% wt/vol, VetOne, Boise, ID) and 0.1 IU/kg BW insulin for the ITT (Sigma Aldrich, St. Louis, MO). All blood samples were processed immediately for plasma and stored as described before. Finally, CT, ultrasound backfat measurements, and body condition scoring were performed on the final day.

Phase III started after parturition and was carried through 24 days of lactation for the first cohort and 38 days of lactation for the second cohort. During this time, the first cohort received the moderate energy soy hull-based diet, and the second cohort continued to receive the corn-based diet (Table 3.1). At parturition, litters were standardized to 2 lambs and all ewes were fed ad libitum for the first 5 days to establish copious milk secretion. Beginning on day 6, all ewes were restricted to 70% of their predicted energy requirements for lactation based on their non-pregnant/non-lactating weight at the start of the experiment. Feeding was 1X/day at 0800 h. Routine procedures during Phase III included blood samples by jugular venipuncture at 0730 h on day 5, 7, 11, 14, and 18 for both cohorts and on additional days 25, 31, and 34 for the second cohort. Blood samples were stored and processed as described above. Ewes were weighed weekly at 1500 h; lambs were weighed at 0900 h on days 1, 3, 5, 8, 10, 12, 14, 16, 18, and 20 for both cohorts and on additional days 23, 26, 29, 32, and 35 for the second cohort. Finally, milk samples were collected on days 2, 6, 10, 14, and 18 for both cohorts and on additional days 26, 30, and 34 for the second cohort. Finally, the 5-day study window was repeated starting on day 20 for the first cohort and day 34 for the second cohort. Procedures and their sequence during the study window were exactly as described for Phase II.

Table 3.1. Ingredient and nutrient composition of the diets

Item	Moderate Energy TMR	High Energy TMR	Moderate Energy Soy Hull Diet	High Energy Soy Hull Diet	Corn Diet	Hay
Ingredient (%DM)						
Corn Silage	38.0	29.1	-	-	-	-
Haylage	20.5	15.7	-	-	-	-
Soy Hulls	-	-	43.1	35.1	-	-
High Moisture Corn	32.0	24.5	-	-	-	-
Corn	-	23.3	23.6	30.9	59.4	-
Wheat Midds	-	-	19.9	19.9	20.1	-
Soybean Meal	9.6	7.4	8.5	9.0	12.8	-
Molasses	-	-	1.61	1.62	2.04	-
CU Sheep Mineral[1]	-	-	1.12	1.12	1.13	-
Calcium Carbonate	-	-	1.12	1.34	2.60	-
Ammonium Chloride	-	-	0.78	0.78	0.62	-
Monocal - 21%	-	-	-	-	0.83	-
Magnesium Chloride	-	-	-	-	0.14	-
Pellet Binder	-	-	0.28	0.28	0.28	-
Chemical Analysis (DM)						
CP (%)	15.6	13.8	17.2	17.7	17.2	10.8
ADF (%)	30.5	21.1	23.8	17.0	6.6	40.9
aNDF (%)	41.1	28.1	39.7	28.3	14.1	63.9
TDN (%)	69.0	73.0	74.0	78.0	82.0	66.0
Ca (%)	0.91	0.63	0.60	0.63	0.87	0.37
P (%)	0.31	0.33	0.40	0.46	0.59	0.26
ME (Mcal/Kg)	2.48	2.63	2.66	2.81	2.95	2.38

[1]Contained 21.2% Ca, 33.5% Salt, 167 ppm Se, 1.37% Zn, 6740 ppm Mn, 4030 ppm Fe, 318 ppm I, 34.5 ppm Co

Analysis of Metabolites and Insulin

Plasma fatty acids, glucose, and β-hydroxybutyrate (BHB) were analyzed using spectrophotometric methods based on the enzymes acyl coenzyme A–oxidase, glucose oxidase, and BHB dehydrogenase, respectively (Block et al., 2001; Caixeta et al., 2017). The plasma concentration of insulin was determined using a double antibody RIA validated in ruminants (Caixeta et al., 2017). The plasma glucose response area was calculated between 0 and 90 min for the GTT and between 0 and 45 min for the ITT; these values were corrected for baseline concentrations (mean of concentrations at −10, −5, and 0 min for both the GTT and ITT). The plasma insulin response area during the GTT was calculated between 0 and 120 min and was corrected for baseline concentrations (mean of concentrations at −10 and −5 min). Inter- and intra-assay coefficients of variation were <10 and <7% respectively for metabolite assays, and <9 and <7% respectively for insulin assays.

Fatness Indices

Body condition scoring was based on the 5-point scale system defined by Russel in 1984 (1=thin, 5=fat) (Russel, 1984). Backfat measurements were obtained using the ultrasound machines described previously during Phase I (both units were validated to obtain the same measurements). During Phases II and III, backfat was measured with a portable ultrasound machine equipped with a 7.5 MHz probe (Easi-Scan II, BCF Technology Ltd., Livingston, UK). Internal electronic calipers were utilized to obtain measurements with each machine. Measurements were taken 1.5 inches from the left side of the spinal cord at the level of the lumbar 5 vertebra. The recorded value was the average of 3 separate measurements.

The CT was performed as follows. Feed and water were respectively removed 12 h and 8 h prior to the scan. Each ewe was premedicated with butorphanol (0.05 mg/kg) and/or

Midazolam (0.1 mg/kg) followed by a 1:1 ketamine/propofol mix (3mg/kg each or until anesthetically induced) intravenously. Additional propofol (1-2 mg/kg) was administered if more induction agent was required for anesthetization. Ewes were then intubated and subjected to inhalant anesthesia (isoflurane) for whole body CT using a 16-slice CT scanner (Aquilion LB, Toshiba American Medical Systems), including 120 kVp, automated mA (SUREExpose-high quality), 1 mm slice thickness, pitch factor 1.0, 512 _ 512 matrix and the smallest possible scan field of view. Ewes were placed in sternal position for CT data acquisition.

Volume of total and internal fat were obtained using a computer algorithm previously adapted for use in sheep (Rosenblatt et al., 2017). In brief, the computer algorithm was implemented using the VisionX V4 software system (Vision and Image Analysis Group, Cornell University, http://www.via.cornell.edu/visionx/). The algorithm was run on a Supermicro server with Quad Dual Core AMD Opteron Processors with 32GB RAM running CentOS 6 (Linux). First, the whole body was segmented from the background, then fat volumes were calculated by summing the volume of pixels that had density values between -190 and -30 Hounsfield units in the proper region (Yoshizumi et al., 1999; Nemoto et al., 2014). Internal fat volumes were estimated from the visceral region of the trunk, which was approximated using a convex hull of an extended rib cage and caudally projected sternum (Rosenblatt et al., 2017). Retroperitoneal fat was included in the internal fat volume measurements (Hung et al., 2014; Nemoto et al., 2014). The process was semi-automated in that it involved an operator marking key anatomical landmarks, such as the extents of the internal region, manually. Some manual adjustments were made as needed to mark the limit of the internal cavity. Data obtained from each individual CT were: (1) whole body volume (cm^3); (2) total fat volume (cm^3); and (3) internal fat volume (cm^3). External fat volumes were obtained by difference between total and internal fat volumes.

Calculation of Fat Depot Dynamics and Statistical Analysis

Fat accretion was calculated by a difference between mid-pregnancy and basal CT data. Basal CT data were estimated for each ewe as follows. Body volume was obtained from the weight-to-volume relation derived from the reference group. Volume of internal and external fat were then calculated as the product of volume and fraction of total volume occupied by internal and external fat in the reference group. Fat mobilization was calculated by difference between late pregnancy and lactation CT data.

All data were analyzed by a mixed model using the fit model procedure of JMP Pro 14.3.0 statistical software (SAS Institute Inc., Cary, NC). Data collected at a single timepoint were analyzed using a model accounting for treatment (lean vs. obese), diet (soy hull vs. corn), and their interactions as fixed effects and animal as the random effect. Data collected over time during pregnancy and lactation were analyzed separately. They were analyzed using a mixed model accounting for treatment (lean vs. obese), time, and their interactions as fixed effects and animal as the random effect. Parametric Pearson Correlations were utilized to determine relationships between plasma glucose and insulin response areas obtained during GTT and ITT and fatness indices. Statistical significance and tendency were respectively set at $P < 0.05$ and $P < 0.10$ for main effects and at $P < 0.10$ and $P < 0.15$ for the interactions.

RESULTS

Comparison of soy hull-based and corn-based diets

The experiment involved two cohorts of ewes fed to estimated energy requirement (lean) or consuming unlimited amounts of energy (obese) for a 50-day premating period and during pregnancy. For the first cohort, feeding levels were achieved by feeding corn silage/haylage TMR until day -90 (all times given relative to parturition on day 0) and soy hull diets (SH) thereafter (Table 3.1). Obese ewes gained weight rapidly over the first 100 days of the experiment whereas lean ewes remained at the same weight (Fig. 3.1A; Obesity × Day, $P<0.0001$). As a result, the weight difference between the two groups exceeded 25 kg by day -105. This difference in body weight did not grow further during the last 80 days of pregnancy. As expected, the weight gain of obese sheep was associated with a nearly 2-fold higher energy intake until day -40 (Fig. 3.1A; Obesity × Day, $P<0.0001$). From that point on, energy intake in obese ewes progressively dropped and became identical to that of lean ewes over the last 15 days of pregnancy.

A major drop in energy intake in late pregnancy has not been reported before in obese ewes consuming high-energy corn- or barley-based diets (Wallace et al., 2005; Long et al., 2010; Fensterseifer et al., 2018). To assess whether this related to use of a high-energy soy hull diet, a second cohort of ewes were subjected to the same design except for the use of a corn-based diet during the second half of pregnancy. As shown in Figure 3.1B, profiles of body weight seen in both lean and obese ewes mirrored those seen in the first cohort. More importantly, a reduction in energy intake was again seen in the obese ewes over the last 40 days of pregnancy. This suggests that stage of gestation rather than the type of high-energy diet is the main factor driving reduced energy intake in obese ewes.

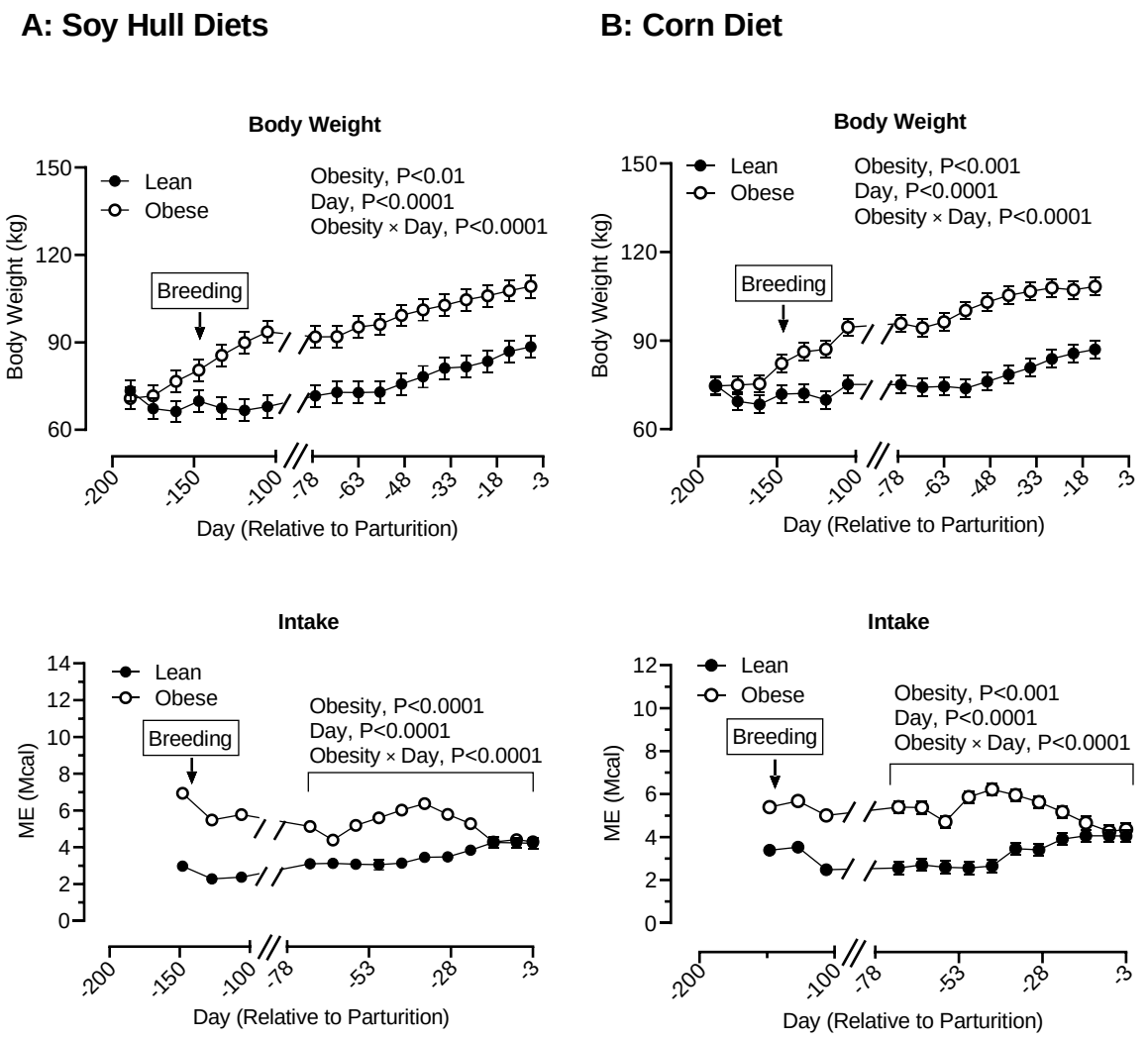

Figure 3.1. Energy intake and body weight profiles of lean and obese ewes. Ewes were fed energy-dense diets before and after breeding in amounts supporting appropriate fat deposition (amounts providing 100% of energy requirements; Lean) or excessive fat deposition (unlimited amounts; Obese). The energy-dense diets were corn silage:haylage TMR for the first 105 days and either soy hull or corn-based dry pelleted diets afterwards. Energy intake and body weight for Lean and Obese ewes receiving soy hull diets (A) or the corn diet (B). Each data point represents the LSM ± SE of 6-8 animals. The effect of obesity, day, and the interaction of obesity and day (Obesity × Day) are reported when significant.

Next, we characterized the profiles of plasma insulin, glucose, and fatty acids (Fig. 3.2). For the soy hull-based diets, plasma glucose was elevated in obese ewes relative to that of lean ewes within 50 days of treatment initiation and remained elevated until declining over the final 3 weeks of gestation (Obesity × Day, $P<0.01$). Obese ewes experienced a gradual increase in plasma insulin reaching a 5-fold elevation by day -45 relative to lean ewes, followed by a gradual reduction over the last 45 days of gestation (Obesity × Day, $P<0.0001$). Declining glucose and insulin in late pregnant ewes may be explained by the coincidental fall in energy intake. Fatty acids were elevated in lean relative to obese ewes except for the last 3 weeks of pregnancy (Obesity × Day, $P<0.01$). Use of the corn diet led to near identical treatment effects on the profiles of plasma glucose, insulin and fatty acids (Fig. 3.2B). In aggregate, the temporal profiles of body weight, energy intake, and plasma variables confirm identical effects of excessive energy independently of the type of diet used during the second half of pregnancy (i.e. soy hull or corn based). Accordingly, both cohorts were combined for all subsequent analyses performed during pregnancy.

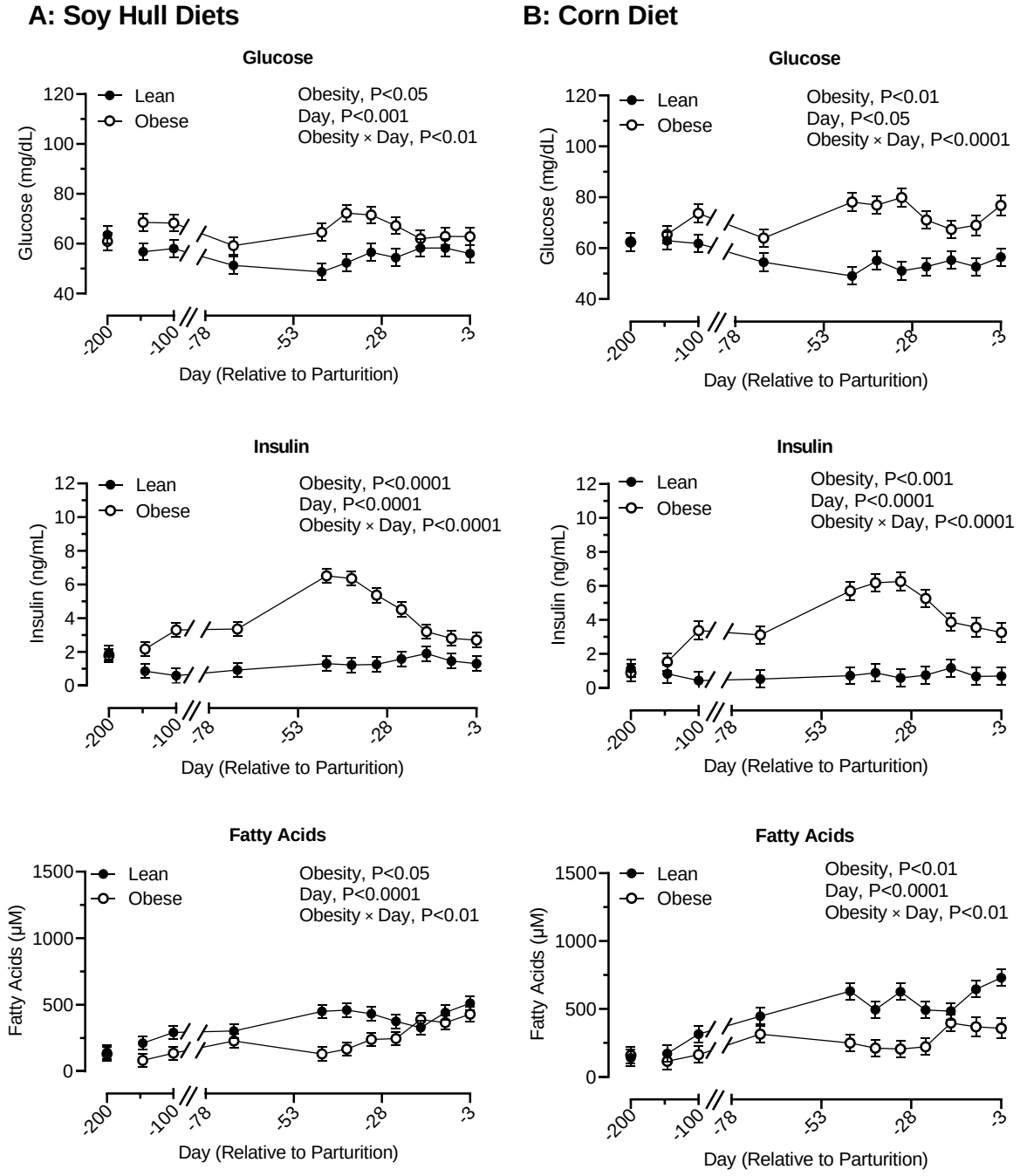

Figure 3.2. Plasma profile of energy-related variables in lean and obese ewes. Ewes were fed energy-dense diets before and after breeding in amounts supporting appropriate fat deposition (amounts providing 100% of energy requirements; Lean) or excessive fat deposition (unlimited amounts; Obese). The energy-dense diets were corn silage:haylage TMR for the first 105 days and either soy hull or corn-based dry pelleted diets afterwards. Plasma glucose, insulin, fatty acids, and β-hydroxybutyrate (BHBA) in Lean and Obese ewes receiving the soy hull diet (A) or corn diet (B). Each data point represents the LSM ± SE of 6-8 animals. The effect of obesity, day, and the interaction of obesity and day (Obesity × Day) are reported when significant.

Effect of fatness on insulin action during mid-pregnancy

Data collected during the mid-pregnancy study window are summarized in Table 3.2. Irrespective of diet, obese ewes consumed >1.6-fold more energy than lean ewes and were 20 kg heavier (Obesity, $P<0.0001$). Adiposity was first quantified using conventional measurements of body condition score (BCS) and backfat thickness. By mid-pregnancy, obese ewes had BCS of 4 or more versus 2.5-3.0 in the lean ewes and nearly twice as much backfat thickness (Obesity, $P<0.0001$). Second, we utilized CT scanning to obtain quantitative estimates of whole body fatness and its distribution between external and internal sites. CT scans obtained from representative mid-pregnant lean and obese ewes are shown in Figure 3.3. When assessed at the level of the thoracic vertebrae 11, obese ewes not only had a larger volume but also more external and internal fat than lean ewes, in both relative and absolute terms (Fig. 3.3A). The same conclusion was obtained from plots obtained after integrating CT scan slices collected over the entire body (Fig. 3.3B).

Numerical CT scan data are presented in Table 3.2. Body and total fat volume were respectively 1.3 and 2.0 fold greater in obese than lean ewes (Obesity, $P<0.0001$). Total fat expressed as % of body volume was respectively 20 and 34% for lean and obese ewes (Obesity, $P<0.0001$). Similar treatment effects were seen when internal and external fat were expressed in the same manner (Obesity, $P<0.0001$). The type of diet fed in late pregnancy had no effect on these variables.

External fat expressed as a percent of total fat was lower in lean than obese ewes (Obesity, $P<0.01$); the reciprocal result was seen for internal fat ($P<0.01$). These results suggested external fat as the predominant site of excess lipid deposition in obese ewes. This was assessed by obtaining the total volume of fat accreted from initiation of treatment until mid-

pregnancy and calculating proportions deposited as internal and external fat (Fig. 3.4). This analysis revealed that 70-78% of fat was accreted in the external location versus only 22-30% in the internal location (Depot, $P<0.001$); fatness had no effect on these variables.

Table 3.2. Whole animal performance and metabolic parameters in lean and obese sheep in mid-pregnancy[1]

	Soy Hull Diet		Corn Diet			P Value[3]		
	Lean	Obese	Lean	Obese	SD	Obesity	Diet	Obesity*Diet
Whole Animal								
Intake (Mcal ME)[2]	3.1	4.8	2.8	6.0	0.8	<0.0001	NS	<0.05
Body Weight (kg)	71.8	91.6	74.2	94.3	9.3	<0.0001	NS	NS
Fatness Indices								
BCS[2]	3.0	4.7	2.9	4.1	0.4	<0.0001	<0.05	NS
Backfat (mm)	7.4	13.4	7.0	18.6	3.7	<0.0001	NS	<0.06
CT Scan								
Volume (cm^3)								
Body	75312	96805	76025	99945	10364	<0.0001	NS	NS
Fat	14889	33495	15180	34526	5610	<0.0001	NS	NS
Fatness (% Body Volume)								
Body	19.7	34.2	19.8	34.2	4.0	<0.0001	NS	NS
Internal	7.8	12.0	8.7	12.4	1.8	<0.0001	NS	NS
External	11.9	22.2	11.0	21.9	2.9	<0.0001	NS	NS
Fraction (% Total Fat)								
Internal	39.8	34.9	45.0	36.4	4.7	<0.01	<0.08	NS
External	60.2	64.1	55.0	63.6	4.5	<0.01	NS	NS
Plasma								
Insulin (ng/mL)	0.87	3.41	0.52	3.11	0.83	<0.0001	NS	NS
Glucose (mg/dL)	51.3	59.2	54.5	64.0	6.6	<0.01	NS	NS
Fatty Acids (μM)	303.4	228.8	446.0	314.2	140.0	<0.1	<0.05	NS
BHBA (mM)[2]	0.55	0.53	0.35	0.41	0.13	NS	<0.01	NS

[1]Ewes were fed soy hull or corn-based diets in amounts supporting appropriate fat deposition (amounts providing 100% of energy requirements; Lean) or excessive fat deposition (unlimited amounts; Obese). Data were collected between day -71 to day -67 (n = 6-8 ewes per treatment)

[2]ME, metabolizable energy; BCS, body condition score; BHBA; β-hydroxybutyric acid

[3]Type I probability error. NS = P>0.1

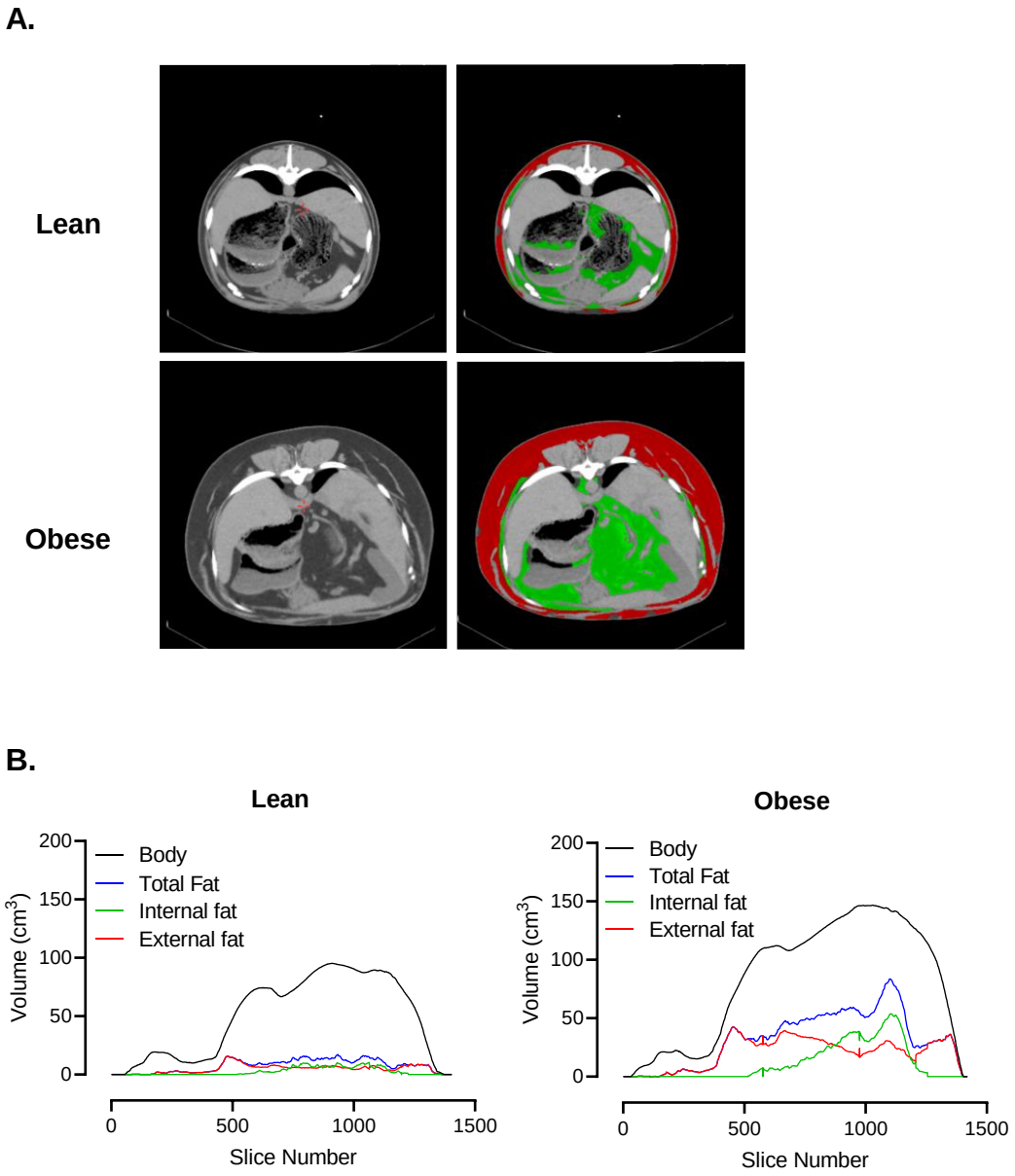

Figure 3.3. Internal and external fat volume by CT scanning. Representative CT scanning data obtained on day 79 of pregnancy. (A) 1 mm-slice obtained at the level of thoracic vertebra 11 of a representative lean or obese sheep. The slices are shown in their native grey scale (left) and after computer-driven detection (right) of internal (green) and external fat (red). (B) Computer-driven reconstruction of whole body volume (black) for a representative lean and obese ewe and volumes occupied by total (blue), internal (green), and external fat (red).

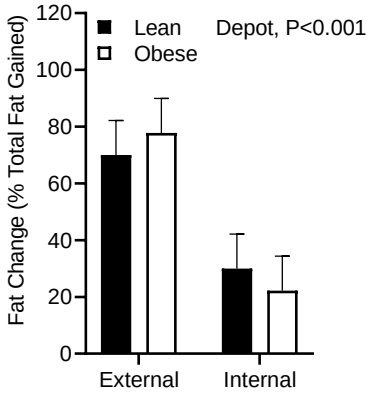

Figure 3.4. Gain of fat by depot location in lean and obese ewes. Ewes were fed energy-dense diets before and after breeding in amounts supporting appropriate fat deposition (amounts providing 100% of energy requirements, lean; or excessive fat deposition, obese). CT data obtained from the pre-treatment reference group before treatment and at mid-pregnancy were used to calculate fat accumulation from internal and external depots. Each bar represents the LSM ± SE of 14 ewes compared to the pre-treatment average.

Next, we assessed effect of fatness on various indices of insulin action. The plasma concentrations of glucose and insulin were elevated in obese sheep samples relative to those of lean sheep irrespective of diet (Table 3.2; Obesity, $P<0.01$ or less). The GTT test revealed slower glucose disposal in SH than corn-fed ewes (Fig. 3.5A; Diet, $P<0.01$), but otherwise did not uncover an effect of fatness, including on glucose-stimulated insulin secretion. In contrast, the ITT test revealed faster insulin-stimulated glucose disposal in lean than obese ewes and no effect of diet (Fig. 3.5B; Obesity, $P<0.01$).

Finally, we assessed associations between dynamic indices of insulin action and various fatness indices. The plasma glucose and insulin response areas during GTT were not associated with any fatness indices (Table 3.3 and not shown). In contrast, weak inverse relationships were found between glucose response area during the ITT and fatness measured by CT scan (external and total fat as a % of body volume), backfat thickness, and BCS. In contrast, the glucose response area during ITT was positively associated with the fraction of total fat accounted by internal fat.

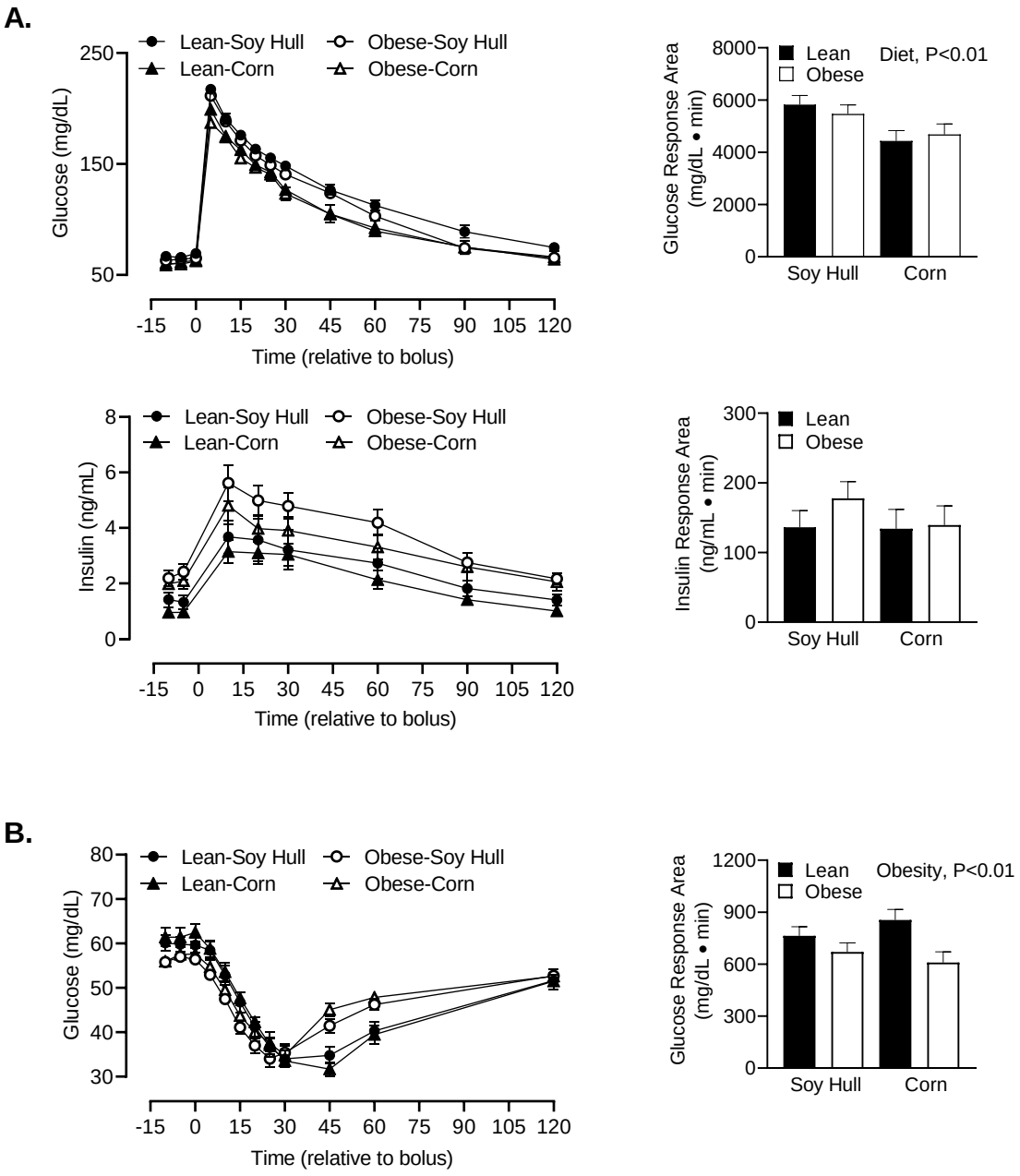

Figure 3.5. Glucose and insulin tolerance in mid-pregnant lean and obese ewes. Ewes were fed energy-dense diets based on either soy hull or corn in amounts supporting appropriate fat deposition (amounts providing 100% of energy requirements; Lean) or excessive fat deposition (unlimited amounts; Obese). (A) Plasma glucose (top) and insulin (bottom) responses during the GTT performed on day 77 of pregnancy. Response areas are shown on the right and were calculated over 90 min for glucose and over 120 min for insulin. (B) Plasma glucose response during the ITT performed on day 78 of pregnancy. Response area is shown on the right and is calculated over 45 min. For all graphs and panels, data shown represent the LSM ± SE of 6-8 ewes, with the effects of obesity, diet, and the interaction of obesity and diet (Obesity × Diet) reported when significant.

Table 3.3. Correlations between fatness indices and glucose response during glucose and insulin tolerance tests in mid-pregnant ewes[1]

	GTT AUC[2]		ITT AUC[2]	
	R	P Value[3]	R	P Value[3]
BCS	0.12	NS	-0.37	<0.06
Backfat	-0.15	NS	-0.36	<0.07
Body fatness	0.06	NS	-0.35	<0.07
Internal Fatness	-0.04	NS	-0.24	NS
External Fatness	0.10	NS	-0.38	<0.05
Internal Fat Fraction	-0.31	NS	0.37	<0.06
External Fat Fraction	0.27	NS	-0.31	NS

[1]Data were collected in lean and obese ewes between day -71 and -67 of pregnancy.

[2]AUC for plasma glucose during glucose tolerance (GTT) and insulin tolerance (ITT).

[3]Type I probability error, NS = P>0.10

Effect of fatness on insulin action during late pregnancy

Data collected during the late pregnancy study window are summarized in Table 3.4. Lean ewes received additional feed during this period in accordance with estimated requirements in late pregnancy (NRC Nutrient Requirements of Sheep, 1985). Nevertheless energy intake remained higher in obese than lean ewes (Obesity, $P<0.01$). Obese ewes maintained a >20 kg weight difference compared to lean ewes and higher values for all indices of fatness (i.e. BCS, backfat, CT scan fat expressed as a volume and as a % of body volume; $P<0.0001$). Notably, all groups gained ~10 kg body weight between mid- and late pregnancy (compare Tables 3.2 & 3.4). This appears to reflect predominantly the growth of the products of conception because total body volume was also increased in all groups by 10,000-12,000 cm^3 in absence of meaningful increases in absolute values of the various fatness indices between mid- and late pregnancy.

The plasma concentration of insulin and glucose were significantly elevated in obese relative to lean ewes (Table 3.4; $P<0.0001$). Both obesity and the soy hull diets impaired glucose disposal during the GTT (Fig. 3.6A; Obesity and Diet, $P<0.001$ or less); insulin secretion was not affected by either factor. Obesity also impaired glucose disposal during the ITT (Fig. 3.6B; Obesity, $P<0.06$). Impairment of glucose disposal by obesity during both ITT and GTT suggest a more potent effect of this factor in late than mid-pregnancy. This possibility was assessed further by computing correlations between the glucose response areas obtained during GTT and ITT and indices of adiposity (Table 3.5). Both number and strength of association increased in late pregnancy relative to results obtained in mid-pregnancy (compare Tables 3.3 & 3.5). Notably, most indices of fatness were now associated with impaired glucose disposal, not only during the ITT but also during the GTT. Unexpectedly, correlations suggested a more negative effect of external than internal fat on indices of glucose disposal.

Table 3.4. Whole animal performance and metabolic parameters in lean and obese sheep in late pregnancy[1]

	Soy Hull Diet		Corn Diet			P Value[3]		
	Lean	Obese	Lean	Obese	SD	Obesity	Diet	Obesity*Diet
Whole Animal								
Intake (Mcal ME)[2]	4.3	4.9	4.1	5.5	0.8	<0.01	NS	NS
Body Weight (kg)	81.3	104.6	83.8	107.8	10.0	<0.0001	NS	NS
Fatness Indices								
BCS[2]	3.0	4.8	2.4	4.9	0.3	<0.0001	<0.05	<0.01
Backfat (mm)	6.3	13.1	6.3	14.7	3.1	<0.0001	NS	NS
CT Scan[6]								
Volume (cm^3)								
Body	86527	111036	86428	112898	10803	<0.0001	NS	NS
Fat	17043	36723	15896	37628	5291	<0.0001	NS	NS
Fatness (% Body Volume)								
Body	19.6	33.5	18.4	33.2	4.0	<0.0001	NS	NS
Internal	7.4	11.1	7.5	10.5	1.9	0.0001	NS	NS
External	12.2	22.4	10.9	22.7	3.0	<0.0001	NS	NS
Fraction (% Total Fat)								
Internal	37.6	33.1	40.7	31.9	5.2	<0.01	NS	NS
External	62.4	67.9	59.3	68.1	5.2	<0.01	NS	NS
Plasma								
Insulin (ng/mL)	1.49	4.57	0.75	5.06	1.39	<0.0001	NS	NS
Glucose (mg/dL)	55.3	67.2	52.7	69.9	6.7	<0.0001	NS	NS
Fatty Acids (μM)	356.8	247.1	492.1	173.7	134.7	<0.001	NS	<0.1
BHBA (mM)[2]	0.51	0.78	0.37	0.45	0.18	<0.05	<0.01	NS

[1]Ewes were fed soy hull or corn-based diets in amounts supporting appropriate fat deposition (amounts providing 100% of energy requirements; Lean) or excessive fat deposition (unlimited amounts; Obese). Data were collected between day -21 to day -17 (n = 4-7 ewes per treatment)

[2]ME, metabolizable energy; BCS, body condition score; BHBA; β-hydroxybutyric acid

[3]Type I probability error. NS = P>0.1

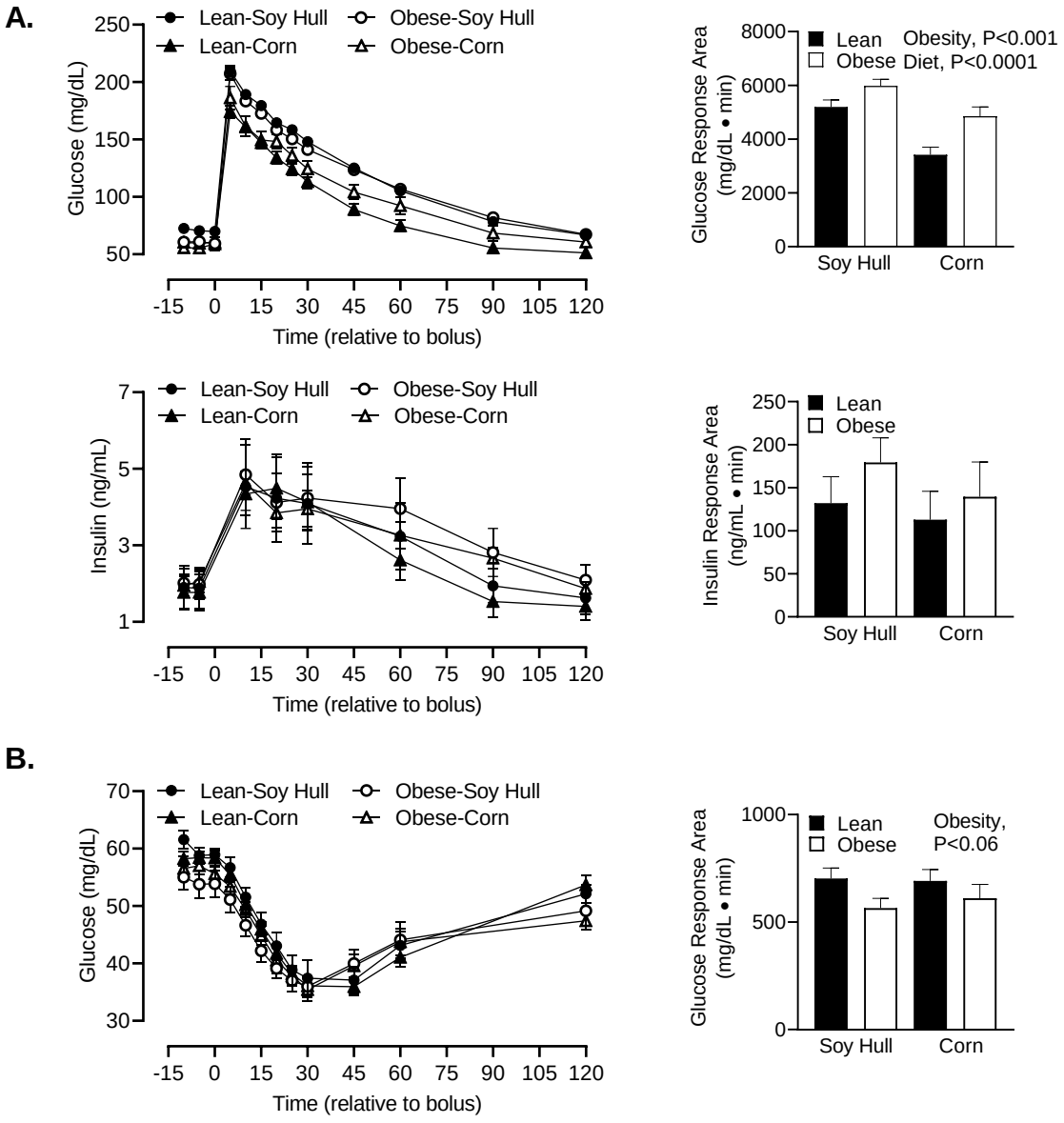

Figure 3.6. Glucose and insulin tolerance in late pregnant lean and obese ewes. Ewes were fed energy-dense diets based on soy hull or corn in amounts supporting appropriate fat deposition (amounts providing 100% of energy requirements; Lean) or excessive fat deposition (unlimited amounts; Obese). (A) Plasma glucose (top) and insulin (bottom) responses during the GTT performed on day 127 of pregnancy. Response areas are shown on the right and were calculated over 90 min for glucose and over 120 min for insulin. (B) Plasma glucose response during the ITT performed on day 128 of pregnancy. Response area is shown on the right and is calculated over 45 min. For all graphs and panels, data shown represent the LSM ± SE of 4-7 ewes, with the effects of obesity, diet, and the interaction of obesity and diet (Obesity x Diet) reported when significant.

Table 3.5. Correlations between fatness indices and glucose response during glucose and insulin tolerance tests in late pregnant ewes[1]

	GTT Glucose AUC[2]		ITT Glucose AUC[2]	
	R	P Value[3]	R	P Value[3]
BCS	0.64	<0.001	-0.44	<0.05
Backfat	0.43	<0.05	-0.45	<0.05
Body fatness	0.57	<0.01	-0.46	<0.05
Internal Fatness	0.42	<0.05	-0.33	<0.10
External Fatness	0.58	<0.01	-0.48	<0.05
Internal Fat Fraction	-0.51	<0.01	0.32	NS
External Fat Fraction	0.53	<0.01	-0.39	<0.05

[1]Data were collected in lean and obese ewes between day -21 and -17 of pregnancy.

[2]AUC for plasma glucose during glucose tolerance (GTT) and insulin tolerance (ITT).

[3]Type I probability error, NS = P>0.10

Effect of fatness on insulin action during early lactation

After parturition, all ewes were fed unlimited amounts of a single diet for 5 days (moderate SH diet for the SH cohort; corn diet for the corn cohort). Starting on day 6, each ewe received a feed allowance covering 70% of lactation requirements calculated on the basis of its body weight on day 0 of the experiment. Ewes were then studied until day 24 (SH ewes) or 38 of lactation (CD ewes).

Temporal profiles of body weight and plasma variables are shown for the SH cohort in Figure 3.7. Obese and lean ewes lost weight at the same rate and mounted similar plasma glucose, insulin, and fatty acid responses to feed restriction (Obesity × Day, $P>0.40$ for all). Plasma BHBA was the only exception, rising to higher concentrations over time in lean than obese ewes (Obesity × Day, $P<0.1$). Lean and obese ewes supported identical lamb growth rates (332.4 vs. 313.3 g/day/lamb) and produced milk of similar composition (data not shown), suggesting that maternal fatness did not impact lactation. Data collected during the lactation study window are given in Table 3.6. Obese ewes were 17 kg heavier than lean ewes (Obesity, $P<0.01$) and higher BCS and backfat thickness (Obesity, $P<0.01$ or less). By CT scan analysis, obese ewes were twice as fat as lean ewes (Obesity, $P<0.0001$) with internal fat accounting for 33% of total fat versus 41% for lean ewes (Obesity, $P<0.01$). Despite substantially greater fatness, obese ewes did not differ from lean ewes in terms of plasma glucose, insulin, fatty acids, or BHBA. Similarly, obese ewes did not suffer from reduced glucose disposal during GTT and ITT or exaggerated insulin secretion during GTT (Fig. 3.8). Overall, these data suggest similar insulin action in energy-deficient obese and lean ewes during lactation.

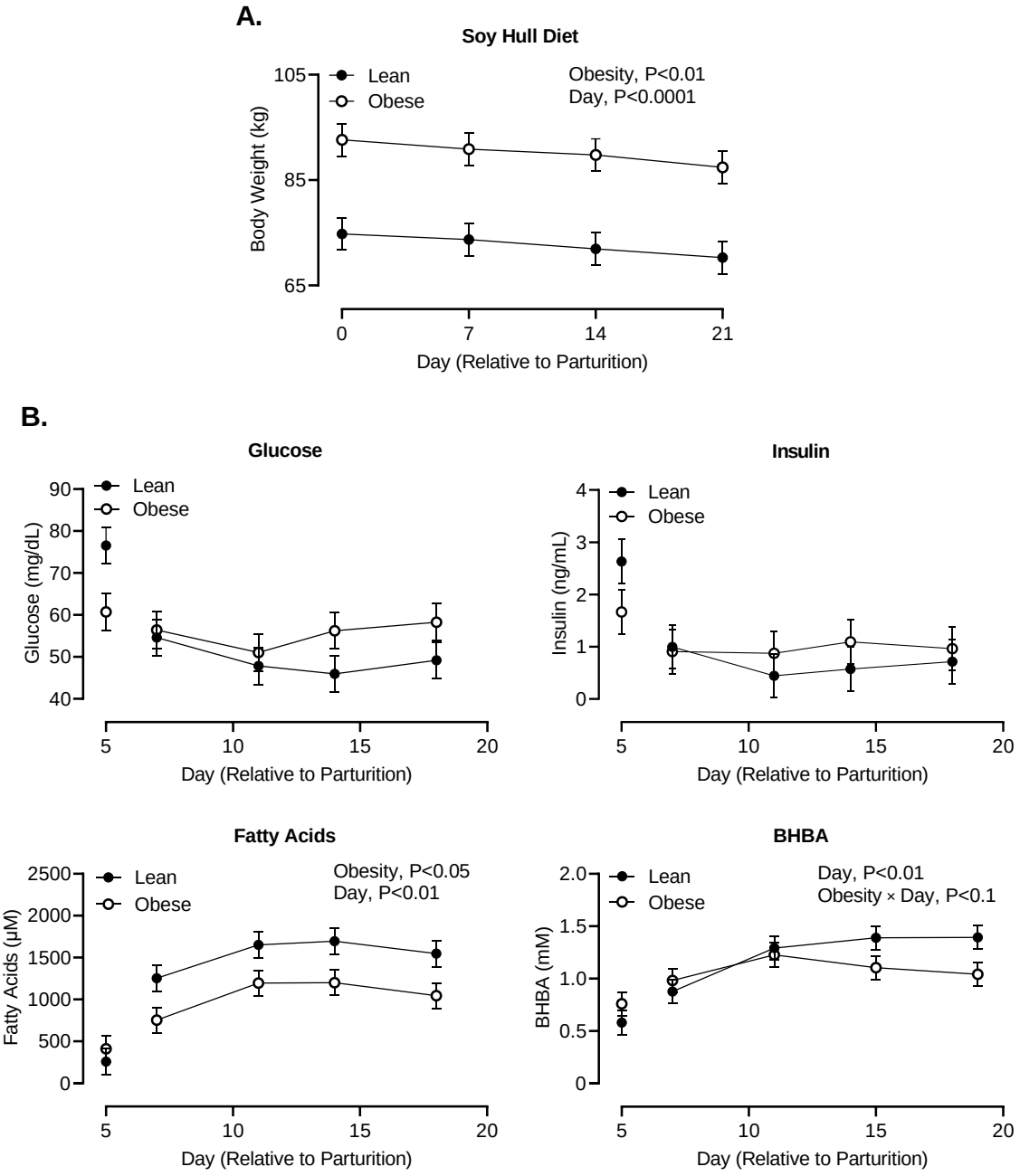

Figure 3.7. Body weight and energy-related variables during lactation in lean and obese ewes fed the soy hull diet. Ewes were fed soy hull diets in amounts supporting appropriate fat deposition (amounts providing 100% of energy requirements; Lean) or excessive fat deposition (unlimited amounts; Obese) from mid-pregnancy until parturition. Both groups were offered unlimited amounts of the soy hull diet for the first 5 days of lactation followed by amounts covering 70% of estimated energy requirements until day 24 of lactation. (A) Body weight. (B) Plasma concentration of glucose, insulin, fatty acids, and β-hydroxybutyrate (BHBA). For all graphs, data shown represent the LSM ± SE of 7 ewes, with effects of obesity, day, and the interaction of obesity and day (Obesity x Day) reported when significant.

Table 3.6. Whole animal performance and metabolic parameters in soy hull-fed lean and obese ewes in early lactation[1]

	Lean	Obese	SD	P Value[3]
Whole Animal				
Body Weight (kg)	70.3	87.4	8.3	<0.01
Fatness Indices				
BCS	2.1	3.7	0.3	<0.0001
Backfat (mm)	4.5	9.1	2.0	<0.01
CT Scan				
Volume (cm^3)				
Body	68907	89145	8939	<0.01
Fat	10875	27786	4420	<0.0001
Fatness (% Body Volume)				
Body	15.5	31.2	5.0	<0.0001
Internal	6.5	10.3	2.4	<0.01
External	9.1	20.9	2.9	<0.0001
Fraction (% Total Fat)				
Internal	41.5	33.0	4.2	<0.01
External	58.5	67.0	4.2	<0.01
Plasma				
Insulin (ng/mL)	0.72	0.97	0.67	NS
Glucose (mg/dL)	49.2	58.3	10.6	NS
Fatty Acids (μM)	1547.8	1045.9	535.0	NS
BHBA (mM)	1.39	1.04	0.42	NS

[1]Ewes received soy hull diets in amounts supporting appropriate fat deposition (amounts providing 100% of energy requirements; Lean) or excessive fat deposition (unlimited amounts; Obese) from mid-pregnancy until parturition. Both groups were offered unlimited amounts for the first 5 days of lactation followed by amounts covering 70% of estimated energy requirements until day 24 of lactation. Data were collected between day 21 and day 24 (n = 7 ewes per treatment)

[2]BCS, body condition score; BHBA, β-hydroxybutric acid

[3]Type I probability error. NS = P>0.1

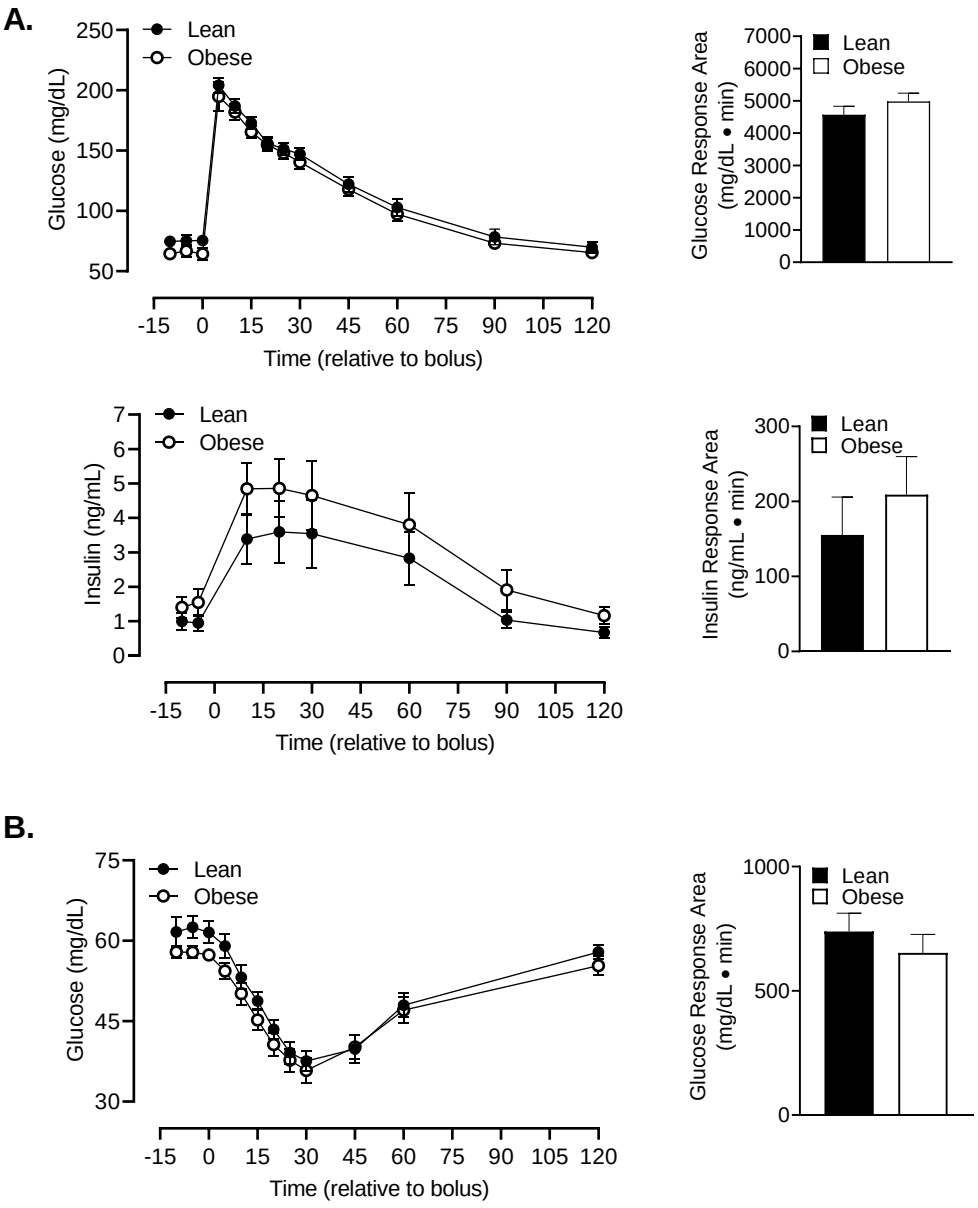

Figure 3.8. Glucose and insulin tolerance test during lactation in lean and obese ewes fed the soy hull diet. Ewes were fed soy hull diets in amounts supporting appropriate fat deposition (amounts providing 100% of energy requirements; Lean) or excessive fat deposition (unlimited amounts; Obese) from mid-pregnancy until parturition. Both groups were offered unlimited amounts of the soy hull diet for the first 5 days of lactation followed by amounts covering 70% of estimated energy requirements until day 24 of lactation. (A) Plasma glucose (top) and insulin (bottom) responses during the GTT performed on day 22 of lactation. Response areas are shown on the right and were calculated over 90 min for glucose and over 120 min for insulin. (B) Plasma glucose response during the ITT performed on day 23 of lactation. Response area is shown on the right and is calculated over 45 min. For all graphs and panels, data shown represent the LSM ± SE of 7 ewes.

The CD cohort was studied until day 38 of lactation to assess whether a longer period of lactation and lipid mobilization would uncover differences between lean and obese ewes. Results were essentially as described for the SH cohort. In brief, body weight and metabolic variables of lean and obese ewes varied in near parallel fashion during lactation (Fig. 3.9). Ewes remained 2-3X as fat as lean ewes according to the various fatness indices measured during the study window at the end of lactation and did not differ in terms of plasma metabolites (Table 3.7). Lamb growth rate (lean vs. obese, 264.4 vs. 274.8 g/day) and milk composition did not differ by maternal fatness. In contrast to results with the SH cohort, obese ewes tended to have impaired glucose disposal but only during the GTT (Fig. 3.10; $P<0.07$); insulin secretion during the GTT was not affected.

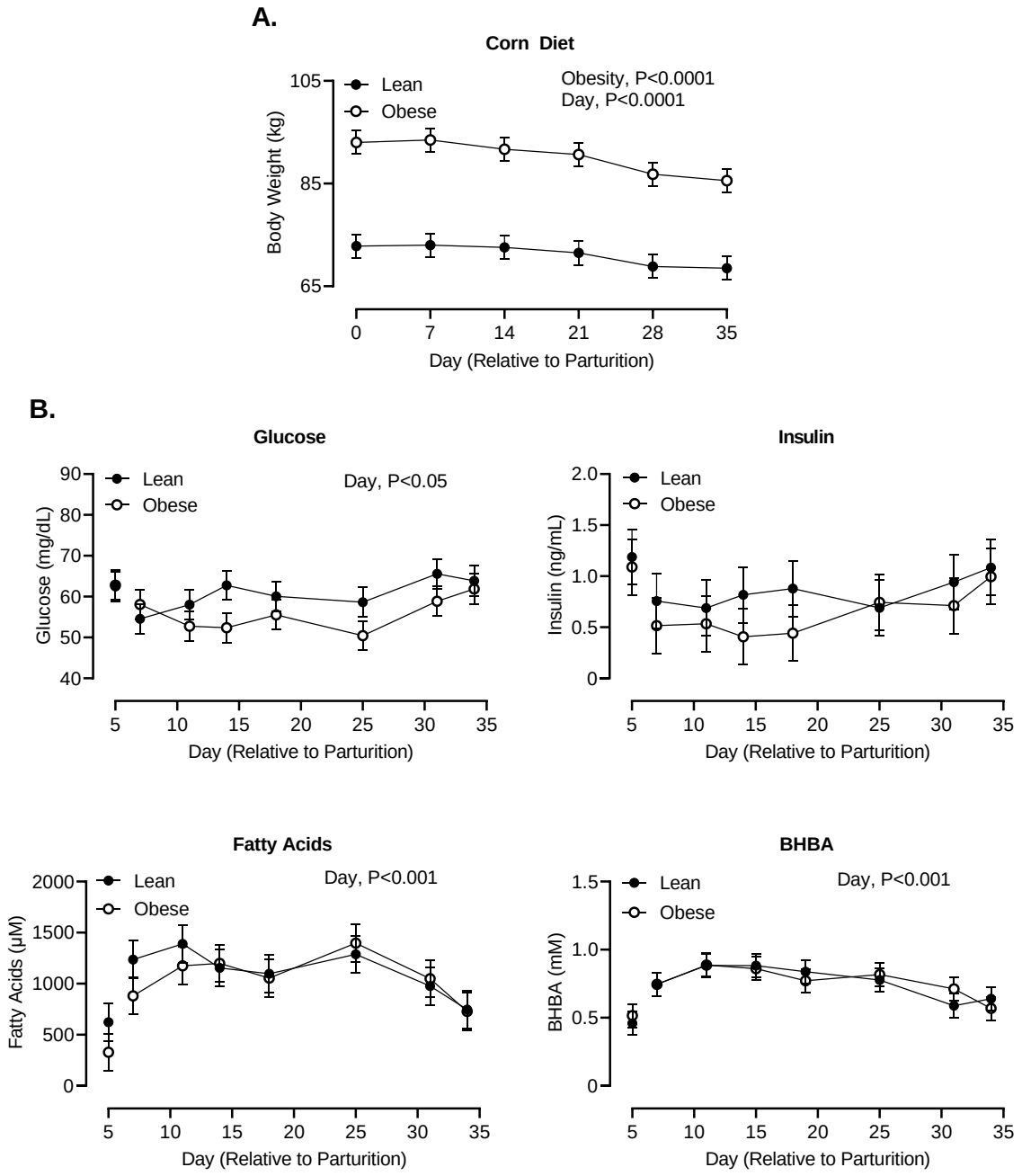

Figure 3.9. Body weight and energy-related variables during lactation in lean and obese ewes fed the corn diet. Ewes were fed a corn diet in amounts supporting appropriate fat deposition (amounts providing 100% of energy requirements; Lean) or excessive fat deposition (unlimited amounts; Obese) during pregnancy. Both groups were offered unlimited amounts of the corn diet for the first 5 days of lactation followed by amounts covering 70% of estimated energy requirements until day 38 of lactation. (A) Body weight. (B) Plasma concentration of glucose, insulin, fatty acids, and β-hydroxybutyrate (BHBA). For all graphs, data shown represent the LSM ± SE of 6 ewes, with effects of obesity, day, and the interaction of obesity and day (Obesity x Day) reported when significant.

Table 3.7. Whole animal performance and metabolic parameters in corn-fed lean and obese ewes in early lactation[1]

	Lean	Obese	SD	P Value[3]
Whole Animal				
Body Weight (kg)	68.5	85.6	4.7	<0.0001
Fatness Indices				
BCS[2]	2.3	3.8	0.4	<0.0001
Backfat (mm)	3.3	8.8	1.9	<0.01
CT Scan				
Volume (cm^3)				
Body	69170	86564	6087	<0.001
Fat	8389	25472	4586	<0.0001
Fatness (% Body Volume)				
Body	11.9	29.3	4.5	<0.0001
Internal	5.7	10.6	1.2	<0.0001
External	6.2	18.7	3.7	<0.001
Fraction (% Total Fat)				
Internal	50.2	36.6	6.9	<0.01
External	49.8	63.4	6.9	<0.01
Plasma				
Insulin (ng/mL)	1.08	1.00	0.92	NS
Glucose (mg/dL)	63.9	61.9	11.3	NS
Fatty Acids (μM)	747.6	728.5	373.8	NS
BHBA (mM)[2]	0.64	0.57	0.19	NS

[1]Ewes received corn diets in amounts supporting appropriate fat deposition (amounts providing 100% of energy requirements; Lean) or excessive fat deposition (unlimited amounts; Obese) from mid-pregnancy until parturition. Both groups were offered unlimited amounts for the first 5 days of lactation followed by amounts covering 70% of estimated energy requirements until day 38 of lactation. Data were collected between day 35 and day 38 (n = 6 ewes per treatment)

[2]BCS, body condition score; BHBA, β-hydroxybutyric acid

[3]Type I probability error. NS = P>0.1

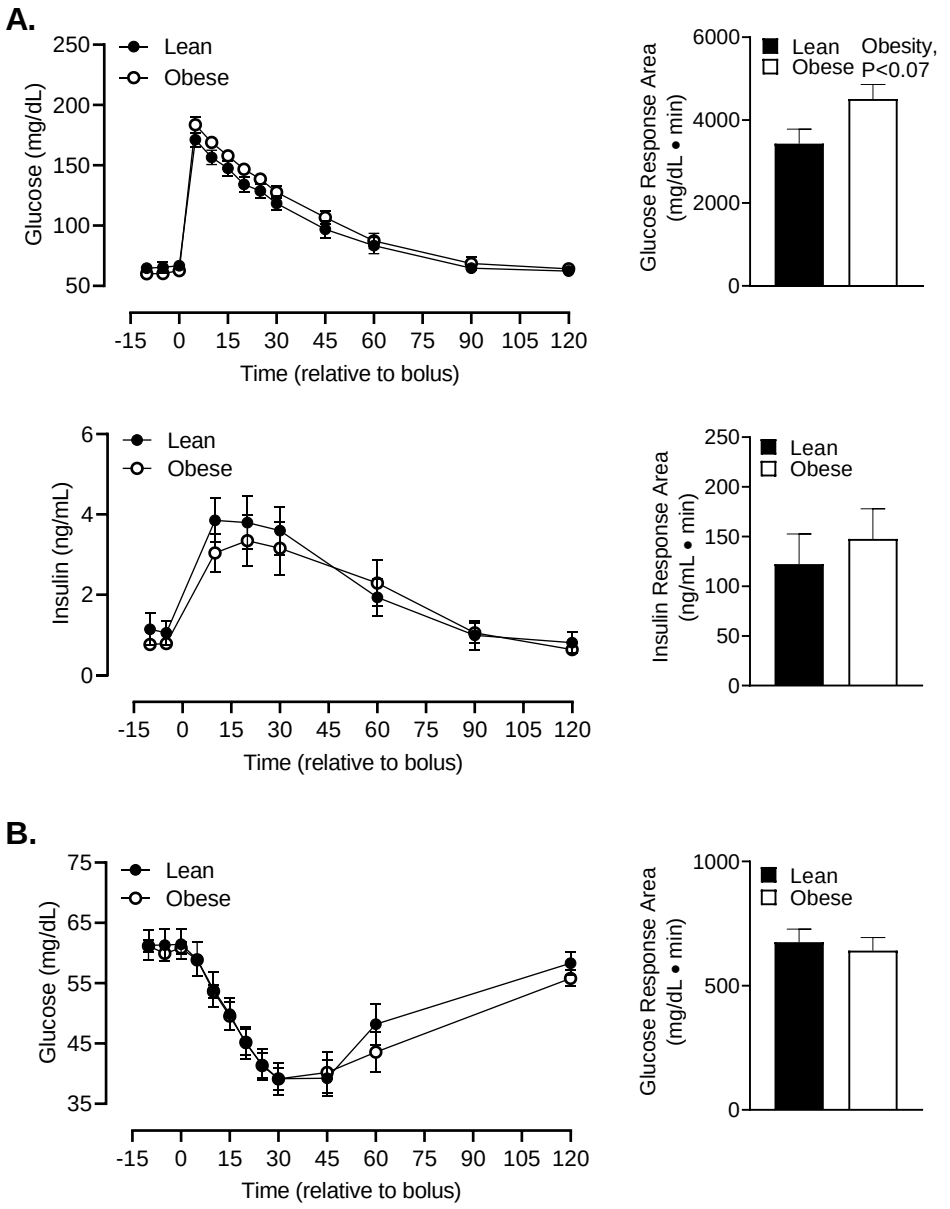

Figure 3.10. Glucose and insulin tolerance test during lactation in lean and obese ewes fed the corn diet. Ewes were fed a corn diet in amounts supporting appropriate fat deposition (amounts providing 100% of energy requirements; Lean) or excessive fat deposition (unlimited amounts; Obese) from mid-pregnancy until parturition. Both groups were offered unlimited amounts of the corn diet for the first 5 days of lactation followed by amounts covering 70% of estimated energy requirements until day 38 of lactation. (A) Plasma glucose (top) and insulin (bottom) responses during the GTT performed on day 36 of lactation. Response areas are shown on the right and were calculated over 90 min for glucose and over 120 min for insulin. (B) Plasma glucose response during the ITT performed on day 37 of lactation. Response area is shown on the right and is calculated over 45 min. For all graphs and panels, data shown represent the LSM ± SE of 6 ewes, with the effect of obesity reported when $P<0.10$.

Correlations between glucose response areas and indices of insulin action were calculated across both diets. Despite little evidence of treatment effects on dynamic indices of insulin action, near significant correlations were observed with most fatness indices but only during the GTT (Table 3.8). Finally, we used CT scan data collected in late pregnancy and in lactation to calculate the total volume of fat mobilized and fractions contributed by internal and external sites (Fig. 3.11). These data show that irrespective of diet, 30% and 70% of fat mobilized originated from the internal and external depot, respectively (Depot, $P<0.0001$).

Table 3.8. Correlations between fatness indices and glucose response during glucose and insulin tolerance tests in early lactating ewes[1]

	GTT Glucose AUC[2]		ITT Glucose AUC[2]	
	R	P Value[3]	R	P Value[3]
BCS	0.34	<0.09	-0.18	NS
Backfat	0.27	NS	-0.34	<0.10
Body fatness	0.38	<0.06	-0.18	NS
Internal Fatness	0.34	<0.09	-0.12	NS
External Fatness	0.38	<0.06	-0.19	NS
Internal Fat Fraction	-0.39	<0.05	0.10	NS
External Fat Fraction	0.39	<0.05	-0.10	NS

[1]Data were collected in lean and obese ewes between day 20 and 38 of lactation.

[2]AUC for plasma glucose during glucose tolerance (GTT) and insulin tolerance (ITT).

[3]Type I probability error, NS = P>0.10

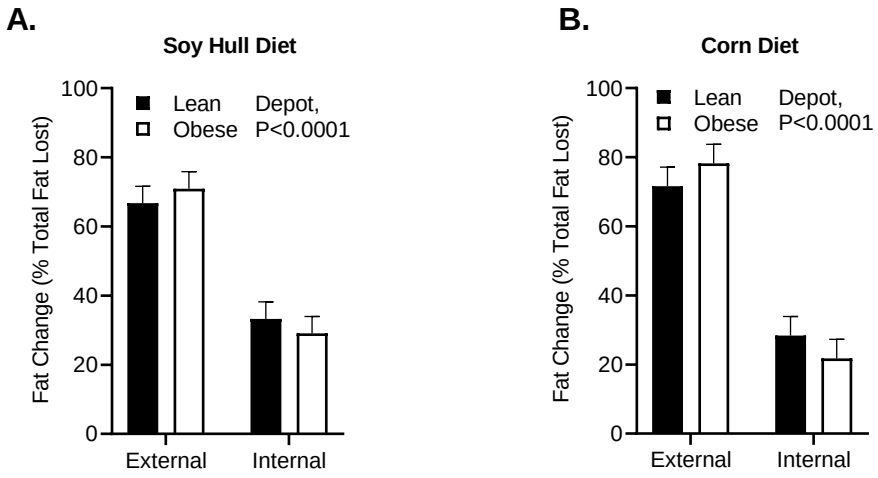

Figure 3.11. Mobilization of fat by depot location in lean and obese ewes. After parturition, lean and obese ewes were offered unlimited amounts for the first 5 days followed by amounts covering 70% of estimated requirements for a period of 24 days (SH) or 38 days (CD). CT data obtained at the end of lactation and in late pregnancy were used to calculate fat mobilization between internal and external depots. Each bar represents the LSM ± SE of 13 ewes. In each panel, effect of depot is reported when significant.

DISCUSSION

Ruminants rely on adequate adipose tissue reserves to achieve optimal productivity during the pregnancy-lactation cycle (Roche et al., 2009; Fthenakis et al., 2012; Pires et al., 2013). For example, dairy cows entering lactation with insufficient reserves are at increased risk for milk fever and metritis, whereas excessive reserves lead to greater susceptibility to infectious and metabolic diseases (Roche et al., 2009; Roche et al., 2013). In addition, ewes with either insufficient or excessive adipose reserves in late pregnancy are at greater risk for developing pregnancy toxemia and hypocalcemia (Andrews, 1997; Fthenakis et al., 2012). Despite the recognition that major functional differences exist between external and internal fat depots (Matsuzawa et al., 1995; Ibrahim, 2010), most studies assessing effects of adiposity on productivity have relied almost exclusively on methods measuring external fat such as body condition scoring and ultrasonographic backfat determination (Boisclair et al., 1986; Wallace et al., 2005; Zhu et al., 2008; Janovick and Drackley, 2010). Accordingly, we used CT scanning to assess changes in external and internal fat volume during periods of dynamic accretion and mobilization and asked how these changes impacted insulin action. We chose insulin action as the physiological variable of interest because of its implication in linking excessive fatness and negative outcomes on productivity and health of ruminants (De Koster and Opsomer, 2013). Our choice of the sheep as the experimental model for these studies was dictated by the limited size capacity of the available CT unit.

We generated ewes differing in fatness by limiting energy consumption to requirements or by allowing unlimited energy intake for a 196-day period before parturition. These treatments were initiated 50 days prior to mating and led to differences in body weight and BCS between lean and obese ewes that were comparable to those achieved in previous work (Wallace et al.,

2005; Ford et al., 2009; George et al., 2010; Tuersunjiang et al., 2013). The energy intake profile, however, differed from previous studies. Starting ~45 days before parturition, the first cohort of obese ewes experienced a gradual decline in energy intake and, accordingly, coincidental reduction in plasma glucose and insulin. Because previous work relied on grains as the sole major source of energy (Wallace et al., 2005; Long et al., 2010; Tuersunjiang et al., 2013), we asked whether these differences related to the use of soy hulls in our diet. However, we observed the exact same energy intake reduction in obese ewes when feeding the corn-based diet of Ford and colleagues to the second cohort (Long et al., 2010), ruling out soy hulls as a causal factor for this phenomenon. Interestingly, Bergman and colleagues observed a reduction in voluntary intake in nonpregnant obese ewes after 25 weeks of excess energy intake (Bergman and Reulein, 1989; McCann et al., 1992). We speculate that our observation of reduced energy consumption near parturition in obese ewes relates to a combination of higher level of overconsumption for a longer period than used by previous investigators [i.e. ~190% vs. 150% for Ford et al., 2009; 196 days vs. ~146 days for Wallace et al., 2005]. The important point in terms of our overall objective is that both diets led to similar differences between lean and obese ewes, as shown by profiles of body weight, glucose, and insulin from initiation of treatment to the end of pregnancy.

Fatness and its effects on insulin action were assessed during study windows conducted in mid- and late pregnancy. By mid-pregnancy obese ewes had increased external adipose tissue relative to lean ewes as indicated by higher body condition scores and backfat thickness. The CT scan data not only confirmed this result, but also showed that the same effect applied to internal fat. The CT data revealed little gain in adipose tissue volume after mid-pregnancy and accordingly fatness differences between lean and obese ewes remained more or less the same by

late pregnancy. The proportion of total fat accounted by internal fat was ~40% and was less in obese than lean ewes. According to CT data, this related to preferential storage of lipids accumulated during pregnancy into external rather than internal fat depots. This was somewhat unexpected because work in non-pregnant sheep show that internal fat accounts for a greater proportion of dissectible fat than subcutaneous fat (sum of omental, mesenteric, and perirenal vs. subcutaneous) (Thompson et al., 1985). Internal depots are also the preferred site of lipid deposition during periods of excess nutrition (Chay-Canul et al., 2011). A similar effect of nutrition was inferred in non-lactating dairy cows on the basis of a growing mass of internal fat depots in the presence of static BCS (Drackley et al., 2014). However, most of these studies did not measure the intermuscular fat depot; this depot is detected by CT and is therefore part of our external fat measurements. In dairy cows, intermuscular fat alone is greater than the sum of all internal depots and twice as heavy as subcutaneous depots (Butler-Hogg et al., 1985). The intermuscular fat depot was also the greatest absolute contributor to changing fatness (Butler-Hogg et al., 1985). Other reasons for these discrepancies could be an underestimation of internal fat depots in pregnant animals by CT scan and difference in the preferred site of lipid deposition between non-pregnant and pregnant animals.

Elevated circulating insulin is a compensatory mechanism seen in states of insulin resistance (Petersen and Shulman, 2018) and has been reported previously in obese mid- and late pregnant ewes (Tuersunjiang et al., 2013). Consistent with this previous work, obese ewes exhibited hyperinsulinemia relative to lean ewes regardless of diet, suggesting elevated insulin resistance. This was conclusively shown in late pregnancy by impaired glucose disposal during both GTT and ITT. Our results, however, are not in complete agreement with those of Ford and colleagues (Tuersunjiang et al., 2013). Using exclusively GTT, they identified insulin resistance

in obese ewes by mid-pregnancy while this test was inconclusive at that point in our work. Moreover, they observed substantially higher insulin secretion during GTT in both mid- and late pregnant obese ewes, whereas we never observed such an effect. Upon closer examination, differences in insulin secretion between lean and obese ewes in their work reflect near absence of a robust insulin response to the GTT glucose bolus in lean sheep rather than exaggerated secretion in the obese ewes. Genotype could be one possible reason for this discrepancy as we used Polypay X Dorset crossbred ewes and Ford and colleagues used Rambouillet X Colombia crossbred ewes.

Previous work in rodents and humans suggest visceral fat depots as a major determinant of insulin resistance (Matsuzawa et al., 1995; Einstein et al., 2008; Liao et al., 2020). For example, indices of insulin responsiveness were negatively correlated with visceral fat mass, but not subcutaneous fat mass in diet-induced obese mice (Chen et al., 2012). Furthermore, removal of omental fat in nonobese dogs improved insulin sensitivity (Lottati et al., 2009). An inverse relation between visceral fatness and insulin action, however, was not detected in our work. First, the internal depot represented a larger fraction of the total fat in lean than obese ewes, and yet lean ewes were more insulin sensitive. Second, we examined correlations between glucose response areas obtained during dynamic tests and various indices of fatness. These correlations were most informative in late pregnancy when the negative effects of obesity on insulin action were greatest. AUC during GTT and ITT were respectively positively and negatively associated with indices of fatness (BCS, backfat, and CT scan fatness); this was expected because increasing glucose response during GTT indicates growing insulin resistance and the opposite during ITT. However, when the proportion of total fat accounted by internal and external fat were used in this analysis, better insulin response was associated with the internal fat fraction.

Our study provided an opportunity to evaluate the effects of pre-existing obesity on performance and insulin action during lactation. Lipid utilization in lactating, well-fed ewes is limited, particularly if unselected for milk production (Bell, 1979). Accordingly, ewes were restricted to 70% of estimated energy requirements in an effort to promote negative energy balance and utilization of lipid reserves. Despite this nutritional restriction, obesity did not impair maternal health as reflected by similar body weight losses and plasma indicators of carbohydrate (e.g. glucose and insulin) and lipid metabolism (e.g. fatty acids and BHBA) in lean and obese ewes. Moreover, the average daily gain of lambs was not affected by maternal fatness and matched those reported for lambs nursing on well-fed ewes or lambs fed unlimited amounts of milk replacer (Greenwood et al., 1998; Wang et al., 2019). More importantly, we found little evidence of reduced insulin action in obese ewes based on the ITT and GTT tests. This suggests that the combination of energy insufficiency and lactation negates the detrimental effects of obesity on insulin action. A resolution of insulin action determined by oral GTT following parturition has been documented in women experiencing gestational diabetes mellitus (Yasuhi et al., 2019; Waters et al., 2020).

CONCLUSION

In summary, we showed obese ewes were more insulin resistant than lean ewes by late pregnancy as demonstrated by increased basal plasma insulin and glucose, as well as decreased glucose disposal during both GTT and ITT tests. Surprisingly, external fat appeared to be more potent than internal fat in driving insulin resistance. In contrast, the insulin resistance effects of obesity were no longer evident in energy-deficient lactating ewes. Overall, longitudinal fat measurements during pregnancy and lactation suggested more dynamic lipid accretion and mobilization in external than internal fat depots.

REFERENCES

Andrews, A. 1997. Pregnancy toxaemia in the ewe. In Practice 19(6):306. doi: 10.1136/inpract.19.6.306

Bell, A. W. 1979. Lipid metabolism in liver and selected tissues and in the whole body of ruminant animals. Progress in Lipid Research 18(3):117-164. doi: 10.1016/0163-7827(79)90013-4 PMID - 396532

Bell, A. W., and D. E. Bauman. 1997. Adaptations of glucose metabolism during pregnancy and lactation. Journal of Mammary Gland Biology and Neoplasia 2(3):265-278.

Bergman, E. N., and S. S. Reulein. 1989. Effects of obesity on insulin sensitivity and responsiveness in sheep. American Journal of Physiology Endocrinology and Metabolism

Block, S. S., W. R. Butler, R. A. Ehrhardt, A. W. Bell, M. E. V. Amburgh, and Y. R. Boisclair. 2001. Decreased concentration of plasma leptin in periparturient dairy cows is caused by negative energy balance. Journal of Endocrinology 171(2):339-348.

Boisclair, Y., D. G. Grieve, J. B. Stone, O. B. Allen, and G. K. MacLeod. 1986. Effect of prepartum energy, body condition, and sodium bicarbonate on production of cows in early lactation. Journal of Dairy Science 69(10):2636-2647. doi: 10.3168/jds.S0022-0302(86)80711-1

Butler-Hogg, B. W., J. D. Wood, and J. A. Bines. 1985. Fat partitioning in British Friesian cows: the influence of physiological state on dissected body composition. The Journal of Agricultural Science 104(3):519-528. doi: 10.1017/s0021859600044282

Caixeta, L. S., S. L. Giesy, C. S. Krumm, J. W. Perfield, A. Butterfield, K. M. Schoenberg, D. C. Beitz, and Y. R. Boisclair. 2017. Effect of circulating glucagon and free fatty acids on hepatic FGF21 production in dairy cows. American Journal of Physiology: Regulatory, Integrative and Comparative Physiology:ajpregu.00197.02017. doi: 10.1152/ajpregu.00197.2017 PMID - 28794103

Chay-Canul, A. J., A. J. Ayala-Burgos, J. C. Ku-Vera, J. G. Magaña-Monforte, and L. O. Tedeschi. 2011. The effects of metabolizable energy intake on body fat depots of adult Pelibuey ewes fed roughage diets under tropical conditions. Tropical Animal Health and Production 43(5):929-936. doi: 10.1007/s11250-011-9785-5 PMID - 21240653

Chen, W., J. L. Wilson, M. Khaksari, M. A. Cowley, and P. J. Enriori. 2012. Abdominal fat analyzed by DEXA scan reflects visceral body fat and improves the phenotype description and the assessment of metabolic risk in mice. American Journal of Physiology Endocrinology and Metabolism 303(5):E635-643. doi: 10.1152/ajpendo.00078.2012 PMID - 22761161

De Koster, J. D., and G. Opsomer. 2013. Insulin resistance in dairy cows. Veterinary Clinics of North America: Food Animal Practice 29(2):299-322. doi: 10.1016/j.cvfa.2013.04.002

Drackley, J. K., R. L. Wallace, D. Graugnard, J. Vasquez, B. F. Richards, and J. J. Loor. 2014. Visceral adipose tissue mass in nonlactating dairy cows fed diets differing in energy density. Journal of Dairy Science 97(6):3420-3430. doi: 10.3168/jds.2014-8014 PMID - 24704224

Duehlmeier, R., I. Fluegge, B. Schwert, and M. Ganter. 2013. Insulin Sensitivity during Late Gestation in Ewes Affected by Pregnancy Toxemia and in Ewes with High and Low Susceptibility to this Disorder. Journal of Veterinary Internal Medicine 27(2):359-366. doi: 10.1111/jvim.12035 PMID - 23397990

Einstein, F. H., S. Fishman, R. H. Muzumdar, X. M. Yang, G. Atzmon, and N. Barzilai. 2008. Accretion of visceral fat and hepatic insulin resistance in pregnant rats. American Journal of Physiology Endocrinology and Metabolism 294(2):E451-E455. doi: 10.1152/ajpendo.00570.2007 PMID - 18073320

Fensterseifer, S. R., K. J. Austin, S. P. Ford, and B. M. Alexander. 2018. Effects of maternal obesity on maternal and fetal plasma concentrations of adiponectin and expression of adiponectin and its receptor genes in cotyledonary and adipose tissues at mid- and late-gestation in sheep. Animal Reproduction Science doi: 10.1016/j.anireprosci.2018.08.033 PMID - 30172606

Ford, S. P., L. Zhang, M. Zhu, M. M. Miller, D. T. Smith, B. W. Hess, G. E. Moss, P. W. Nathanielsz, and M. J. Nijland. 2009. Maternal obesity accelerates fetal pancreatic β-cell but not α-cell development in sheep: prenatal consequences. American Journal of Physiology: Regulatory, Integrative and Comparative Physiology 297(3):R835-R843. doi: 10.1152/ajpregu.00072.2009 PMID - 19605766

Fthenakis, G. C., G. Arsenos, C. Brozos, I. A. Fragkou, N. D. Giadinis, I. Giannenas, V. S. Mavrogianni, E. Papadopoulos, and I. Valasi. 2012. Health management of ewes during pregnancy. Animal Reproduction Science 130(3-4):198-212. doi: 10.1016/j.anireprosci.2012.01.016 PMID - 22356932

George, L. A., A. B. Uthlaut, N. M. Long, L. Zhang, Y. Ma, D. T. Smith, P. W. Nathanielsz, and S. P. Ford. 2010. Different levels of overnutrition and weight gain during pregnancy have differential effects on fetal growth and organ development. Reproductive Biology and Endocrinology 8:75. doi: 10.1186/1477-7827-8-75 PMID - 20576133

Greenwood, P. L., A. S. Hunt, J. W. Hermanson, and A. W. Bell. 1998. Effects of birth weight and postnatal nutrition on neonatal sheep: I. Body growth and composition, and some aspects of energetic efficiency. Journal of Animal Science 76(9):2354-2367. doi: 10.2527/1998.7692354x

Hung, C. S., J. K. Lee, C. Y. Yang, H. R. Hsieh, W. Y. Ma, M. S. Lin, P. H. Liu, S. R. Shih, J. M. Liou, L. M. Chuang, M. F. Chen, J. W. Lin, J. N. Wei, and H. Y. Li. 2014. Measurement of visceral fat: should we include retroperitoneal fat? PloS One 9(11):e112355. doi: 10.1371/journal.pone.0112355

Ibrahim, M. M. 2010. Subcutaneous and visceral adipose tissue: structural and functional differences. Obesity Reviews 11(1):11-18. doi: 10.1111/j.1467-789x.2009.00623.x PMID - 19656312

Janovick, N. A., and J. K. Drackley. 2010. Prepartum dietary management of energy intake affects postpartum intake and lactation performance by primiparous and multiparous Holstein cows1. Journal of Dairy Science 93(7):3086-3102. doi: https://doi.org/10.3168/jds.2009-2656

Liao, C.-C., W. H.-H. Sheu, S.-Y. Lin, W.-J. Lee, and I. T. Lee. 2020. The Relationship Between Abdominal Body Composition and Metabolic Syndrome After a Weight Reduction Program in Adult Men with Obesity. Diabetes, Metabolic Syndrome and Obesity: Targets and Therapy 13:1-8. doi: 10.2147/dmso.s228954 PMID - 32021346

Long, N. M., L. A. George, A. B. Uthlaut, D. T. Smith, M. J. Nijland, P. W. Nathanielsz, and S. P. Ford. 2010. Maternal obesity and increased nutrient intake before and during gestation in the ewe results in altered growth, adiposity, and glucose tolerance in adult offspring1. Journal of Animal Science 88(11):3546-3553. doi: 10.2527/jas.2010-3083 PMID - 20622177

Lottati, M., C. M. Kolka, D. Stefanovski, and E. L. Kirkman. 2009. Greater omentectomy improves insulin sensitivity in nonobese dogs. Obesity doi: 10.1038/oby.2008.642

Matsuzawa, Y., I. Shimomura, T. Nakamura, Y. Keno, K. Kotani, and K. Tokunaga. 1995. Pathophysiology and Pathogenesis of Visceral Fat Obesity. Obesity Research 3(S2):187s-194s. (https://doi.org/10.1002/j.1550-8528.1995.tb00462.x) doi: https://doi.org/10.1002/j.1550-8528.1995.tb00462.x

McCann, J. P., E. N. Bergman, and D. H. Beermann. 1992. Dynamic and static phases of severe dietary obesity in sheep: food intakes, endocrinology and carcass and organ chemical composition. The Journal of Nutrition 122(3):496-505.

Mulligan, F. J., and M. L. Doherty. 2008. Production diseases of the transition cow. Veterinary Journal 176(1):3-9. doi: 10.1016/j.tvjl.2007.12.018 PMID - 18342556

Nemoto, M., T. Yeernuer, Y. Masutani, Y. Nomura, S. Hanaoka, S. Miki, T. Yoshikawa, N. Hayashi, and K. Ohtomo. 2014. Development of automatic visceral fat volume calculation software for CT volume data. Journal of Obesity 2014:495084. doi: 10.1155/2014/495084

Petersen, M. C., and G. I. Shulman. 2018. Mechanisms of Insulin Action and Insulin Resistance. Physiological Reviews 98(4):2133-2223. doi: 10.1152/physrev.00063.2017 PMID - 30067154

Pires, J. A. A., C. Delavaud, Y. Faulconnier, D. Pomiès, and Y. Chilliard. 2013. Effects of body condition score at calving on indicators of fat and protein mobilization of periparturient Holstein-Friesian cows. Journal of Dairy Science 96(10):6423-6439. doi: https://doi.org/10.3168/jds.2013-6801

Roche, J. R., N. C. Friggens, J. K. Kay, M. W. Fisher, K. J. Stafford, and D. P. Berry. 2009. Invited review: Body condition score and its association with dairy cow productivity, health, and welfare. Journal of Dairy Science 92(12):5769-5801. doi: 10.3168/jds.2009-2431

Roche, J. R., J. K. Kay, N. C. Friggens, J. J. Loor, and D. P. Berry. 2013. Assessing and Managing Body Condition Score for the Prevention of Metabolic Disease in Dairy Cows. Veterinary Clinics of North America: Food Animal Practice 29(2):323-336. doi: 10.1016/j.cvfa.2013.03.003 PMID - 23809894

Rosenblatt, A. J., P. V. Scrivani, Y. R. Boisclair, A. P. Reeves, J. M. Ramos-Nieves, Y. Xie, and H. N. Erb. 2017. Evaluation of a semi-automated computer algorithm for measuring total fat and visceral fat content in lambs undergoing in vivo whole body computed tomography. Veterinary Journal 228:46-52. doi: 10.1016/j.tvjl.2017.10.012 PMID - 29153108

Ruda, L., C. Raschka, K. Huber, R. Tienken, U. Meyer, S. Dänicke, and J. Rehage. 2019. Gain and loss of subcutaneous and abdominal fat depot mass from late pregnancy to 100 days in milk in German Holsteins. Journal of Dairy Research 86(3):296-302. doi: 10.1017/s0022029919000542 PMID - 31409432

Russel, A. 1984. Body condition scoring of sheep. In Practice 6(3):91-93. doi: 10.1136/inpract.6.3.91

Thompson, J. M., R. M. Butterfield, and D. Perry. 1985. Food intake, growth and body composition in Australian Merino sheep selected for high and low weaning weight. 2. Chemical and dissectible body composition. Animal Science 40(1):71-84. doi: 10.1017/S000335610003186X

Tuersunjiang, N., J. F. Odhiambo, N. M. Long, D. R. Shasa, P. W. Nathanielsz, and S. P. Ford. 2013. Diet reduction to requirements in obese/overfed ewes from early gestation prevents glucose/insulin dysregulation and returns fetal adiposity and organ development to control levels. American Journal of Physiology Endocrinology and Metabolism 305(7):E868-878. doi: 10.1152/ajpendo.00117.2013 PMID - 23921140

Wallace, J. M., J. S. Milne, and R. P. Aitken. 2005. The effect of overnourishing singleton-bearing adult ewes on nutrient partitioning to the gravid uterus. British Journal of Nutrition 94(4):533-539.

Wang, S., T. Ma, G. Zhao, N. Zhang, Y. Tu, F. Li, K. Cui, Y. Bi, H. Ding, and Q. Diao. 2019. Effect of Age and Weaning on Growth Performance, Rumen Fermentation, and Serum Parameters in Lambs Fed Starter with Limited Ewe-Lamb Interaction. Animals 9(10)doi: 10.3390/ani9100825

Waters, T. P., S. Y. Kim, A. J. Sharma, P. Schnellinger, J. K. Bobo, R. T. Woodruff, L. A. Cubbins, M. Haghiac, J. Minium, L. Presley, H. Wolfe, S. Hauguel-de Mouzon, W. Adams, and P. M. Catalano. 2020. Longitudinal changes in glucose metabolism in

women with gestational diabetes, from late pregnancy to the postpartum period. Diabetologia 63(2):385-394. doi: 10.1007/s00125-019-05051-0

Yasuhi, I., H. Yamashita, K. Maeda, M. Nomiyama, T. Mizunoe, K. Tada, M. Yorozu, M. Ogawa, T. Kodama, K. Yamaguchi, N. Okura, K. Kawakami, Y. Maekawa, and K. Hayashi. 2019. High-intensity breastfeeding improves insulin sensitivity during early post-partum period in obese women with gestational diabetes. Diabetes/Metabolism Research and Reviews 35(4):e3127. doi: 10.1002/dmrr.3127

Yoshizumi, T., T. Nakamura, M. Yamane, A. H. Islam, M. Menju, K. Yamasaki, T. Arai, K. Kotani, T. Funahashi, S. Yamashita, and Y. Matsuzawa. 1999. Abdominal fat: standardized technique for measurement at CT. Radiology 211(1):283-286. doi: 10.1148/radiology.211.1.r99ap15283

Zhu, M. J., B. Han, J. Tong, C. Ma, J. M. Kimzey, K. R. Underwood, Y. Xiao, B. W. Hess, S. P. Ford, P. W. Nathanielsz, and M. Du. 2008. AMP-activated protein kinase signalling pathways are down regulated and skeletal muscle development impaired in fetuses of obese, over-nourished sheep. The Journal of Physiology 586(10):2651-2664. doi: 10.1113/jphysiol.2007.149633 PMID - 18372306

CHAPTER 4

FGF21 IMPROVES INSULIN SENSITIVITY IN GROWING SHEEP

INTRODUCTION

Insulin resistance is a key adaptation of ruminants when faced with an insufficient glucose supply (Bell and Bauman, 1997). For example, insulin sensitivity declines during late pregnancy in the sheep, sparing glucose for insulin-independent tissues such as the placenta. However, excessive insulin resistance can cause metabolic disease such as pregnancy toxemia and lead to loss of productivity in the ewe (Duehlmeier et al., 2013). Another example is early lactation in dairy cows. When reduced insulin response favors diversion of the glucose supply to the mammary gland where uptake is independent of insulin (Bell and Bauman, 1997; De Koster and Opsomer, 2013). Like in sheep, excessive insulin resistance can cause metabolic diseases such as ketosis in cattle. Mechanisms underlying variation in insulin response are not well understood in ruminants. Moreover, there are no strategies to counter excessive insulin resistance in these animals.

An interesting development in this context is the discovery of FGF21 (Nishimura et al., 2000; Kharitonenkov et al., 2005). FGF21 belongs to the FGF superfamily, but lacks the heparin binding domain (HBD) which enables it to act as a hormone (Ornitz, 2000). A consequence to lacking the HBD is that FGF21 requires presence of the co-receptor β-klotho in order to bind and activate the receptor (Adams et al., 2012a). Exogenous FGF21 administration not only normalizes basal glucose and insulin in obese rodents or primates, but it also improves glucose clearance during glucose or insulin tolerance tests (Kharitonenkov et al., 2005; Véniant et al., 2012; Adams et al., 2013). In addition, these effects are commonly coupled with an increase in the insulin-sensitizing adipokine adiponectin (Holland et al., 2013). Given this, we recently explored the role of FGF21 in early lactating dairy cows; contrary to findings in rodents, FGF21 treatment failed to improve indices of insulin action under basal conditions or during glucose

tolerance tests (Krumm et al., 2019). These dairy cows experienced a substantial energy deficit whereas virtually all previous FGF21 work in rodents involved animals in positive energy balance (Kharitonenkov et al., 2005; Lin et al., 2013).

These data raise the possibility that energy balance is a key factor regulating the insulin sensitizing effects of FGF21. Accordingly, we hypothesize that the insulin-sensitizing effect of FGF21 would be seen in sheep when in positive energy balance. We first characterize essential elements of the FGF21 endocrine system in the sheep. We then tested whether FGF21 was capable of insulin-sensitizing effects when administered to grazing sheep in positive energy balance.

MATERIALS AND METHODS

Animals and Design

All procedures were conducted with the approval of the Cornell University Institutional Care and Use Committee.

Experiment 1: Description of the FGF21 System in Sheep

Four Finn × Dorset female sheep of uniform age and body weight (10.6 ± 1.3 months; 52.5 ± 4.1 kg) were used to survey tissue expression of FGF21, β-klotho, and FGFR isoforms. Sheep were offered an unlimited amount of a pelleted diet consisting of corn, wheat midds, soy hulls, soybean meal, and mineral/vitamin supplement in the ratio of 46:20:15:13:4. Sheep were slaughtered by stunning with a captive bolt and exsanguinated, followed by tissue collection within 30 min. Tissues collected were liver, subcutaneous, omental, and retroperitoneal adipose tissue, kidney, muscle, and lung. Tissues were snap frozen in liquid nitrogen upon collection and stored at -80ºC until further analysis.

Experiment 2: Pharmacokinetics and bioactivity of human FGF21

Six Finn × Dorset female sheep of uniform age (12.9 ± 0.1 months), body condition (3.58 ± 0.11), and weight (64.5 ± 2.2 kg) were used. Sheep were fitted with bilateral intrajugular catheters (Tygon S-54-HL, 1.02-mm i.d. × 1.78-mm o.d.; Saint-Gobain Performance Plastics, Akron, OH) 1 wk prior to treatment. They were then assigned to a crossover design with experimental periods of 24 h separated by a 7 d washout period. Treatment consisted of a single i.v. bolus of either excipient solution (control) or recombinant human FGF21 (FGF21) at the dose of 5 mg/kg metabolic body weight ($BW^{0.75}$; MBW). The dose was prepared with the

human FGF21 variant LY2405319 with 84% identity with ovine FGF21 and engineered for enhanced in vivo stability (Altschul et al., 1997; Altschul et al., 2005). It was produced in Pichia pastoris, purified to homogeneity using reversed-phase and anion-exchange chromatography, and prepared as a 33 mg/mL solution in an excipient solution of 10 mM citrate, 150 mM NaCl, pH 7.0 (Eli Lilly, Indianapolis, IN) (Adams et al., 2013; Kharitonenkov et al., 2013). Blood samples were collected at fixed times (-60, -30, -1, 1, 5, 20, 40, and 60 min and 2, 4, 6, 8, and 12 h relative to the bolus at time 0). Blood was mixed with heparin (15 IU/mL) and centrifuged at 3,020 rpm (2171 × *g*) for 15 min at 4°C. Resulting plasma was stored in aliquots at -20°C until analyzed for FGF21. In addition, adipose tissue biopsies were taken at -10, 15, and 30 min relative to bolus administration. Biopsies of tailhead adipose tissue were performed as previously described (Krumm et al., 2019). In brief, the site was surgically prepared followed by incision through the skin and dissection of adipose tissue. Pre-bolus biopsies were obtained from the left side of the tailhead and post-bolus biopsies were obtained from the right side of the tailhead. Tissue was snap frozen in liquid nitrogen and stored at -80°C until further analysis.

Experiment 3: Chronic Effect of FGF21

Six Finn × Dorset female sheep of uniform age (9.4 ± 0.1 months), body condition (3.38 ± 0.09), and weight (49.7 ± 1 kg) were selected and moved to individual tie stalls under a controlled environment (20°C , light on 0730 – 2000 h). Sheep were randomly allocated to a crossover design with treatments consisting of daily s.c. injections of excipient solution (control) or the human FGF21 variant LY2405319 (FGF21) at the dose of 15 mg/kg MBW. Treatments lasted 13 days and were separated by a 14-day intervening period. Sheep were fitted with bilateral intrajugular catheters (Tygon S-54-HL, 1.02-mm i.d. × 1.78-mm o.d.; Saint-Gobain

Performance Plastics, Akron, OH) 1 wk before initiation of the treatment period. Throughout the experiment, sheep were offered *ad libitum* levels of a dry TMR (Table 4.1), partitioned into meals offered every 4 h using in-house automatic feeders.

On the first day of the experimental period, treatments were administered as a single s.c. injection at 0800 h. Blood samples were obtained at fixed times relative to the injection (-60, -30, 0, 5, 15, 30, and 60 min and 2, 4, 6, 8, 12, 16, and 24 h), immediately mixed with heparin (15 IU/mL), and centrifuged at 3,020 rpm (2171 × *g*) for 15 min at 4ºC. Resulting plasma was stored at -20ºC until analyzed for metabolites and hormones.

For the remainder of the experimental period, treatments were administered as twice daily injections at 0800 and 2000 h. Blood samples (3 samples over 1 h) were taken from 1000-1100 h on experimental d -1, 3, 6, 9, 12 and processed immediately for plasma. Glucose tolerance tests (GTT) and epinephrine challenges (EC) were performed on d 12 and 13 of treatment respectively; the bolus of glucose (0.25 g/kg BW, 50% wt/vol, VetOne, Boise, ID) or epinephrine (1.4 μg/kg BW, Anpro Pharmaceutical, Arcadia, CA, USA) was administered at 1030 h. Other variables measured during each experimental period included beginning and ending body weight and body condition score using the 5-point scale (1=thin, 5=fat) (Russel, 1984) and daily feed intake. The nutrient and chemical composition of the TMR was determined using wet chemistry analysis (Dairy One Cooperative Inc., Ithaca, NY).

Table 4.1. Ingredient and nutrient composition of the diet

Item	
Ingredient (% of DM)	
Corn (coarsely cracked)	48.2
Hay	19.9
Soy Hulls	17.4
Soybean Meal	8.6
Corn Oil	2.2
Limestone	1.6
CU Sheep Mineral[1]	1.2
Vitamin E premix[2]	0.9
Chemical Analysis	
CP (% of DM)	13.60
ADF (% of DM)	20.40
aNDF (% of DM)	33.70
TDN (% of DM)	71.00
Ca (% of DM)	0.71
P (% of DM)	0.32
ME (Mcal/Kg of DM)	2.56

[1]Contained 21.2% Ca, 33.5% Salt, 167 ppm Se, 1.37% Zn, 6740 ppm Mn, 4030 ppm Fe, 318 ppm I, 34.5 ppm Co

[2]Contained 20,000 U/lb Vitamin E

Analysis of Metabolites, Insulin, IGF-1, and FGF21

Plasma fatty acids and glucose were analyzed using spectrophotometric methods based on the enzymes acyl coenzyme A–oxidase and glucose oxidase, respectively (Block et al., 2001). The plasma concentration of insulin was determined using a double antibody RIA validated in ruminants (Caixeta et al., 2017). The plasma glucose response area was calculated between 0 and 90 min for the GTT and between 0 and 60 min for the epinephrine challenge; these values were corrected for baseline concentrations (mean of concentrations at −15, −10 and −5 min for the GTT; –30, –15, –10, –5, and –1 min for the epinephrine challenge). The plasma insulin response area during the GTT was calculated between 0 and 120 min and was corrected for baseline concentrations (mean of concentrations at −10 and −5 min). The fatty acid response area during the epinephrine challenge was calculated between 0 and 60 min and was corrected for baseline concentrations (mean of concentrations at –30, –15, –10, –5, –1, 120, 130, and 140 min). The plasma concentrations of IGF-1 and FGF21 were determined using double antibody assays previously validated in bovine plasma (Greenwood et al., 2002; Caixeta et al., 2017). Inter- and intra-assay coefficients of variation were <6 and <5% respectively for metabolite assays, and <10 and <7% respectively for hormone assays.

Pharmacokinetic Analysis of Human FGF21

The concentrations of plasma FGF21 after the i.v. bolus were analyzed using noncompartmental analyses with a commercial software (PK Solutions 2.0, Summit Research Services, Montrose, CO) (Ramos-Nieves et al., 2019). This software uses a curve-stripping procedure to resolve the concentration–time curves into a series of exponential terms that correspond to the kinetic phases of circulating FGF21. The initial total FGF21 concentration was estimated through linear extrapolation of the first 2 plasma concentration values to time

zero. Area under the concentration–time curve from 0 to 12 h ($AUC_{0–12\ h}$) was estimated using the trapezoid method up to the last measured concentration at 12 h post-bolus. The apparent terminal disposition rate constant (λz) was determined using linear regression analysis of the terminal portion of the log plasma concentration–time curve. Elimination half-life ($t_{1/2}$) and clearance rate were calculated as ln (2)/λz and dose/ $AUC_{0–12\ h}$, respectively. The volume of distribution (Vd) was estimated as $D/AUC_{0-\infty}\cdot\lambda z$ where D is the ratio of dose to body weight. Mean residence time (mRT) was estimated as $AUMC_{0-\infty}C/AUC_{0-\infty}$ where $AUMC_{0-\infty}$ is the area under the concentration·time-time curve extrapolated to infinity.

Western Immunoblotting

Adipose tissue was homogenized in 1 mL of lysis buffer (10 mM Tris, pH 7.6, 10 mL/L of Triton X-100, 1 mM EGTA, 150 mM NaCl, 1 mM EDTA) supplemented with commercial proteases and phosphatase inhibitors (Halt phosphatase inhibitor mixture EDTA-free; Thermo Fisher). Homogenates were clarified by centrifugation (10,000 × g for 20 min at 4°C). Protein concentrations of cellular extracts were determined using a bicinchoninic acid protein assay kit (Thermo Fisher, Waltham, MA). Fixed amounts of protein (25 μg) were separated on 9% polyacrylamide gels under reducing conditions and transferred onto nitrocellulose membranes (Protran, Schleicher, and Schuell Bioscience, Dassel, Germany). Membranes were immersed in blocking solution (50 mM Tris, pH 7.4, 200 mM NaCl, 1 mL/L of Tween 20, 50 g/L of bovine serum albumin). For signaling proteins, membranes were incubated with 1:1,000 dilution of primary antibodies obtained from Cell Signaling (Danvers, MA) against p44/42 MAPK (ERK1/2) and threonine 202/tyrosine 204 phosphorylated ERK1/2 (pERK1/2). Signals were developed with a 1:20,000 dilution of IRDye 800 anti-rabbit secondary antibody (LI-COR

Biotechnology, Lincoln, NE) followed by visualization and quantification with the LI-COR Odyssey infrared imaging system using the 800-nm channel.

For determination of plasma adiponectin, samples (10 μl of a 1:20 dilution) were separated on 12% polyacrylamide gels and transferred onto nitrocellulose membranes. Membranes were immersed in blocking solution of TBS-T (50 mM Tris, pH 7.4, 200 mM NaCl, 1 mL/L of Tween 20, 50 g/L of nonfat dry milk) for 1 hr and then immunodecorated overnight at 4°C in blocking solution and a 1:5,000 dilution of a primary antibody against human adiponectin (a gift from T. Funahashi, Osaka University, Osaka, Japan) validated in cattle (Krumm et al., 2018). Signals were developed with a 1:20,000 dilution of IRDye 800 anti-mouse secondary antibody (LI-COR Biotechnology, Lincoln, NE) followed by visualization and quantification with the LI-COR Odyssey infrared imaging system using the 800-nm channel.

RNA Extraction and Analysis of Gene Expression

Tissue samples were lysed with Qiazol (Qiagen, Valencia, CA) followed by total RNA purification using RNeasy Mini columns and on-column RNase-free DNase treatment (Qiagen). Quality of RNA was determined using the RNA Nano Lab Chip kit and bioanalyzer (Agilent, Palo Alto, CA) with samples having an RNA integrity number average of 7.9 ± 0.1. Reverse transcription reactions were performed with 1 μg of total RNA in a total 20 μL volume with the high-capacity cDNA reverse transcription kit and RNase inhibitor (Applied Biosystems, Foster City, CA). Gene expression was analyzed by quantitative real-time PCR (qPCR) using Power SYBR Green Mix (Applied Biosystems). Real-time PCR assays were performed in duplicate with a total 25 μL reaction volume containing 500 nM concentration of each primer and reverse transcribed mRNA (25 ng except 2.5 ng for the internal standard gene 18S). The sequences of all primers used are given in Supplemental Table S1. Primer pairs were designed using Primer-

BLAST software (http://www.ncbi.nlm.nih.gov/tools/primer-blast/). For all genes, each member of the primer pair was located in adjoining exons and shown by blast analysis to anneal exclusively to the target sequence. For all primer pairs, amplification efficiency ranged from 90-103% and yielded a single product by melting curve analysis. Data were analyzed using a relative standard curve based on a serial 4-fold dilution of pooled cDNA except when quantifying the relative abundance of the FGFR isoforms. In this case, the efficiency-corrected change in cycle threshold value method was used as previously described with all assays performed at the same detection threshold (Tacer et al., 2010; Schoenberg et al., 2011). 18S expression was used as the invariant control and any mRNA with a cycle number greater than 34 was declared undetectable.

Statistical Analysis

All data were analyzed by a mixed model using the fit model procedure of JMP Pro 14.3.0 statistical software (SAS Institute Inc., Cary, NC). Expression data describing the FGF21 system were analyzed with tissue as a fixed effect and animal as the random effect. Data collected at a single time point or collated over the treatment period were analyzed using a model accounting for treatment (control vs. FGF21) and period as fixed effects and animal as the random effect. Data collected over time were analyzed using a mixed model accounting for treatment (control vs. FGF21), time, period, and their interactions as fixed effects and animal as the random effect. Statistical significance and tendency were respectively set at $P < 0.05$ and $P < 0.10$ for main effects and at $P < 0.10$ and $P < 0.15$ for the FGF21 × Time interactions.

RESULTS

Components of the FGF21 system in the sheep

To identify possible sites of FGF21 production, tissues were collected from growing female sheep and assayed by RT-qPCR for FGF21 expression (Fig. 4.1A). The FGF21 cycle threshold number (Ct) was 29.2 ± 0.8 in liver whereas it was barely above the limit of detection in subcutaneous and retroperitoneal adipose tissue and in kidney, and undetectable in omental fat and skeletal muscle; as a consequence, FGF21 expression was 17-fold higher in liver than in other expressing tissues (Tissue, $P<0.05$).

FGF21 signaling is restricted to tissues expressing the co-receptor β-klotho. β-klotho expression was highest in retroperitoneal adipose tissue and in liver followed by subcutaneous and omental adipose tissue and finally kidney (Fig. 4.1A, Tissue, $P<0.0001$); β-klotho expression was barely detectable in muscle and absent in lungs.

Next, we measured the abundance of the β-klotho interacting FGF receptors FGFR1c, FGFR2c and FGFR3c in liver and subcutaneous adipose tissue. The FGF receptor expression profile was specific to each tissue, with over 69% of all receptors accounted by FGFR2c in liver and 98% by FGFR1c in subcutaneous adipose tissue (Fig. 4.1B). The sum total of β-klotho interacting FGF receptors was 3.7-fold higher in subcutaneous adipose tissue than in liver (Fig. 4.1C, $P<0.05$). The other fat depots were similar to subcutaneous adipose tissue in terms of FGF receptor profile and sum total of β-klotho interacting FGF receptors (results not shown). These results identify liver as a major site of FGF21 expression in the sheep and adipose tissue and liver as possible FGF21 target tissues.

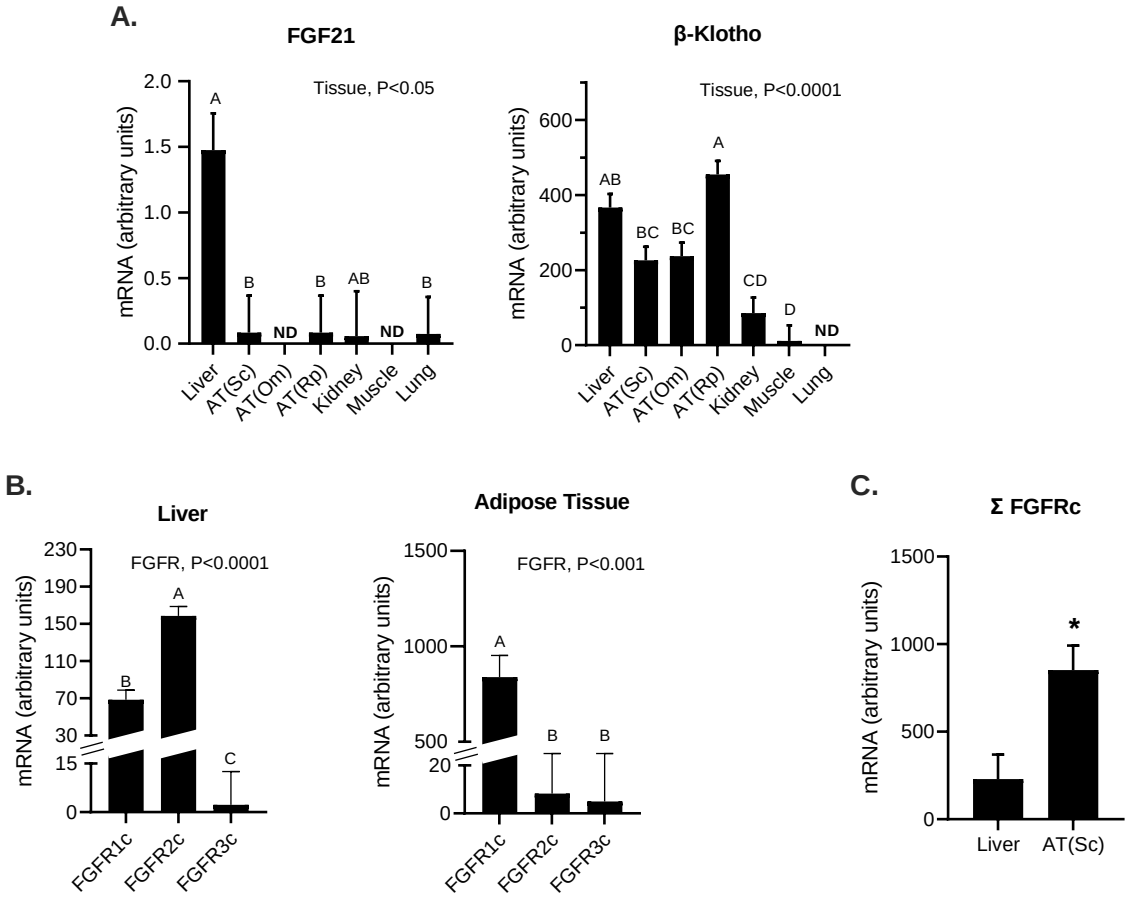

Figure 4.1. Expression of the components of the FGF21 signaling system. Tissues were obtained from 8-month old growing female sheep. All bars represent the LSM ± SE of 4 animals. (A) mRNA abundance of FGF21 and β-klotho across selected tissues. AT, adipose tissue; Sc, subcutaneous; Om, omental; Rp, retroperitoneal. The significant effect of Tissue is reported. Bars with different letters are significantly different at P<0.05; ND, non detectable. (B) mRNA abundance of β-klotho interacting FGF receptors in liver and subcutaneous (sc) adipose tissue. Bars with different letters differ at P<0.05. (C) Combined mRNA expression of β-klotho interacting FGF receptors in liver and subcutaneous adipose tissue [AT(Sc)]. *, P<0.05.

Pharmacokinetics and Bioactivity of Human FGF21 in the sheep

Disposition of human FGF21 was assessed by administering a single i.v. bolus of excipient solution or human FGF21 at the dose of 5 mg/kg MBW followed by blood sampling over the next 12 h. The concentration of plasma FGF21 was similar prior to bolus in control and FGF21 treated sheep (0.8 ± 0.3 vs 1.3 ± 0.6 ng/mL). Plasma FGF21 reached a peak of 53,803 ng/ml within 1 minute of FGF21 administration followed by a steady decline to 6.5 ng/ml after 12 h (Fig 4.2). Analysis of the concentration-time curve predicted a maximal concentration of 61,451 ng/mL at 0 min and an elimination $t_{1/2}$ of 94 min (Table 4.2). Other relevant pharmacokinetic parameters are reported in Table 4.2. As expected, plasma FGF21 did not vary significantly in sheep receiving the excipient bolus and averaged 0.9 ng/ml (Fig 4.2).

To determine whether human FGF21 is bioactive in the sheep, adipose tissue biopsies were taken immediately before and at fixed times after bolus administration. In tissues collected 15 min after bolus, FGF21 caused a 3.1-fold increase in immunoreactive pERK1/2 whereas the excipient had no effect (Figure 4.3A, FGF21 × Time, $P<0.0001$). In rodents, FGF21 signaling is followed by expression of rapid response genes such as EGR1 (Fisher et al., 2011). Although both treatments increased EGR1 expression 30 min after bolus, the increase was greater after the FGF21 than excipient bolus (FGF21 × Time, $P<0.07$). These results confirm bioactivity of the human FGF21 variant LY2405319 in the sheep and adipose tissue as a FGF21 target.

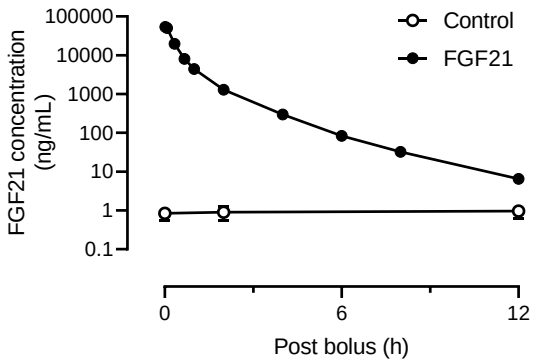

Figure 4.2. Disposition of FGF21 in plasma. Growing female sheep received an i.v. bolus of excipient (Control) or human FGF21 (FGF21) at the dose of 5 mg/kg MBW. Blood samples were analyzed after bolus at 0.017, 0.083, 0.33, 0.67, 1, 2, 4, 6, 8, and 12 h for FGF21 and at 0.017, 2, and 12 h for control. All data points represent the LSM ± SE of 6 sheep.

Table 4.2. Pharmacokinetic parameters of FGF21 after a single i.v. bolus injection[1]

Parameters[2]	Average ± SE
C_i (ng/mL)	61,451 ± 1,747
Vd (mL/kg)	163 ± 7
AUC (ng • min/mL)	1,494,352 ± 73,627
Elimination $t_{1/2}$ (min)	94 ± 4
mRT (min)	37 ± 2
Cl (mL/min/kg)	1.2 ± 0.06

[1]Female sheep (n=6) received a single i.v. bolus of human FGF21 at the dose of 5 mg/kg metabolic body weight, ($BW^{0.75}$).

[2]Ci, initial concentration; Vd, volume of distribution; AUC, area under the concentration-time curve extrapolated to infinity; $t_{1/2}$, half-life; mRT, mean residence time; Cl, clearance rate.

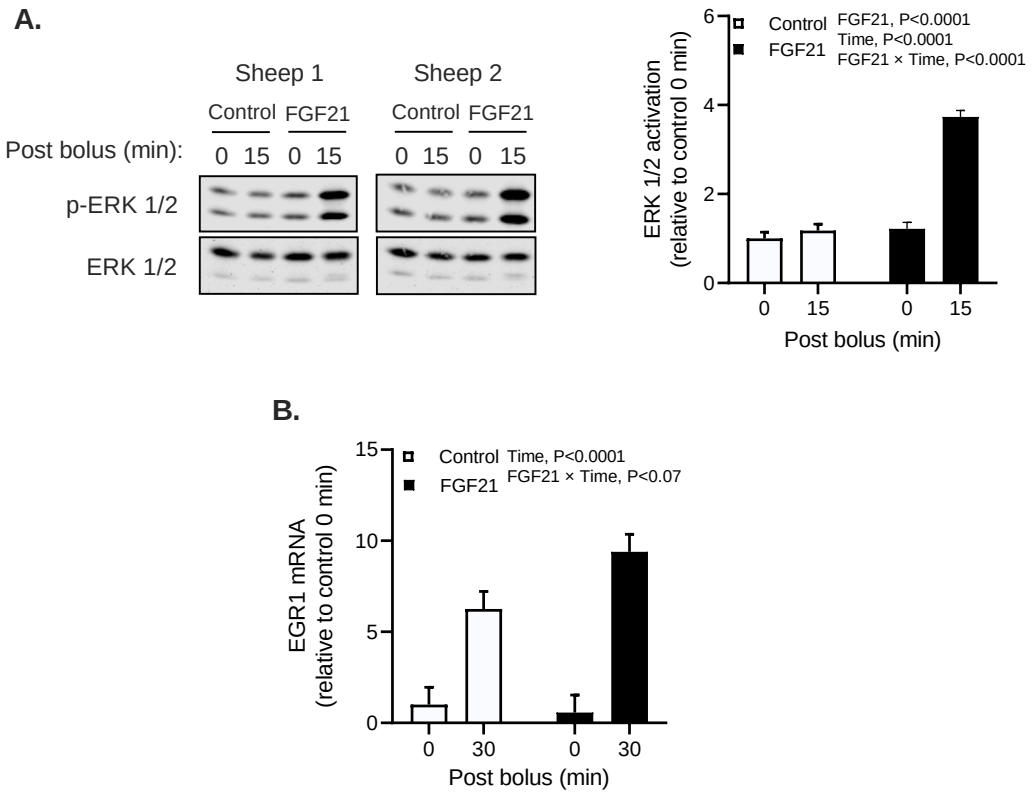

Figure 4.3. FGF21 signaling in white adipose tissue. Growing female sheep received an i.v. bolus of excipient (Control) or human FGF21 (FGF21) at the dose of 5 mg/kg MBW. (A) Biopsies of subcutaneous adipose tissue were obtained immediately before i.v. bolus at time 0 and then 15 min later. Total cellular extracts were prepared and analyzed by Western Immunoblotting. Left: threonine 202/tyrosine 204 phosphorylated (p-ERK1/2) and total p44/42 mitogen-activated protein kinase (ERK1/2) abundance in adipose tissue extracts from representative control and FGF21-treated sheep. Right: ERK1/2 activation (ratio of phosphorylated to total ERK1/2) was calculated and expressed relative to time 0. Each bar represents the LSM ± SE of 6 sheep. (B) Total RNA was isolated from adipose tissue obtained at time 0 and 30 min relative to the i.v. bolus and analyzed for the abundance of EGR1 mRNA. Expression is expressed relative to time 0. Each bar represents the LSM ± SE of 6 sheep. For all panels, the effects of FGF21 treatment, time, and the interaction between FGF21 treatment and time (FGF21 × Time) are reported when significant.

Effects of FGF21 treatment on growth and metabolic parameters

Acute metabolic effects A final study involved a 13-day treatment period with the excipient solution (control) or human FGF21 (FGF21) at the dose of 15 mg/kg MBW/day. To assess acute FGF21 effects, the first dose was administered as a single injection followed by frequent blood sampling over the next 24 h. At time 0, plasma FGF21 concentration in both groups of sheep averaged 0.75 ± 0.23 ng/mL and remained at this level in the sheep receiving the excipient solution (Figure 4.4A). In contrast, the plasma FGF21 concentration rose within 30 min to a near peak of 1806 ± 140 ng/ml in the FGF21 group, followed by a decline to 224 ± 83 ng/ml over the next 23 h.

The concentration of plasma fatty acids declined over the first 12 h post-bolus and then rebounded (Fig. 4.4B, Time, $P<0.02$) but was not affected by treatment. The concentration of plasma glucose was lower in FGF21 than excipient-treated sheep, particularly between 8 and 24 h post-bolus (Fig 4.4C, FGF21 × Time, $P<0.01$). The concentration of plasma insulin was lower in FGF21 than excipient-treated sheep 30 min post-bolus followed by a rebound over the next 2.5 h (Fig 4.4D, FGF21 × Time, $P<0.07$). Plasma adiponectin remained invariant irrespective of time and treatment (Fig. 4.4E).

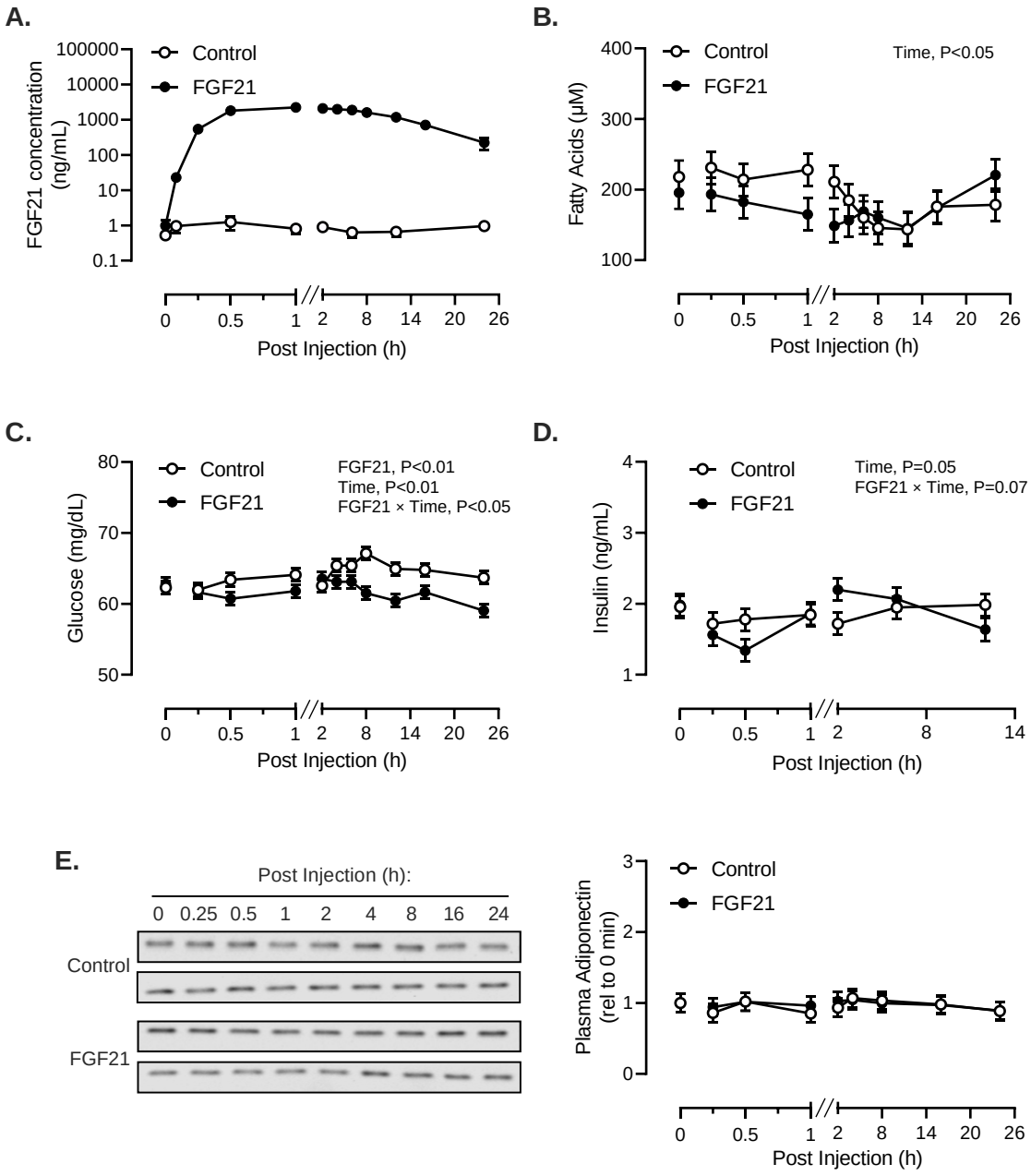

Figure 4.4. Acute effects of FGF21 treatment on plasma variables. Growing female sheep were treated with a single s.c. injection of excipient (Control) or human FGF21 (FGF21) at the dose of 15 mg/kg MBW. Blood samples were collected over the first 24 h of treatment. (A-D) Plasma concentration of FGF21, fatty acids, glucose, and insulin. All data points represent the LSM ± SE of 6 sheep. (E) Plasma concentration of adiponectin measured by Western blotting. Left: Adiponectin signals from representative control and FGF21 treated sheep. Right: Plasma adiponectin abundance expressed relative to time 0. For all panels, effects of FGF21 treatment, time, and the interaction of FGF21 treatment and time (FGF21 x Time) are reported when significant.

Chronic growth and metabolic effects For the remainder of the experimental period, treatments were administered as twice daily injection. Initial body weight did not differ between treatment (control, 52.7 ± 1.3 kg; FGF21, 51.3 ± 1.3 kg) and FGF21 had no effect on voluntary feed intake (control, 1.13 ± 0.04 kg; FGF21, 1.09 ± 0.04 kg) and weight gain (control, 1.83 ± 0.68 kg; FGF21, 1.67 ± 0.68 kg).

Plasma samples were obtained 2 h after the first daily bolus. Under this mode of administration, plasma FGF21 remained stable over the treatment period at 2.2 ± 0.3 and 2012 ± 55 ng/ml for excipient and FGF21-treated animals (Fig. 4.5A). FGF21 tended to reduced plasma IGF-I starting on day 6 of treatment (Fig 4.5B, FGF21, $P < 0.09$). FGF21 caused a reduction in plasma glucose throughout the entire treatment period (Fig. 4.5C, $P< 0.01$) and a similar depressing effect on plasma insulin except for a rebound by the end of treatment (Fig 4.5D, FGF21 × Time, $P<0.05$).

To assess the possibility that FGF21 effects on glucose and insulin represented insulin sensitization, sheep were administered a glucose tolerance test on day 12 of treatment. FGF21 treatment resulted in a slightly lower plasma glucose profile and tended to cause a lower glucose response area (Fig 4.6A, FGF21, $P=0.06$). FGF21 also lowered the plasma insulin profile but did not lead to a significant reduction in the response area (Fig 4.6B).

FGF21 treatment did not have any effects on plasma fatty acids (Fig. 4.5E). To assess whether FGF21 alters β-adrenergic responsiveness of adipose tissue, sheep were administered an epinephrine challenge test on day 13 of treatment. The fatty acid response area, calculated over 60 min, tended to be increased by FGF21 treatment (Fig. 4.7A, $P<0.07$), suggesting an elevated β-adrenergic responsiveness. FGF21 had no significant effect on the glucose response during the epinephrine challenge test (Fig. 4.7B).

Effects on the insulin-sensitizing hormone adiponectin FGF21 increased plasma adiponectin by 2-fold over the treatment period whereas excipient treatment had no effect (Fig 4.8A, $P<0.05$). To determine the timing of this effect, plasma adiponectin was analyzed every 3 or 4 days; the positive effect of FGF21 became apparent on day 3 of treatment and continued to increase until reaching a plateau on day 9 of treatment (Fig 4.8B, FGF21 × Time, $P<0.01$).

Table 4.3. Animal performance during chronic FGF21 treatment

Variable	Control	FGF21	SEM	Probability level[2]
Start Weight (kg)	52.7	51.3	1.3	NS
Weight gain (kg)	1.83	1.67	0.68	NS
Intake (kg/d)	1.13	1.09	0.04	NS
Energy intake (%maintenance)[3]	139.3	132.9	7.2	0.06
Rectal Temperature (°F)	101.9	102.3	0.2	NS

[1]Growing female sheep received s.c. injections of excipient (control) or human FGF21 (FGF21) at the dose of 15 mg/kg MBW/day for 13 days.

[2]Type I probability error. NS = P>0.10

[3]Metabolizable energy intake expressed as a % of maintenance energy requirement.

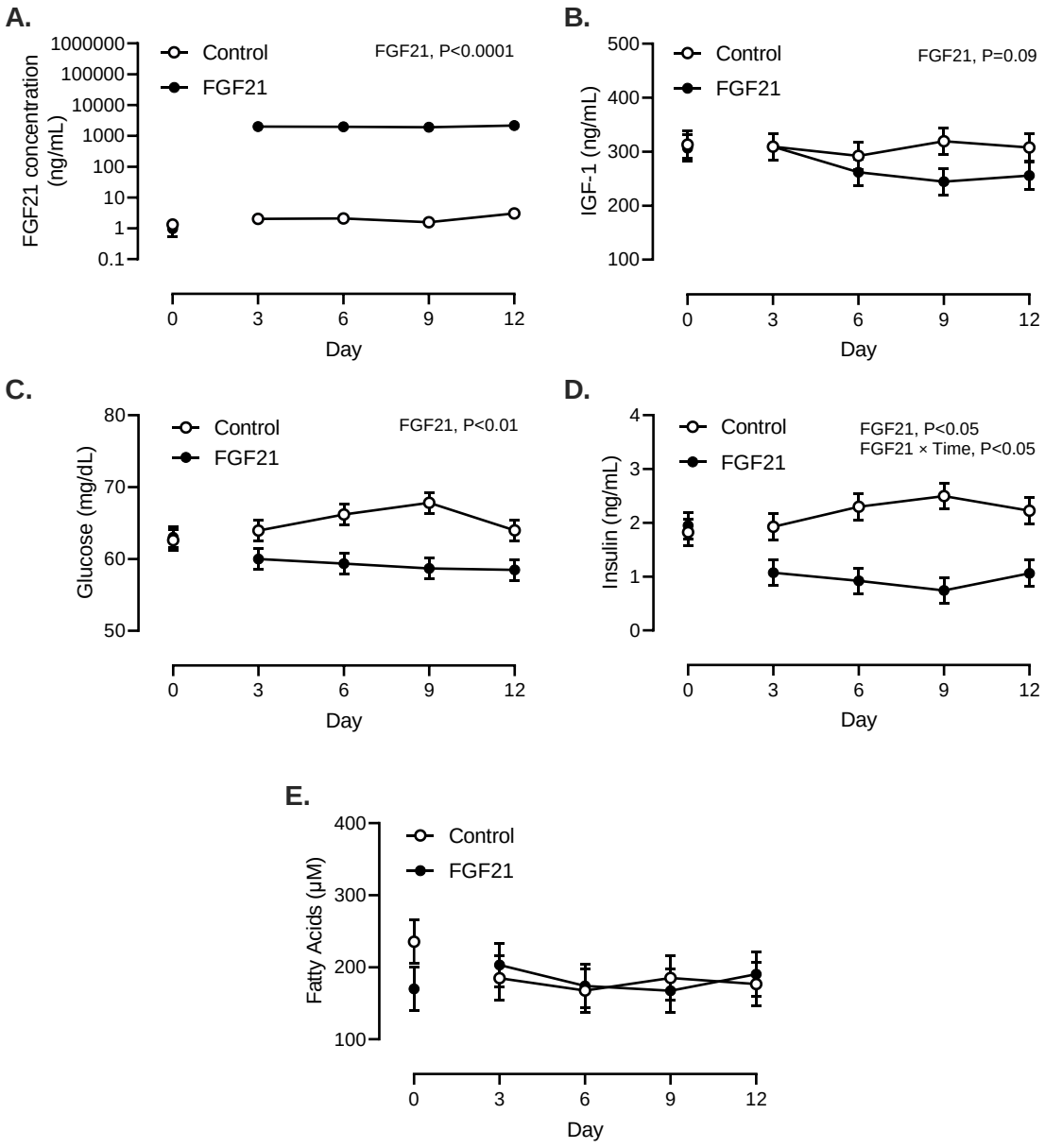

Figure 4.5. Effects of chronic FGF21 treatment on plasma variables. Growing female sheep received daily s.c. injection of excipient (Control) or human FGF21 (FGF21) at the dose of 15 mg/kg MBW/day. Treatments were administered as a single injection on the first day of treatment and as twice daily injection thereafter. (A-E) Plasma samples collected every 3 days during the treatment period were analyzed for the concentration of FGF21, IGF-1, glucose, insulin, and fatty acids. All data points represent the LSM ± SE of 6 sheep. Effects of FGF21 treatment, time, and the interaction of FGF21 treatment and time (FGF21 × Time) are reported when significant.

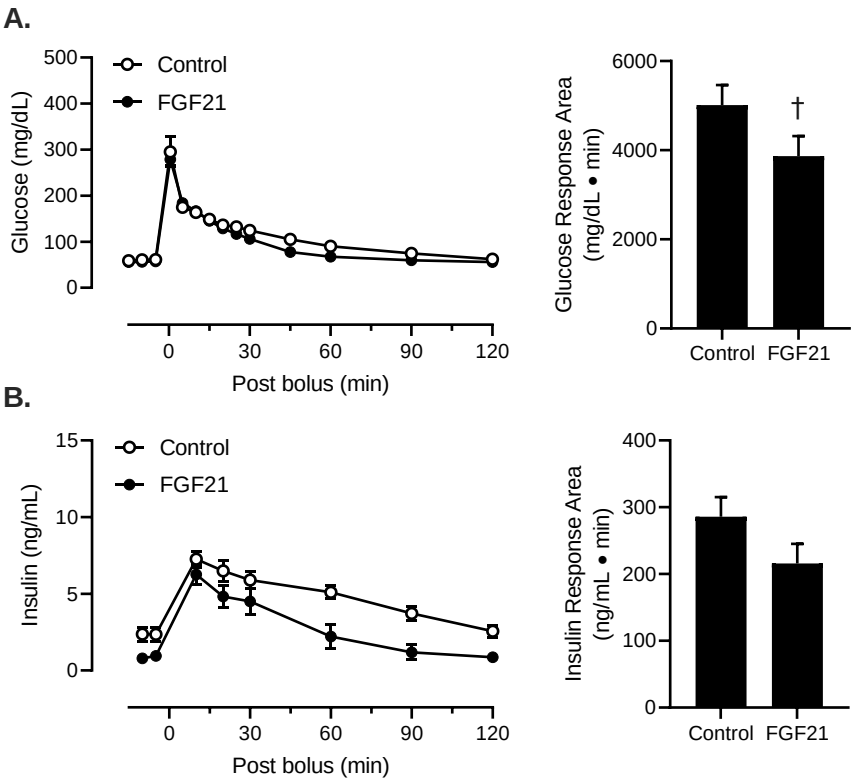

Figure 4.6. Chronic effects of FGF21 treatment on glucose tolerance. Growing female sheep received daily s.c. injection of excipient (Control) or human FGF21 (FGF21) at the dose of 15 mg/kg MBW/day. Treatments were administered as a single injection on the first day of treatment and as twice daily injection thereafter. A glucose tolerance test was performed on day 12 of treatment. (A) Plasma glucose concentration and glucose response area calculated over 90 min; †, $P<0.07$. (B) Plasma insulin concentration and insulin response area calculated over 120 min. All points and bars represent the LSM ± SE of 6 sheep.

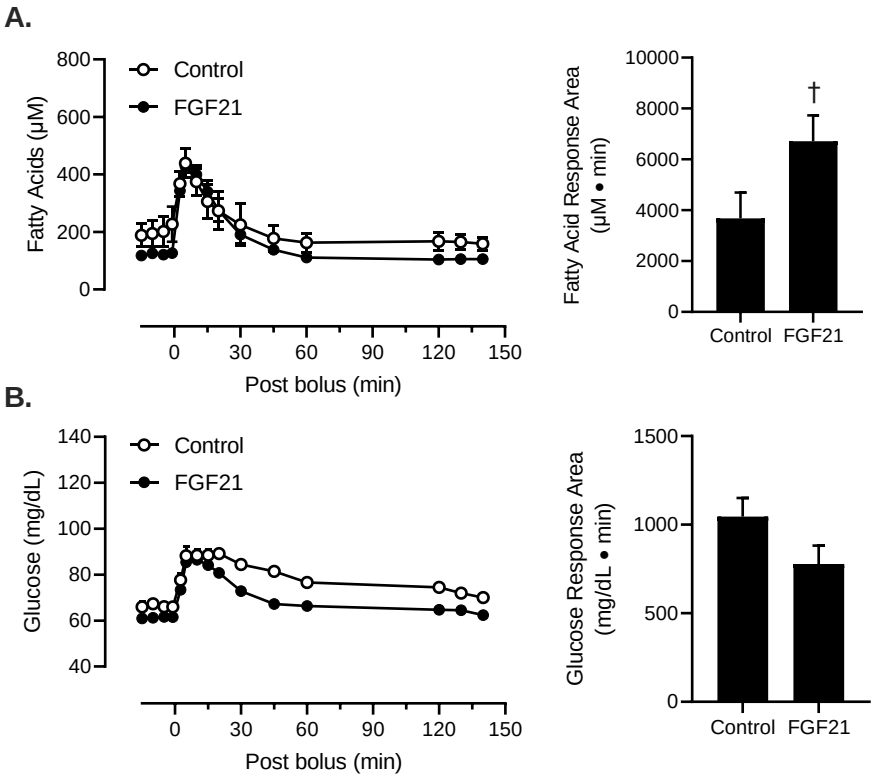

Figure 4.7. Effects of chronic FGF21 treatment on epinephrine response. Growing female sheep received daily s.c. injection of excipient (Control) or human FGF21 (FGF21) at the dose of 15 mg/kg MBW/day. Treatments were administered as a single injection on the first day of treatment and as twice daily injection thereafter. An epinephrine challenge was performed on day 13 of treatment. (A) Plasma fatty acid concentrations and fatty acid response area calculated over 60 min; †, $P<0.07$. (B) Plasma glucose concentration and glucose response area calculated over 60 min. All points and bars represent the LSM ± SE of 6 sheep.

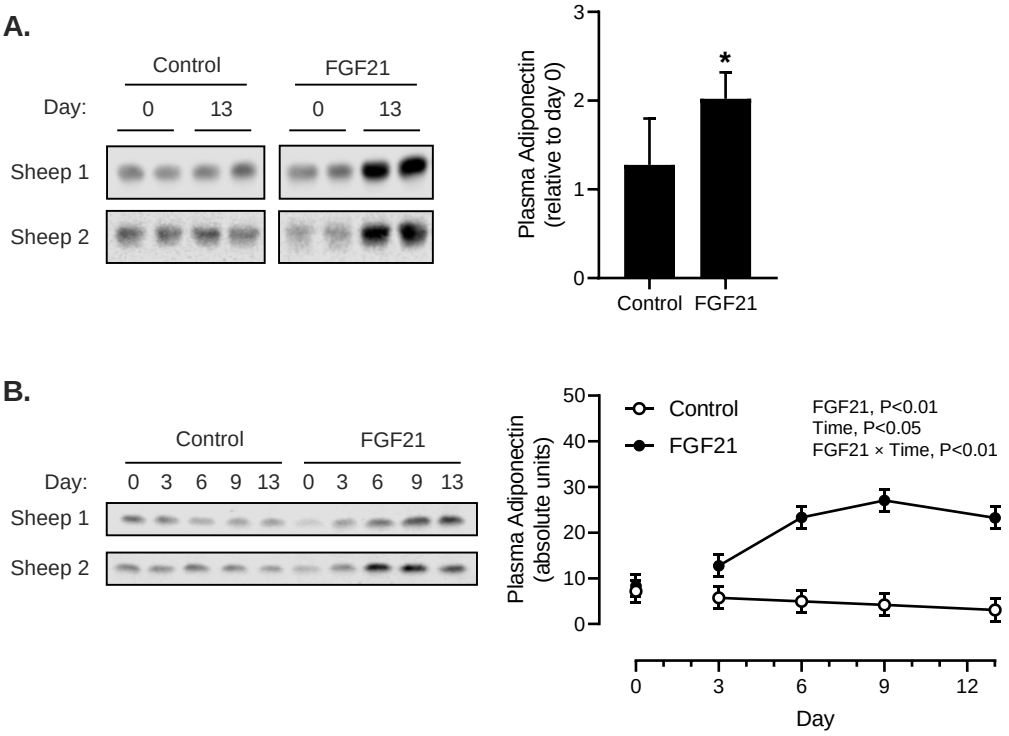

Figure 4.8. Effect of chronic FGF21 treatment on plasma adiponectin. Growing female sheep received daily s.c. injection of excipient (Control) or human FGF21 (FGF21) at the dose of 15 mg/kg MBW/day. Treatments were administered as a single injection on the first day of treatment and as twice daily injection thereafter. (A) Left: Plasma samples collected before (day 0) and at the term of the period of treatment (day 13) were analyzed by Western Immunoblotting for adiponectin abundance. Adiponectin signals are shown for 2 representative sheep. Right: The adiponectin signal was calculated and expressed relative to time 0, with each bar representing the LSM ± SE of 6 sheep. *, P<0.05. (B) Left: Plasma samples were collected at regular intervals during treatment and analyzed by Western Immunoblotting for adiponectin abundance. Adiponectin signals are shown for 2 representative sheep. Right: Plasma adiponectin abundance over the treatment period. Effects of FGF21 treatment and the interaction of FGF21 treatment and time (FGF21 × Time) are reported when significant.

DISCUSSION

Exogenous FGF21 administration consistently reduces plasma insulin and glucose as well as improves insulin action during glucose tolerance or insulin tolerance tests in rodent and primate models (Kharitonenkov et al., 2005; Coskun et al., 2008; Adams et al., 2013). FGF21 work in these species has been focused on its therapeutic potential and therefore performed almost exclusively in states of energy surplus such as obesity and type 2 diabetes. In contrast, our interest has been to explore the insulin-sensitizing effect of FGF21 in the energy insufficient dairy cow (Krumm et al., 2019). The absence of such effect in this model led us to hypothesize that effect of FGF21 on insulin action requires a positive energy balance. Given the limited availability of FGF21, we chose to perform this work in sheep, a smaller but closely related ruminant.

In absence of previous FGF21 work in sheep, we first sought to characterize sites of FGF21 production, and target tissues. Our data identifies liver as the predominant site of FGF21 expression and barely detectable expression in adipose tissue. This pattern of FGF21 expression is nearly identical to those previously described in cattle (Schoenberg et al., 2011) and humans (Dushay et al., 2010), and contrasts with that of mice where basal expression is nearly as high in adipose tissue as in liver (Cui et al., 2014).

Next we identified potential FGF21 target tissues by measuring expression of its receptor complexes and FGF21-dependent signaling events. FGFs signal through a family of tyrosine kinase receptors (FGFR1-4). Most members of the FGF superfamily can bind these receptors with high affinity in large part due to presence of the heparin binding domain. This domain is missing in FGF21 with the consequence that high affinity binding depends on the presence of the co-receptor β-klotho (Suzuki et al., 2008). It follows that high β-klotho expression is required

for FGF21 signaling. In mice, β-klotho expression is highest in brown adipose tissue, followed by liver and white adipose tissue. Other expressing tissues include gall bladder, pancreas, and brain (Tacer et al., 2010; Hultman et al., 2019). The present study revealed β-klotho was highest in adipose and liver and this pattern is quite similar to that seen in cattle where expression was highest in internal white adipose depots, followed by peripheral adipose depots and liver (Schoenberg et al., 2011). With respect to FGFR, at least 7 isoforms exist, arising from the combination of 4 genes and alternative splicing. Of these, however, only FGFR1c-3c are capable of interacting with β-klotho and of mediating FGF21 signaling. More recent work however, suggests that virtually all FGF21 signaling *in vivo* is through FGFR1c (Adams et al., 2012b). In support of this, FGFR1 knockout mice put on a high fat diet and treated with FGF21 displayed blunted FGF21 signaling and insulin sensitizing responses. In addition, adiponectin was not increased and dyslipidemia was not improved (Adams et al., 2012b). Our results in the sheep show that FGFR1c expression accounts for 98% of all FGFR in adipose and is 12-fold more abundant in adipose than liver. Similar results were obtained in cattle where FGFR1c accounted for more than 99% of all FGFR in adipose tissue and was expressed at substantially higher levels in adipose tissue than in liver (Schoenberg et al., 2011).

The gold standard method to identify target tissue is documentation of FGF21 signaling events immediately after administration. The predominant early signaling event triggered by FGF21 is ERK 1/2 phosphorylation, followed later by increased expression of early response genes such as c-fos or Egr1. In mice, ERK 1/2 phosphorylation is consistently upregulated in adipose tissue, but only Fisher et al. reported upregulation in liver (Kurosu et al., 2007; Fisher et al., 2011). We now identified adipose tissue as an FGF21 target tissue in the sheep on the basis of the combined increase in ERK 1/2 phosphorylation and Egr1 expression in close agreement

with what we previously reported in early lactating dairy cows. Because of difficulties in obtaining liver biopsies in the sheep, we could not perform similar measurements in liver. However, we previously reported negligible FGFR1c expression combined with the absence of FGF21 signaling events in bovine liver. With similarly low FGFR1c expression, ovine liver is also unlikely to be a direct FGF21 target tissue in the sheep. Finally, we took advantage of this experiment to characterize disposition of the human FGF21 variant LY2405319 in the sheep. This work revealed a half-life of 94 min. Intravenous administration of human FGF21 in cattle, monkeys, and mice yielded half-lives of 194, 120, and 90 min were reported (Kharitonenkov et al., 2007; Xu et al., 2009; Caixeta et al., 2019).

FGF21 research in rodents and primates has focused on its potential as a therapy for type 2 diabetes, an effort motivated by the observation that FGF21 is a potent stimulator of glucose uptake in adipocytes (Kharitonenkov et al., 2005). For example, FGF21 lowers plasma glucose and insulin within 1 hr of injection in rodent models of obesity including the *ob/ob* and diet induced obese mice; these effects are sustained during chronic administration (Kharitonenkov et al., 2005; Xu et al., 2009). Using dynamic tests such as GTT, these FGF21 effects have been traced to improvement in insulin-mediated glucose disposal. Our results in growing sheep are in broad agreement with the rodent work: FGF21 treatment reduced plasma glucose and insulin both acutely and chronically and this effect was associated with improved glucose disposal during GTT. In contrast, FGF21 had no effect on these outcomes in early lactating, energy deficient dairy cows (Krumm et al., 2019). These results suggest that beneficial effects of FGF21 on carbohydrate metabolism require a state of positive energy balance.

One possible mechanism explaining effects of FGF21 on glucose metabolism is stimulation of adiponectin production. Adiponectin is a 30-kDa protein hormone secreted

exclusively by adipose tissue. Genetically engineered mouse models suggest that this adipokine improves insulin action: knockout models exhibit insulin insensitivity while transgenic models show improved insulin action (Maeda et al., 2002; Nawrocki et al., 2006; Kim et al., 2007). Circulating adiponectin is increased following both acute and chronic FGF21 administration in mice (Camporez et al., 2013; Holland et al., 2013; Lin et al., 2013). Adiponectin knockout mice were used to ask whether FGF21 effects depended on adiponectin; adiponectin absence negated much of the insulin-sensitizing effects of FGF21 (Holland et al., 2013; Lin et al., 2013). Interestingly, we observed a significant increase in adiponectin with chronic FGF21 treatment, but this effect was not seen in energy-deficient dairy cows. Our data are consistent with adiponectin as a mediator of FGF21 action on carbohydrate metabolism.

FGF21 is reported to have contrasting effects on lipolysis depending on the energy status. Hotta et al. reported that FGF21 stimulated lipolysis in the fed state, but inhibited it during fasting (Hotta et al., 2009). In addition, mice overexpressing FGF21 exhibit increased lipolytic activity in adipose tissue in addition to elevated circulating fatty acids when fed (Inagaki et al., 2007). A lipolytic effect also was demonstrated in alcohol-treated fed mice: alcohol increases circulating FGF21, and this was shown to increase circulating catecholamines and plasma fatty acids (Zhao et al., 2015). FGF21 treatment reduced plasma fatty acids in early lactating cows suggesting an antilipolytic effect during negative energy balance (Caixeta et al., 2019). In the present study, FGF21 had no effect on basal lipolysis, but increased the lipolytic response to epinephrine. Overall, these data suggest that FGF21 effects on lipolysis in ruminants depend on the energy status, as demonstrated in rodents.

FGF21 has been effective in rodent and primate models in reducing adiposity and accordingly, body weight. These effects were traced to a stimulation of thermogenesis in rodents

and to a reduction in appetite in primates (Fisher et al., 2012; Adams et al., 2013; Owen et al., 2014). In our sheep, there was no effect on voluntary intake, nor were there any effects on body weight. Finally, FGF21 modulates GH action in rodents. This was demonstrated in mice expressing FGF21, which displayed stunted growth as well as evidence of GH resistance and decreased plasma IGF-1 (Inagaki et al., 2008). FGF21-treated sheep tended to have lower plasma IGF-1 than control animals, but average daily gain or final body weight were not affected. This suggests FGF21 modulation on GH action in growing sheep may be minimal, although this remains to be explored further.

CONCLUSION

In conclusion, we have shown the FGF21 system is similarly organized in sheep compared with other species. Specifically, liver is the main tissue expressing FGF21 and adipose tissue is an important target tissue. In addition, we have shown that FGF21 treatment could improve insulin sensitivity and increase circulating adiponectin. This contrasts with what we reported previously in the energy deficient dairy cow, suggesting that energy balance might be an important determinant of FGF21 insulin-sensitizing actions. Future work is needed in the same ruminant species to test FGF21 effects during contrasting energy status.

REFERENCES

Adams, A. C., C. C. Cheng, T. Coskun, and A. Kharitonenkov. 2012a. FGF21 requires βklotho to act in vivo. PloS One 7(11):e49977. doi: 10.1371/journal.pone.0049977 PMID - 23209629

Adams, A. C., C. A. Halstead, B. C. Hansen, A. R. Irizarry, J. A. Martin, S. R. Myers, V. L. Reynolds, H. W. Smith, V. J. Wroblewski, and A. Kharitonenkov. 2013. LY2405319, an Engineered FGF21 Variant, Improves the Metabolic Status of Diabetic Monkeys. PloS One 8(6):e65763. doi: 10.1371/journal.pone.0065763 PMID - 23823755

Adams, A. C., C. Yang, T. Coskun, C. C. Cheng, R. E. Gimeno, Y. Luo, and A. Kharitonenkov. 2012b. The breadth of FGF21's metabolic actions are governed by FGFR1 in adipose tissue. Molecular Metabolism 2(1):31-37. doi: 10.1016/j.molmet.2012.08.007 PMID - 24024127

Altschul, S. F., T. L. Madden, A. A. Schäffer, J. Zhang, Z. Zhang, W. Miller, and D. J. Lipman. 1997. Gapped BLAST and PSI-BLAST: a new generation of protein database search programs. Nucleic Acids Research 25(17):3389-3402. doi: 10.1093/nar/25.17.3389

Altschul, S. F., J. C. Wootton, E. M. Gertz, R. Agarwala, A. Morgulis, A. A. Schäffer, and Y. K. Yu. 2005. Protein database searches using compositionally adjusted substitution matrices. FEBS Journal 272(20):5101-5109. doi: 10.1111/j.1742-4658.2005.04945.x

Bell, A. W., and D. E. Bauman. 1997. Adaptations of glucose metabolism during pregnancy and lactation. Journal of Mammary Gland Biology and Neoplasia 2(3):265-278.

Block, S. S., W. R. Butler, R. A. Ehrhardt, A. W. Bell, M. E. V. Amburgh, and Y. R. Boisclair. 2001. Decreased concentration of plasma leptin in periparturient dairy cows is caused by negative energy balance. Journal of Endocrinology 171(2):339-348.

Caixeta, L. S., S. L. Giesy, C. S. Krumm, J. W. Perfield, A. Butterfield, and Y. R. Boisclair. 2019. Fibroblast growth factor-21 (FGF21) administration to early-lactating dairy cows. II. Pharmacokinetics, whole-animal performance, and lipid metabolism. Journal of Dairy Science doi: 10.3168/jds.2019-16696 PMID - 31548064

Caixeta, L. S., S. L. Giesy, C. S. Krumm, J. W. Perfield, A. Butterfield, K. M. Schoenberg, D. C. Beitz, and Y. R. Boisclair. 2017. Effect of circulating glucagon and free fatty acids on hepatic FGF21 production in dairy cows. American Journal of Physiology: Regulatory, Integrative and Comparative Physiology:ajpregu.00197.02017. doi: 10.1152/ajpregu.00197.2017 PMID - 28794103

Camporez, J. P. G., F. R. Jornayvaz, M. C. Petersen, D. Pesta, B. A. Guigni, J. Serr, D. Zhang, M. Kahn, V. T. Samuel, M. J. Jurczak, and G. I. Shulman. 2013. Cellular Mechanisms by Which FGF21 Improves Insulin Sensitivity in Male Mice. Endocrinology 154(9):3099-3109. doi: 10.1210/en.2013-1191 PMID - 23766126

Coskun, T., H. A. Bina, M. A. Schneider, J. D. Dunbar, C. C. Hu, Y. Chen, D. E. Moller, and A. Kharitonenkov. 2008. Fibroblast growth factor 21 corrects obesity in mice. Endocrinology 149(12):6018-6027. doi: 10.1210/en.2008-0816 PMID - 18687777

Cui, Y., S. L. Giesy, M. Hassan, K. Davis, S. Zhao, and Y. R. Boisclair. 2014. Hepatic FGF21 production is increased in late pregnancy in the mouse. American Journal of Physiology: Regulatory, Integrative and Comparative Physiology 307(3):R290-298. doi: 10.1152/ajpregu.00554.2013 PMID - 24898837

De Koster, J. D., and G. Opsomer. 2013. Insulin resistance in dairy cows. Veterinary Clinics of North America: Food Animal Practice 29(2):299-322. doi: 10.1016/j.cvfa.2013.04.002

Duehlmeier, R., I. Fluegge, B. Schwert, and M. Ganter. 2013. Insulin Sensitivity during Late Gestation in Ewes Affected by Pregnancy Toxemia and in Ewes with High and Low Susceptibility to this Disorder. Journal of Veterinary Internal Medicine 27(2):359-366. doi: 10.1111/jvim.12035 PMID - 23397990

Dushay, J., P. C. Chui, G. S. Gopalakrishnan, M. Varela–Rey, M. Crawley, F. M. Fisher, M. K. Badman, M. L. Martinez–Chantar, and E. Maratos–Flier. 2010. Increased Fibroblast Growth Factor 21 in Obesity and Nonalcoholic Fatty Liver Disease. Gastroenterology 139(2):456-463. doi: 10.1053/j.gastro.2010.04.054 PMID - 20451522

Fisher, F. M., J. L. Estall, A. C. Adams, P. J. Antonellis, H. A. Bina, J. S. Flier, A. Kharitonenkov, B. M. Spiegelman, and E. Maratos-Flier. 2011. Integrated Regulation of Hepatic Metabolism by Fibroblast Growth Factor 21 (FGF21) in Vivo. Endocrinology 152(8):2996-3004. doi: 10.1210/en.2011-0281 PMID - 21712364

Fisher, F. M., S. Kleiner, N. Douris, E. C. Fox, R. J. Mepani, F. Verdeguer, J. Wu, A. Kharitonenkov, J. S. Flier, E. Maratos-Flier, and B. M. Spiegelman. 2012. FGF21 regulates PGC-1α and browning of white adipose tissues in adaptive thermogenesis. Genes and Development 26(3):271-281. doi: 10.1101/gad.177857.111 PMID - 22302939

Greenwood, P. L., A. S. Hunt, R. M. Slepetis, K. D. Finnerty, C. Alston, D. H. Beermann, and A. W. Bell. 2002. Effects of birth weight and postnatal nutrition on neonatal sheep: III. Regulation of energy metabolism. Journal of Animal Science 80(11):2850-2861. doi: 10.2527/2002.80112850x

Holland, W. L., A. C. Adams, J. T. Brozinick, H. H. Bui, Y. Miyauchi, C. M. Kusminski, S. M. Bauer, M. Wade, E. Singhal, C. C. Cheng, K. Volk, M.-S. S. Kuo, R. Gordillo, A. Kharitonenkov, and P. E. Scherer. 2013. An FGF21-adiponectin-ceramide axis controls energy expenditure and insulin action in mice. Cell Metabolism 17(5):790-797. doi: 10.1016/j.cmet.2013.03.019 PMID - 23663742

Hotta, Y., H. Nakamura, M. Konishi, Y. Murata, H. Takagi, S. Matsumura, K. Inoue, T. Fushiki, and N. Itoh. 2009. Fibroblast growth factor 21 regulates lipolysis in white adipose tissue but is not required for ketogenesis and triglyceride clearance in liver. Endocrinology 150(10):4625-4633. doi: 10.1210/en.2009-0119 PMID - 19589869

Hultman, K., J. M. Scarlett, A. F. Baquero, A. Cornea, Y. Zhang, C. B. G. Salinas, J. Brown, G. J. Morton, E. J. Whalen, K. L. Grove, F. H. Koegler, M. W. Schwartz, and A. J. Mercer. 2019. The central fibroblast growth factor receptor/beta klotho system: Comprehensive mapping in Mus musculus and comparisons to nonhuman primate and human samples using an automated in situ hybridization platform. Journal of Comparative Neurology 527(12):2069-2085. doi: 10.1002/cne.24668 PMID - 30809795

Inagaki, T., P. Dutchak, G. Zhao, X. Ding, L. Gautron, V. Parameswara, Y. Li, R. Goetz, M. Mohammadi, V. Esser, J. K. Elmquist, R. D. Gerard, S. C. Burgess, R. E. Hammer, D. J. Mangelsdorf, and S. A. Kliewer. 2007. Endocrine regulation of the fasting response by PPARalpha-mediated induction of fibroblast growth factor 21. Cell Metabolism 5(6):415-425. doi: 10.1016/j.cmet.2007.05.003 PMID - 17550777

Inagaki, T., V. Y. Lin, R. Goetz, M. Mohammadi, D. J. Mangelsdorf, and S. A. Kliewer. 2008. Inhibition of growth hormone signaling by the fasting-induced hormone FGF21. Cell Metabolism 8(1):77-83. doi: 10.1016/j.cmet.2008.05.006 PMID - 18585098

Kharitonenkov, A., J. M. Beals, R. Micanovic, B. A. Strifler, R. Rathnachalam, V. J. Wroblewski, S. Li, A. Koester, A. M. Ford, T. Coskun, J. D. Dunbar, C. C. Cheng, C. C. Frye, T. F. Bumol, and D. E. Moller. 2013. Rational design of a fibroblast growth factor 21-based clinical candidate, LY2405319. PloS One 8(3):e58575. doi: 10.1371/journal.pone.0058575 PMID - 23536797

Kharitonenkov, A., T. L. Shiyanova, A. Koester, A. M. Ford, R. Micanovic, E. J. Galbreath, G. E. Sandusky, L. J. Hammond, J. S. Moyers, R. A. Owens, J. Gromada, J. T. Brozinick, E. D. Hawkins, V. J. Wroblewski, D.-S. S. Li, F. Mehrbod, S. R. Jaskunas, and A. B. Shanafelt. 2005. FGF-21 as a novel metabolic regulator. Journal of Clinical Investigation 115(6):1627-1635. doi: 10.1172/JCI23606 PMID - 15902306

Kharitonenkov, A., V. J. Wroblewski, A. Koester, Y.-F. F. Chen, C. K. Clutinger, X. T. Tigno, B. C. Hansen, A. B. Shanafelt, and G. J. Etgen. 2007. The metabolic state of diabetic monkeys is regulated by fibroblast growth factor-21. Endocrinology 148(2):774-781. doi: 10.1210/en.2006-1168 PMID - 17068132

Kim, J. Y., E. van de Wall, M. Laplante, A. Azzara, M. E. Trujillo, S. M. Hofmann, T. Schraw, J. L. Durand, H. Li, G. Li, L. A. Jelicks, M. F. Mehler, D. Y. Hui, Y. Deshaies, G. I. Shulman, G. J. Schwartz, and P. E. Scherer. 2007. Obesity-associated improvements in metabolic profile through expansion of adipose tissue. Journal of Clinical Investigation 117(9):2621-2637. doi: 10.1172/jci31021

Krumm, C. S., S. L. Giesy, L. S. Caixeta, J. W. Perfield, H. Sauerwein, B. L. Moore, and Y. R. Boisclair. 2019. Fibroblast growth factor-21 (FGF21) administration to early-lactating dairy cows. I. Effects on signaling and indices of insulin action. Journal of Dairy Science doi: 10.3168/jds.2019-16695 PMID - 31548053

Krumm, C. S., S. L. Giesy, C. L. Orndorff, and Y. R. Boisclair. 2018. Variation in x-box binding protein 1 (XBP1) expression and its dependent endoplasmic reticulum chaperones does

not regulate adiponectin secretion in dairy cows. Journal of Dairy Science doi: 10.3168/jds.2017-14048 PMID - 29550138

Kurosu, H., M. Choi, Y. Ogawa, A. S. Dickson, R. Goetz, A. V. Eliseenkova, M. Mohammadi, K. P. Rosenblatt, S. A. Kliewer, and M. Kuro-o. 2007. Tissue-specific Expression of βKlotho and Fibroblast Growth Factor (FGF) Receptor Isoforms Determines Metabolic Activity of FGF19 and FGF21. Journal of Biological Chemistry 282(37):26687-26695. doi: 10.1074/jbc.m704165200 PMID - 17623664

Lin, Z., H. Tian, Karen S. L. Lam, S. Lin, Ruby C. L. Hoo, M. Konishi, N. Itoh, Y. Wang, Stefan R. Bornstein, A. Xu, and X. Li. 2013. Adiponectin Mediates the Metabolic Effects of FGF21 on Glucose Homeostasis and Insulin Sensitivity in Mice. Cell Metabolism 17(5):779-789. doi: 10.1016/j.cmet.2013.04.005 PMID - 23663741

Maeda, N., I. Shimomura, K. Kishida, H. Nishizawa, M. Matsuda, H. Nagaretani, N. Furuyama, H. Kondo, M. Takahashi, Y. Arita, R. Komuro, N. Ouchi, S. Kihara, Y. Tochino, K. Okutomi, M. Horie, S. Takeda, T. Aoyama, T. Funahashi, and Y. Matsuzawa. 2002. Diet-induced insulin resistance in mice lacking adiponectin/ACRP30. Nature Medicine 8(7):731-737. doi: 10.1038/nm724

Nawrocki, A. R., M. W. Rajala, E. Tomas, U. B. Pajvani, A. K. Saha, M. E. Trumbauer, Z. Pang, A. S. Chen, N. B. Ruderman, H. Chen, L. Rossetti, and P. E. Scherer. 2006. Mice lacking adiponectin show decreased hepatic insulin sensitivity and reduced responsiveness to peroxisome proliferator-activated receptor gamma agonists. Journal of Biological Chemistry 281(5):2654-2660. doi: 10.1074/jbc.M505311200

Nishimura, T., Y. Nakatake, M. Konishi, and I. N. e. Acta. 2000. Identification of a novel FGF, FGF-21, preferentially expressed in the liver. Biochimica et Biophysica Acta

Ornitz, D. M. 2000. FGFs, heparan sulfate and FGFRs: complex interactions essential for development. Bioessays 22(2):108-112. doi: 10.1002/(sici)1521-1878(200002)22:2<108::aid-bies2>3.0.co;2-m PMID - 10655030

Owen, B. M., X. Ding, D. A. Morgan, K. C. Coate, A. L. Bookout, K. Rahmouni, S. A. Kliewer, and D. J. Mangelsdorf. 2014. FGF21 acts centrally to induce sympathetic nerve activity, energy expenditure, and weight loss. Cell Metabolism 20(4):670-677. doi: 10.1016/j.cmet.2014.07.012 PMID - 25130400

Ramos-Nieves, J. M., S. L. Giesy, W. S. Schwark, A. Gertler, and Y. R. Boisclair. 2019. Technical note: Effects of pegylation and route of administration on leptin kinetics in newborn lambs. Journal of Animal Science doi: 10.1093/jas/skz218 PMID - 31250023

Russel, A. 1984. Body condition scoring of sheep. In Practice 6(3):91-93. doi: 10.1136/inpract.6.3.91

Schoenberg, K. M., S. L. Giesy, K. J. Harvatine, M. R. Waldron, C. Cheng, A. Kharitonenkov, and Y. R. Boisclair. 2011. Plasma FGF21 is elevated by the intense lipid mobilization of

lactation. Endocrinology 152(12):4652-4661. doi: 10.1210/en.2011-1425 PMID - 21990311

Suzuki, M., Y. Uehara, K. Motomura-Matsuzaka, J. Oki, Y. Koyama, M. Kimura, M. Asada, A. Komi-Kuramochi, S. Oka, and T. Imamura. 2008. betaKlotho is required for fibroblast growth factor (FGF) 21 signaling through FGF receptor (FGFR) 1c and FGFR3c. Molecular Endocrinology 22(4):1006-1014. doi: 10.1210/me.2007-0313 PMID - 18187602

Tacer, K. F., A. L. Bookout, X. Ding, H. Kurosu, G. B. John, L. Wang, R. Goetz, M. Mohammadi, M. Kuro-o, D. J. Mangelsdorf, and S. A. Kliewer. 2010. Research resource: Comprehensive expression atlas of the fibroblast growth factor system in adult mouse. Molecular Endocrinology 24(10):2050-2064. doi: 10.1210/me.2010-0142 PMID - 20667984

Véniant, M. M., R. Komorowski, P. Chen, S. Stanislaus, K. Winters, T. Hager, L. Zhou, R. Wada, R. Hecht, and J. Xu. 2012. Long-Acting FGF21 Has Enhanced Efficacy in Diet-Induced Obese Mice and in Obese Rhesus Monkeys. Endocrinology 153(9):4192-4203. doi: 10.1210/en.2012-1211 PMID - 22798348

Xu, J., S. Stanislaus, N. Chinookoswong, Y. Y. Lau, T. Hager, J. Patel, H. Ge, J. Weiszmann, S.-C. C. Lu, M. Graham, J. Busby, R. Hecht, Y.-S. S. Li, Y. Li, R. Lindberg, and M. M. Véniant. 2009. Acute glucose-lowering and insulin-sensitizing action of FGF21 in insulin-resistant mouse models--association with liver and adipose tissue effects. American Journal of Physiology Endocrinology and Metabolism 297(5):E1105-1114. doi: 10.1152/ajpendo.00348.2009 PMID - 19706786

Zhao, C., Y. Liu, J. Xiao, L. Liu, S. Chen, M. Mohammadi, C. J. McClain, X. Li, and W. Feng. 2015. FGF21 mediates alcohol-induced adipose tissue lipolysis by activation of systemic release of catecholamine in mice. Journal of Lipid Research 56(8):1481-1491. doi: 10.1194/jlr.m058610 PMID - 26092866

CHAPTER 5

SUMMARY AND CONCLUSIONS

Ruminants entering the transition period with either insufficient or excessive adiposity are at increased risk for developing infectious or metabolic diseases (Mulligan and Doherty, 2008; Fthenakis et al., 2012; Pires et al., 2013). In addition, the functionality and dynamics of internal and external fat depots are different (Ibrahim, 2010). Approaches to measure internal depots are lacking in ruminants with the consequence that virtually all ruminant studies investigating effects of adipose reserves on health or productivity are based on external fat (Boisclair et al., 1986; Zhu et al., 2008; Janovick and Drackley, 2010). Although Ford and colleagues utilized DEXA scanning to quantify total body fatness, they did not differentiate between internal and external depots (Tuersunjiang et al., 2013). Moreover, visceral obesity is linked with insulin resistance in various species, and insulin action is an important determinant of overall health (Einstein et al., 2008; Lottati et al., 2009; LeBlanc, 2014). We therefore conducted a study in lean and obese ewes through pregnancy and lactation to determine the dynamics of external and internal fat.

Ewes were either fed to estimated energy requirements or offered unlimited amounts of energy to generate differences in fatness. This feeding treatment was initiated 50 days prior to mating, allowing obese ewes to become over 25 kg heavier by mid-pregnancy while lean ewes maintained their weight. This approach is similar to work reported previously (Wallace et al., 2005; George et al., 2010; Tuersunjiang et al., 2013). By mid-pregnancy, obese ewes were twice as fat as determined by CT scanning, with little additional fat gain between mid- and late pregnancy. Surprisingly, external fat accounted for a larger proportion of total fat relative to internal fat in both lean and obese ewes. Fat was also preferentially accreted and mobilized to and from the external depot. Previous work in nonpregnant sheep shows that internal fat (sum of omental, mesenteric, and perirenal) accounts for a larger proportion of dissectible fat depots than

subcutaneous fat (Thompson et al., 1985). Similarly, studies in cows and sheep identified internal depots as the preferred site of lipid accretion during times of excess energy consumption (Chay-Canul et al., 2011; Drackley et al., 2014). However, these studies do not account for the intermuscular fat depot. Butler-Hogg and colleagues showed that the intermuscular fat depot is not only the largest depot in dairy cattle, but it is also the most dynamic during accretion and mobilization (Butler-Hogg et al., 1985). Since intermuscular fat is detected by CT scanning, it is included in our external fat measurement. It is also possible pregnancy and lactation alter the preferred site of fat accretion and mobilization in sheep.

Ford and colleagues demonstrated not only increased basal plasma insulin and glucose, but also impaired glucose clearance during GTT in obese relative to lean ewes in both mid- and late pregnancy (Tuersunjiang et al., 2013). In our ewes, basal plasma insulin and glucose are elevated and glucose response is impaired during ITT in obese relative to lean at both timepoints. In contrast to Ford and colleagues, however, obese ewes never experienced impaired glucose-stimulated insulin secretion during GTT. The main difference between their work and ours is the lack of a robust insulin response in their lean ewes (Tuersunjiang et al., 2013).

Visceral obesity is associated with reduced insulin action in both dogs and mice (Lottati et al., 2009; Chen et al., 2012). Relative to total body adiposity, indices of fatness (BCS, backfat, and CT scan fatness) were positively and negatively correlated with glucose response areas during GTT and ITT respectively. Upon analyzing correlations between different depots and GTT and ITT responses, the external depot was more closely associated with impaired insulin action than the internal depot. One possible explanation for this observation is the growing evidence that intermuscular fat directly impairs muscle insulin sensitivity in humans (Sachs et al., 2019); this remains to be evaluated in ruminant species.

In lactation, ewes were restricted to 70% of their estimated energy requirements starting on day 6 to promote increased fat mobilization. Despite this challenge, obesity did not impair health as determined by similar body weight loss and similar plasma profiles for insulin, glucose, fatty acids, and BHBA in lean and obese ewes. In addition, lamb growth and milk composition was unaffected by maternal fatness. Importantly, there was no difference between glucose disposal during GTT and ITT tests between groups. Women experiencing gestational diabetes experience a similar resolution in insulin sensitivity following parturition (Waters et al., 2020). Overall, these data implicate external fat as the primary site of accretion and mobilization as well as the main driver behind insulin resistance in pregnant and lactating ewes. While this is not what other studies observed previously (Drackley et al., 2014; Ruda et al., 2019), these other studies have not taken intermuscular fat (included in the external fat in our study) into account. One study that evaluated the dynamics of intermuscular fat suggested this depot is not only quite extensive, but it also is one of the most affected depots during accretion and mobilization (Butler-Hogg et al., 1985). Future experiments are needed in nonpregnant, nonlactating ewes to determine if the same fat depot dynamics are observed. In addition, further work is needed to specifically assess the role of intermuscular fat on insulin action.

The second focus of this thesis was an assessment of FGF21 as an insulin sensitizer in the sheep. FGF21 is a novel hormone that consistently reduces plasma insulin and glucose as well as improves glucose clearance in rodent and primate models (Kharitonenkov et al., 2005; Coskun et al., 2008; Adams et al., 2013). Almost all FGF21 work has focused on animals in positive energy balance (e.g. obesity and type 2 diabetes). In contrast, we recently explored the insulin-sensitizing potential of FGF21 in early lactating dairy cattle (Krumm et al., 2019). The lack of any such effect in these energy-deficient ruminants led us to hypothesize that FGF21 action may

depend on energy balance. In a first step towards answering this question, we asked whether FGF21 could elicit insulin-sensitizing effects in sheep in a state of positive energy balance. We started by characterizing the FGF system in sheep. We found that liver was the predominant site of FGF21 production, which is similar to results reported previously in cattle and humans (Dushay et al., 2010; Schoenberg et al., 2011). Next we identified the target tissues by measuring expression of the FGF21 obligate co-receptor, β-klotho (Adams et al., 2012a), and its preferred receptor, FGFR1c (Adams et al., 2012b). This work confirmed adipose and liver as two possible target tissues. In addition to expression patterns, we took biopsies of adipose tissue following FGF21 administration and quantified signaling events. Both ERK 1/2 phosphorylation and Egr1 mRNA expression were upregulated in adipose tissue following stimulation, confirming adipose tissue as a primary target. This is again similar to results reported in cattle (Schoenberg et al., 2011).

Following characterization of the FGF system, we next tested acute and chronic effects of FGF21 administration. In both *ob/ob* and diet-induced obese mouse models, FGF21 reduces plasma glucose and insulin within 1 h (Kharitonenkov et al., 2005; Xu et al., 2009). When subjected to GTT, FGF21-treated subjects exhibit an improvement in insulin-mediated glucose disposal. Overall, our results in growing sheep agree with the rodent literature; FGF21 treatment reduced plasma glucose and insulin both acutely and chronically, and this effect was confirmed by improved glucose disposal during GTT.

Additional actions of FGF21 in rodents include increasing plasma adiponectin (Holland et al., 2013; Lin et al., 2013) and increased lipolysis (Inagaki et al., 2007; Hotta et al., 2009). Our data are consistent with these data, showing that FGF21 increased plasma adiponectin and increased epinephrine-stimulated lipolysis; basal lipolysis was not impacted as plasma fatty acids

did not differ between control and FGF21-treated animals. In contrast, FGF21 did not cause any changes in adiponectin nor was there any increase in lipolysis in the energy insufficient dairy cow; in fact, FGF21 appeared to have an antilipolytic effect (Schoenberg et al., 2011). Overall, these data suggest FGF21 action in ruminants depends on energy status. Future work is needed in nonpregnant, nonlactating ewes to assess impact of energy balance on FGF21 action and its ability to improve insulin action during insulin-resistant states such as pregnancy and obesity.

REFERENCES

Adams, A. C., C. C. Cheng, T. Coskun, and A. Kharitonenkov. 2012a. FGF21 requires βklotho to act in vivo. PloS One 7(11):e49977. doi: 10.1371/journal.pone.0049977 PMID - 23209629

Adams, A. C., C. A. Halstead, B. C. Hansen, A. R. Irizarry, J. A. Martin, S. R. Myers, V. L. Reynolds, H. W. Smith, V. J. Wroblewski, and A. Kharitonenkov. 2013. LY2405319, an Engineered FGF21 Variant, Improves the Metabolic Status of Diabetic Monkeys. PloS One 8(6):e65763. doi: 10.1371/journal.pone.0065763 PMID - 23823755

Adams, A. C., C. Yang, T. Coskun, C. C. Cheng, R. E. Gimeno, Y. Luo, and A. Kharitonenkov. 2012b. The breadth of FGF21's metabolic actions are governed by FGFR1 in adipose tissue. Molecular Metabolism 2(1):31-37. doi: 10.1016/j.molmet.2012.08.007 PMID - 24024127

Boisclair, Y., D. G. Grieve, J. B. Stone, O. B. Allen, and G. K. MacLeod. 1986. Effect of prepartum energy, body condition, and sodium bicarbonate on production of cows in early lactation. Journal of Dairy Science 69(10):2636-2647. doi: 10.3168/jds.S0022-0302(86)80711-1

Butler-Hogg, B. W., J. D. Wood, and J. A. Bines. 1985. Fat partitioning in British Friesian cows: the influence of physiological state on dissected body composition. The Journal of Agricultural Science 104(3):519-528. doi: 10.1017/s0021859600044282

Chay-Canul, A. J., A. J. Ayala-Burgos, J. C. Ku-Vera, J. G. Magaña-Monforte, and L. O. Tedeschi. 2011. The effects of metabolizable energy intake on body fat depots of adult Pelibuey ewes fed roughage diets under tropical conditions. Tropical Animal Health and Production 43(5):929-936. doi: 10.1007/s11250-011-9785-5 PMID - 21240653

Chen, W., J. L. Wilson, M. Khaksari, M. A. Cowley, and P. J. Enriori. 2012. Abdominal fat analyzed by DEXA scan reflects visceral body fat and improves the phenotype description and the assessment of metabolic risk in mice. American Journal of Physiology Endocrinology and Metabolism 303(5):E635-643. doi: 10.1152/ajpendo.00078.2012 PMID - 22761161

Coskun, T., H. A. Bina, M. A. Schneider, J. D. Dunbar, C. C. Hu, Y. Chen, D. E. Moller, and A. Kharitonenkov. 2008. Fibroblast growth factor 21 corrects obesity in mice. Endocrinology 149(12):6018-6027. doi: 10.1210/en.2008-0816 PMID - 18687777

Drackley, J. K., R. L. Wallace, D. Graugnard, J. Vasquez, B. F. Richards, and J. J. Loor. 2014. Visceral adipose tissue mass in nonlactating dairy cows fed diets differing in energy density. Journal of Dairy Science 97(6):3420-3430. doi: 10.3168/jds.2014-8014 PMID - 24704224

Dushay, J., P. C. Chui, G. S. Gopalakrishnan, M. Varela–Rey, M. Crawley, F. M. Fisher, M. K. Badman, M. L. Martinez–Chantar, and E. Maratos–Flier. 2010. Increased Fibroblast

Growth Factor 21 in Obesity and Nonalcoholic Fatty Liver Disease. Gastroenterology 139(2):456-463. doi: 10.1053/j.gastro.2010.04.054 PMID - 20451522

Einstein, F. H., S. Fishman, R. H. Muzumdar, X. M. Yang, G. Atzmon, and N. Barzilai. 2008. Accretion of visceral fat and hepatic insulin resistance in pregnant rats. American Journal of Physiology Endocrinology and Metabolism 294(2):E451-E455. doi: 10.1152/ajpendo.00570.2007 PMID - 18073320

Fthenakis, G. C., G. Arsenos, C. Brozos, I. A. Fragkou, N. D. Giadinis, I. Giannenas, V. S. Mavrogianni, E. Papadopoulos, and I. Valasi. 2012. Health management of ewes during pregnancy. Animal Reproduction Science 130(3-4):198-212. doi: 10.1016/j.anireprosci.2012.01.016 PMID - 22356932

George, L. A., A. B. Uthlaut, N. M. Long, L. Zhang, Y. Ma, D. T. Smith, P. W. Nathanielsz, and S. P. Ford. 2010. Different levels of overnutrition and weight gain during pregnancy have differential effects on fetal growth and organ development. Reproductive Biology and Endocrinology 8:75. doi: 10.1186/1477-7827-8-75 PMID - 20576133

Holland, W. L., A. C. Adams, J. T. Brozinick, H. H. Bui, Y. Miyauchi, C. M. Kusminski, S. M. Bauer, M. Wade, E. Singhal, C. C. Cheng, K. Volk, M.-S. S. Kuo, R. Gordillo, A. Kharitonenkov, and P. E. Scherer. 2013. An FGF21-adiponectin-ceramide axis controls energy expenditure and insulin action in mice. Cell Metabolism 17(5):790-797. doi: 10.1016/j.cmet.2013.03.019 PMID - 23663742

Hotta, Y., H. Nakamura, M. Konishi, Y. Murata, H. Takagi, S. Matsumura, K. Inoue, T. Fushiki, and N. Itoh. 2009. Fibroblast growth factor 21 regulates lipolysis in white adipose tissue but is not required for ketogenesis and triglyceride clearance in liver. Endocrinology 150(10):4625-4633. doi: 10.1210/en.2009-0119 PMID - 19589869

Ibrahim, M. M. 2010. Subcutaneous and visceral adipose tissue: structural and functional differences. Obesity Reviews 11(1):11-18. doi: 10.1111/j.1467-789x.2009.00623.x PMID - 19656312

Inagaki, T., P. Dutchak, G. Zhao, X. Ding, L. Gautron, V. Parameswara, Y. Li, R. Goetz, M. Mohammadi, V. Esser, J. K. Elmquist, R. D. Gerard, S. C. Burgess, R. E. Hammer, D. J. Mangelsdorf, and S. A. Kliewer. 2007. Endocrine regulation of the fasting response by PPARalpha-mediated induction of fibroblast growth factor 21. Cell Metabolism 5(6):415-425. doi: 10.1016/j.cmet.2007.05.003 PMID - 17550777

Janovick, N. A., and J. K. Drackley. 2010. Prepartum dietary management of energy intake affects postpartum intake and lactation performance by primiparous and multiparous Holstein cows1. Journal of Dairy Science 93(7):3086-3102. doi: https://doi.org/10.3168/jds.2009-2656

Kharitonenkov, A., T. L. Shiyanova, A. Koester, A. M. Ford, R. Micanovic, E. J. Galbreath, G. E. Sandusky, L. J. Hammond, J. S. Moyers, R. A. Owens, J. Gromada, J. T. Brozinick, E. D. Hawkins, V. J. Wroblewski, D.-S. S. Li, F. Mehrbod, S. R. Jaskunas, and A. B.

Shanafelt. 2005. FGF-21 as a novel metabolic regulator. Journal of Clinical Investigation 115(6):1627-1635. doi: 10.1172/JCI23606 PMID - 15902306

Krumm, C. S., S. L. Giesy, L. S. Caixeta, J. W. Perfield, H. Sauerwein, B. L. Moore, and Y. R. Boisclair. 2019. Fibroblast growth factor-21 (FGF21) administration to early-lactating dairy cows. I. Effects on signaling and indices of insulin action. Journal of Dairy Science doi: 10.3168/jds.2019-16695 PMID - 31548053

LeBlanc, S. J. 2014. Reproductive tract inflammatory disease in postpartum dairy cows. animal 8:54-63. doi: https://doi.org/10.1017/S1751731114000524

Lin, Z., H. Tian, Karen S. L. Lam, S. Lin, Ruby C. L. Hoo, M. Konishi, N. Itoh, Y. Wang, Stefan R. Bornstein, A. Xu, and X. Li. 2013. Adiponectin Mediates the Metabolic Effects of FGF21 on Glucose Homeostasis and Insulin Sensitivity in Mice. Cell Metabolism 17(5):779-789. doi: 10.1016/j.cmet.2013.04.005 PMID - 23663741

Lottati, M., C. M. Kolka, D. Stefanovski, and E. L. Kirkman. 2009. Greater omentectomy improves insulin sensitivity in nonobese dogs. Obesity doi: 10.1038/oby.2008.642

Mulligan, F. J., and M. L. Doherty. 2008. Production diseases of the transition cow. Veterinary Journal 176(1):3-9. doi: 10.1016/j.tvjl.2007.12.018 PMID - 18342556

Pires, J. A. A., C. Delavaud, Y. Faulconnier, D. Pomiès, and Y. Chilliard. 2013. Effects of body condition score at calving on indicators of fat and protein mobilization of periparturient Holstein-Friesian cows. Journal of Dairy Science 96(10):6423-6439. doi: https://doi.org/10.3168/jds.2013-6801

Ruda, L., C. Raschka, K. Huber, R. Tienken, U. Meyer, S. Dänicke, and J. Rehage. 2019. Gain and loss of subcutaneous and abdominal fat depot mass from late pregnancy to 100 days in milk in German Holsteins. Journal of Dairy Research 86(3):296-302. doi: 10.1017/s0022029919000542 PMID - 31409432

Sachs, S., S. Zarini, D. E. Kahn, K. A. Harrison, L. Perreault, T. Phang, S. A. Newsom, A. Strauss, A. Kerege, J. A. Schoen, D. H. Bessesen, T. Schwarzmayr, E. Graf, D. Lutter, J. Krumsiek, S. M. Hofmann, and B. C. Bergman. 2019. Intermuscular adipose tissue directly modulates skeletal muscle insulin sensitivity in humans. American Journal of Physiology Endocrinology and Metabolism 316(5):E866-E879. doi: 10.1152/ajpendo.00243.2018 PMID - 30620635

Schoenberg, K. M., S. L. Giesy, K. J. Harvatine, M. R. Waldron, C. Cheng, A. Kharitonenkov, and Y. R. Boisclair. 2011. Plasma FGF21 is elevated by the intense lipid mobilization of lactation. Endocrinology 152(12):4652-4661. doi: 10.1210/en.2011-1425 PMID - 21990311

Thompson, J. M., R. M. Butterfield, and D. Perry. 1985. Food intake, growth and body composition in Australian Merino sheep selected for high and low weaning weight. 2. Chemical and dissectible body composition. Animal Science 40(1):71-84. doi: 10.1017/S000335610003186X

Tuersunjiang, N., J. F. Odhiambo, N. M. Long, D. R. Shasa, P. W. Nathanielsz, and S. P. Ford. 2013. Diet reduction to requirements in obese/overfed ewes from early gestation prevents glucose/insulin dysregulation and returns fetal adiposity and organ development to control levels. American Journal of Physiology Endocrinology and Metabolism 305(7):E868-878. doi: 10.1152/ajpendo.00117.2013 PMID - 23921140

Wallace, J. M., J. S. Milne, and R. P. Aitken. 2005. The effect of overnourishing singleton-bearing adult ewes on nutrient partitioning to the gravid uterus. British Journal of Nutrition 94(4):533-539.

Waters, T. P., S. Y. Kim, A. J. Sharma, P. Schnellinger, J. K. Bobo, R. T. Woodruff, L. A. Cubbins, M. Haghiac, J. Minium, L. Presley, H. Wolfe, S. Hauguel-de Mouzon, W. Adams, and P. M. Catalano. 2020. Longitudinal changes in glucose metabolism in women with gestational diabetes, from late pregnancy to the postpartum period. Diabetologia 63(2):385-394. doi: 10.1007/s00125-019-05051-0

Xu, J., S. Stanislaus, N. Chinookoswong, Y. Y. Lau, T. Hager, J. Patel, H. Ge, J. Weiszmann, S.-C. C. Lu, M. Graham, J. Busby, R. Hecht, Y.-S. S. Li, Y. Li, R. Lindberg, and M. M. Véniant. 2009. Acute glucose-lowering and insulin-sensitizing action of FGF21 in insulin-resistant mouse models--association with liver and adipose tissue effects. American Journal of Physiology Endocrinology and Metabolism 297(5):E1105-1114. doi: 10.1152/ajpendo.00348.2009 PMID - 19706786

Zhu, M. J., B. Han, J. Tong, C. Ma, J. M. Kimzey, K. R. Underwood, Y. Xiao, B. W. Hess, S. P. Ford, P. W. Nathanielsz, and M. Du. 2008. AMP-activated protein kinase signalling pathways are down regulated and skeletal muscle development impaired in fetuses of obese, over-nourished sheep. The Journal of Physiology 586(10):2651-2664. doi: 10.1113/jphysiol.2007.149633 PMID - 18372306

Appendix I. Ovine primers used in real-time PCR analysis

Gene[1]		Sequence[2]	Product (bp)	Accession No.
FGF21	F	GCCAGGAGTCATTCAGATCT	110	XM_027977590.1
	R	GGAAGCTGCAGGCTTTGGG		
β-klotho	F	TTCCCTGTGATTTCTCCTGGG	113	XM_004010055.4
	R	GTTGCCCGTCACATTCCACA		
FGFR1c	F	GCAAGGTGTACAGTGACCCACA	134	XM_027962636.1
	R	TTTGTCGGTGGTGTTAACTCCGG		
FGFR2c	F	ACGTGCTTGGCGGGTAATT	69	XM_012103045.3
	R	AGGAGCTGGCAGAACTGTCAA		
FGFR3c	F	TACGTCACCGTGCTCAAGAC	73	XM_027971319.1
	R	CATTGCGCAAGGACAGAACC		
FGFR4	F	GAATGGGCACATTTACCCC	67	XM_015095970.2
	R	CAGTTTCTTCTCCATGCGCTG		
Egr1	F	CAAGCGAGCAGCCCTACGA	103	NM_001142506.1
	R	GTGGTTTGGCTGGGGTAACTC		
18s	F	GATCCATTGGAGGGCAAGTCT	75	KY129860.1
	R	GCAGCAACTTTAATATACGCTATTGG		

[1]Primers were designed to measure the abundance of fibroblast growth factor-21 (FGF21), β-klotho, fibroblast growth factor receptor (FGFR)-1c, FGFR2c, FGFR3c, FGFR4, early growth response (Egr1), and 18S ribosomal RNA (18S).

[2]Primer sequences are shown in a 5' to 3' orientation.